

Novel Transaminases for the Preparation of Pharmaceutically Relevant Chiral Amines

I n a u g u r a l d i s s e r t a t i o n

zur

Erlangung des akademischen Grades eines

Doktors der Naturwissenschaften

(Dr. rer. Nat.)

der

Mathematisch-Naturwissenschaftlichen Fakultät

der

Ernst-Moritz-Arndt-Universität Greifswald

vorgelegt von

Martin Steffen Weiß

geboren am 25.07.1987

in Heidelberg

Greifswald, Juli 2017

Dekan: Prof. Dr. Werner Weitschies

1. Gutachter: Jun.-Prof. Dr. Matthias Höhne

2. Gutachter: Prof. Dr. Per Berglund

Tag der Promotion: 08.12.2017

Contents

1	Summary and List of Publications	V
2	Preparation of Chiral Amines	1
2.1	Traditional Ways to Access Chiral Amines	1
2.2	Alternative Biocatalytic Approaches	3
2.2.1	Monoamine Oxidases (MAOs)	5
2.2.2	Imine Reductases (IREDs) and Reductive Aminases	6
2.2.3	Amine Dehydrogenases (AmDHs)	6
2.2.4	Transaminases (TAs)	7
3	Enzyme Screening Assays <i>versus</i> Instrumental Analytics	15
3.1	Principle Screening Options for Transaminases	16
3.1.1	Transaminase Assay Principles	16
3.1.2	Towards High-throughput Options for Transaminases	18
4	Protein-Engineering of <i>Ruegeria</i> sp. TM1040 Transaminase	21
4.1	Requisite Substrates and Project Strategy	21
4.2	Screening Assays for the Target Substrates	23
4.2.1	Adaption of the Glycine Oxidase Assay	24
4.3	Identification of a Starting Scaffold and Bioinformatic Analysis	29
4.3.1	Quinonoid Analysis and Rational Mutagenesis	30
4.4	Validation of the Identified Sequence Motif	32
4.4.1	Preparative Scale Synthesis of Chiral Amines I.1 – I.3	34
4.5	Diversification of the Scaffolds	35
4.5.1	Mutating Position 59 and Neighboring Residues Enhances the Activity Against the Bicyclic-bridged Substrate	36
4.5.2	Aliphatic Amino Acids in Position 87 Enable Acceptance of the Spatially Bulky Substrate	40
5	Conclusion	45
	References	49
6	Articles I – IV	59

List of abbreviations

3FCR-TA	Transaminase from <i>Ruegeria</i> sp. TM1040	GO	Glycine oxidase
3GJU-TA	<i>Mesorhizobium loti</i> maff303099	HPLC	High performance liquid chromatography
3HMU-TA	Transaminase from <i>Ruegeria pomeroyi</i>	IPA	Isopropylamine
AADH	Amino acid dehydrogenase	IREC	Imine reductase
AAO	Amino acid oxidase	L-AAO	L-Amino acid oxidase
AmDH	Amine dehydrogenase	L-Ala	L-Alanine
(A)TA	(Amine) transaminase	λ	Wave length
Cv-TA	Transaminase from <i>Chromobacterium violaceum</i>	LC/MS	Liquid chromatography–mass spectrometry
D-AAO	D-Amino acid oxidase	LDH	Lactate dehydrogenase
D-Ala	D-Alanine	MAO	Monoamine oxidase
DMSO	Dimethyl sulfoxide	MTP	Microtiter plate
ee	Enantiomeric excess	NADH	Nicotinamide adenine dinucleotide
ep-PCR	Error-prone polymerase chain reaction	PEA	α -phenylethylamine
FACS	Fluorescence-activated cell sorting	PLP	Pyridoxal 5'-phosphate
GDH	Glucose dehydrogenase	VibFlu-TA	Transaminase from <i>Vibrio fluvialis</i>

Furthermore, the single letter code for amino acids and regular SI units were applied.

1 Summary and List of Publications

Chiral amines represent high-value fine chemicals serving as key intermediate products in pharmaceutical, chemical and agrochemical industries. In the past decades, application of amine transaminases (ATAs) for stereoselective amination of prochiral ketones emerged to an environmentally benign and economically attractive alternative to transition metal-catalyzed asymmetric synthesis to afford optically pure amines at industrial scale. However, the restricted substrate scope of wild-type transaminases prohibited the conversion of particularly sterically demanding substrates, making protein engineering indispensable.

The following thesis covers elaboration of a novel assay for transaminases (**Article I**) and identification and development of transaminase variants in order to achieve biocatalytic preparation of a set of pharmaceutically relevant model amines, ideally in optically pure form for both stereoisomers, preferentially using asymmetric synthesis and most preferably using isopropylamine as cost-efficient amine donor co-substrate (**Article II-IV**). The aforementioned target amines and the corresponding precursor ketones (see **Scheme 4.1**) were conceived and provided by the company F. Hoffmann-La Roche to attain suitable biocatalysts for a variety of potential intermediates for active pharmaceutical ingredients.

Protein engineering of the transaminase scaffolds investigated in this thesis comprised: Initial screening for suitable starting enzyme scaffolds, structure-guided rational design of these scaffolds to enable bulky planar substrate acceptance, elaboration of a sequence motif, verification of the motif and preparative-scale asymmetric synthesis reactions (**Article II**). For non-planar and structurally different target substrates, namely spatially bulky or bi-cyclic bridged substrates, the transaminase variants were specifically refined and a different evolutionary route had to be pursued (**Article III** and **Article IV**). These results (**Article II**) represent not only the first successful endeavor to engineer a PLP-fold type I amine transaminase (commonly denoted as (*S*)-selective) for the conversion of highly sterically demanding substrates, but also generally expanded the scope of available fold type I amine transaminases by enzymes having a novel and exceptionally broad substrate spectrum.

Aside from structure-guided rational protein engineering, as well non-rational methods, such as site-specific saturation mutagenesis or directed evolution, were applied for protein-engineering. In order to do so for all of the target compounds, a novel high-throughput solid phase activity assay for transaminases that was actually developed during the master thesis, was refined and published (**Article I**). In the context of this thesis, the same assay principle was as well adapted for quantification of specific activities in liquid phase (**Article III**). A comparison of different methodologies for developing agar plate assays and a detailed step by step protocol of our transaminase assay are illustrated in a book chapter.

Articles:

Article I Glycine oxidase based high-throughput solid-phase assay for substrate profiling and directed evolution of (*R*)- and (*S*)-selective amine transaminases.

Martin S. Weiß, Ioannis V. Pavlidis, Clare Vickers, Matthias Höhne and Uwe T. Bornscheuer. *Anal. Chem.*, **2014**, 86, 11847–11853.*

Article II Identification of (*S*)-selective transaminases for the asymmetric synthesis of bulky chiral amines.

Ioannis V. Pavlidis, Martin S. Weiß, Maika Genz, Paul Spurr, Steven P. Hanlon, Beat Wirz, Hans Iding and Uwe T. Bornscheuer. *Nat. Chem.*, **2016**, 8, 1076–1082.†

Article III Protein-engineering of an amine transaminase for the stereoselective synthesis of a pharmaceutically relevant bicyclic amine.

Martin S. Weiß, Ioannis V. Pavlidis, Paul Spurr, Steven P. Hanlon, Beat Wirz, Hans Iding and Uwe T. Bornscheuer. *Org. Biomol. Chem.*, **2016**, 14, 10249–10254.‡

Article IV Amine transaminase engineering for spatially bulky substrate acceptance.

Martin S. Weiß, Ioannis V. Pavlidis, Paul Spurr, Steven P. Hanlon, Beat Wirz, Hans Iding and Uwe T. Bornscheuer. *ChemBioChem*, **2017**, 18, 1022–1026.§

Book Chapter:

Book Chapter Solid Phase Agar Plate Assay for Screening Amine Transaminases.

(*In press*) Martin S. Weiß, Matthias Höhne and Uwe T. Bornscheuer. *Methods in Molecular Biology*¶

*Reproduced with permission from ACS. The article is available under the ACS AuthorChoice license (<http://pubs.acs.org/doi/full/10.1021/ac503445y>) and further permissions related to the article shall be submitted to the ACS.

†Reproduced according to the Nature Publishing Group's online author reuse guidelines. The article is online available under <http://www.nature.com/nchem/journal/v8/n11/abs/nchem.2578.html>.

‡Reproduced by permission of The Royal Society of Chemistry. The article is freely available under <http://pubs.rsc.org/en/Content/ArticleLanding/2016/OB/C6OB02139E>.

§Copyright Wiley-VCH Verlag GmbH & Co. KGaA. Reproduced with permission.

¶Accepted manuscript. The final type-set book chapter will appear in: Protein Engineering: Methods and Protocols, ISBN: 978-1-4939-7364-4, Springer Publishing Company.

2 Preparation of Chiral Amines

Until 1984, about 88 % of all chiral drugs were formulated and delivered as racemates, when E.J. Ariens claimed that the therapeutically inactive enantiomer in racemic formulations should actually be considered as impurity, due to its possible cause of side-effects.^[1, 2] This novel awareness for the significance of stereochemistry in therapeutic action triggered a revolution of pharmacology, gradually increasing single enantiomer entities, while decreasing racemate formulations. Twenty years later, in 2004, only three of all 16 newly approved synthetic drugs were achiral, while all the other 13 were single enantiomers.^[2] This move from racemates to single enantiomers was driven by strict regulations of regulatory authorities in the late 1980s, which required pharmaceutical companies to investigate the stereochemical features of their drug candidates in the early stage of development.^[2] In most cases, single enantiomers were selected for further development, while racemates were only selected exceptionally, in case of similar pharmacological and toxicological properties, synergetic effects or spontaneous racemization of the individual enantiomers.^[2] In addition to that, there is a general trend to chiral entities, independently from these regulations, as the amount of new non-chiral drugs constantly decreased over the past two decades.^[2]

This change had also a great impact on the pharmaceutical and agrochemical industries, whose total revenue was estimated to exceed 20 billion US dollar for the year 2000, of which the greatest shares belong to the pharmaceutical industry.^[3] Optically active intermediates had an estimated fraction of 15 % of the market and sales of these special intermediates annually increased by 7 - 8 %.^[3]

Chiral amines represent a major fraction of these high-value products and primarily serve as building blocks for the synthesis of pharmaceutical drugs (**Figure 2.1**) and agrochemicals but are as well applied as chiral auxiliaries or chiral resolving agents in chemical industry. The increased demand for optically pure amines poses a challenge to provide efficient, sustainable and economical solutions to afford any kind of desired chiral amine in sufficient quantities and enantiomeric purities.

2.1 Traditional Ways to Access Chiral Amines

Historically, chiral amines are prepared by chiral resolution, which implies separation of the different enantiomers by diastereomeric salt crystallization, chiral derivatization or chromatographic methods involving chiral stationary phases.^[6] However, all these methods share one major drawback: They have a restricted maximum yield of 50 %, as only one enantiomer is exploitable, independently from the methods' individual demand for more or less cost intensive equipment

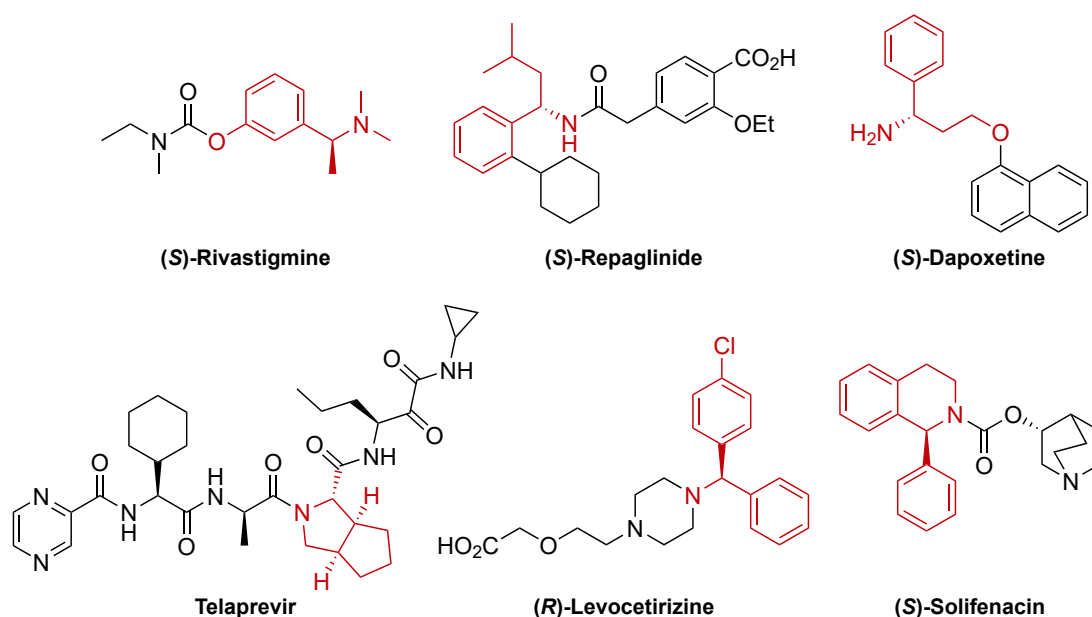


Figure 2.1: Exemplary pharmaceutical drugs that contain chiral amine building blocks (high-lighted in red). Structures were taken from references [4, 5] with minor corrections.

and processing.

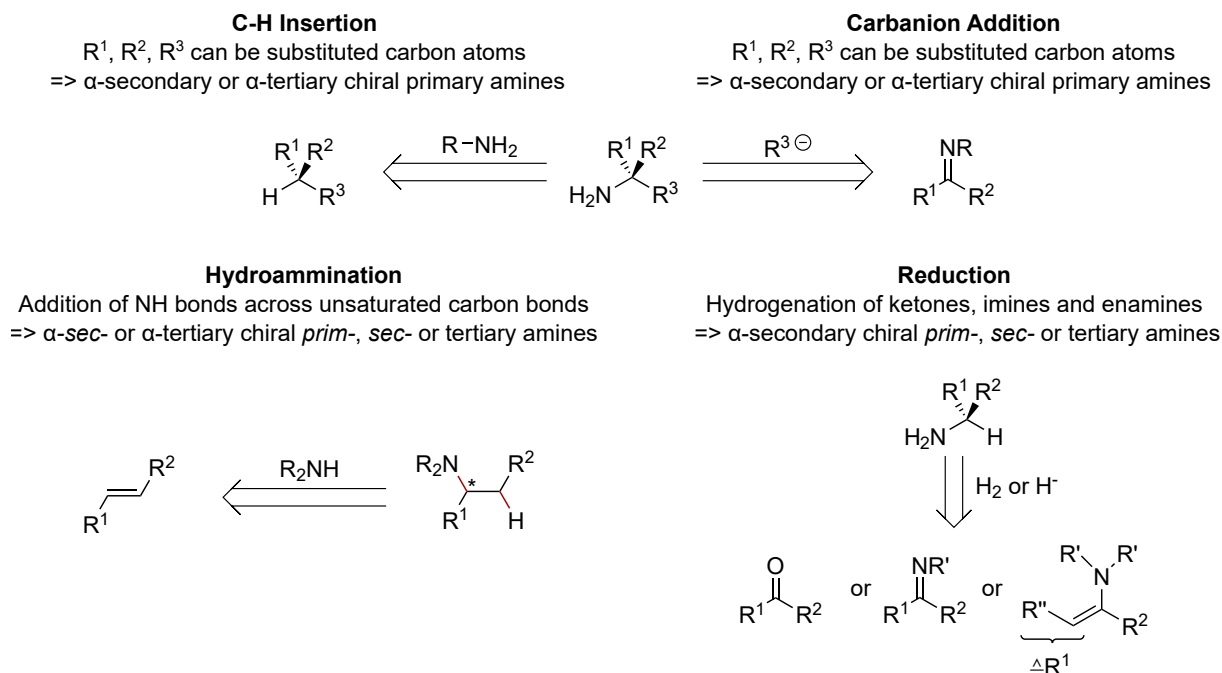
Thus, the direct chemical asymmetric synthesis of the desired enantiomer is highly attractive and was intensively studied. Over the past three decades innumerable diverse synthetic strategies were developed and further optimized for the efficient preparation of chiral amines with high yields at high to excellent enantiomeric purities (**Scheme 2.1**).^[7–10]

The synthetic strategies are subdivided by their type of reaction and have different scope of applications depending on the type of the desired amine product and the starting synthons. Hydroamination reactions allow the addition of N-H bonds across unsaturated carbon atoms,^[11, 12] affording primary, secondary or tertiary amines that are α -secondary or α -tertiary chiral[†]. The C-H insertion reaction allows the amination of a C-H σ -bonds affording α -secondary or α -tertiary chiral primary amines.^[13] The addition of carbanions to imines and subsequent imine cleavage reaction affords α -secondary or α -tertiary chiral primary amines.^[9, 14] The last type of reaction comprises asymmetric reductions of prochiral ketones via imine formation affording α -secondary chiral primary amines or reductions of enamines affording α -secondary chiral primary, secondary or tertiary amines.^[7–9, 15]

Research was predominately focused on reductive approaches for the synthesis of α -chiral primary amines to which also the target amine compounds of this thesis belong. Thus, the majority of these primary amines are synthetically prepared by reductions and only in some cases, typically if the reductive approaches fail to provide useful enantiomeric excess, other approaches such as the carbanion addition are considered as alternatives.^[9]

Nevertheless, all of the aforementioned methods require metal catalysis, in most of the cases transition metals such as Ti, Cu, Zn, Ru, Rh, Pd, Ir to achieve sufficient yields without side-

[†]Explanation of α -secondary or α -tertiary chiral amines: The carbon atom bearing the amine functionality is chiral and secondary or tertiary.



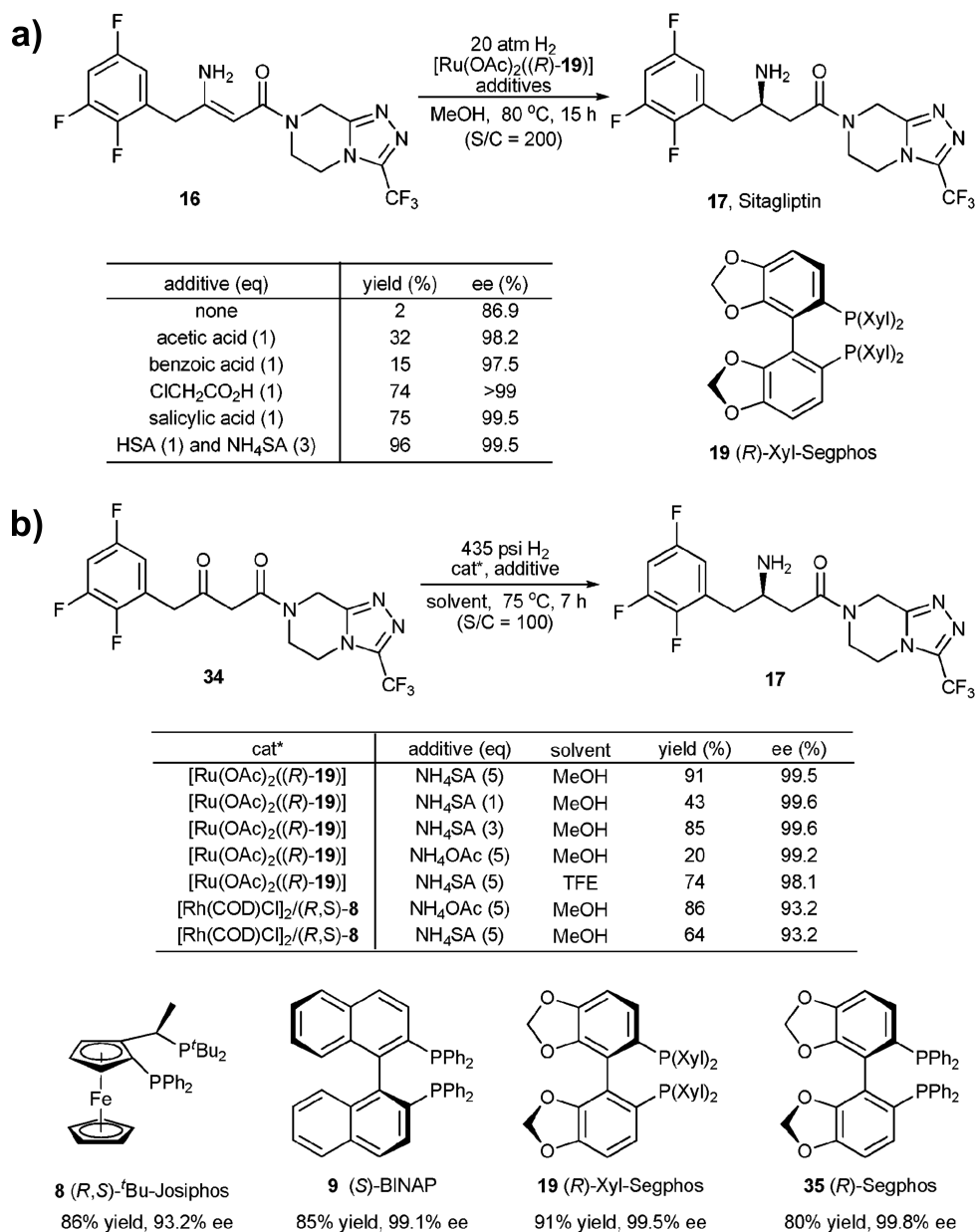
Scheme 2.1: General synthetic strategies to afford chiral amines. This thesis focuses on alternative strategies using transaminases to access α-secondary chiral primary amines, which is in most of the cases synthetically achieved by reduction and carbanion addition strategies (right).

product formation. In addition to that, complex and expensive chiral ligands are required to control stereoselectivity for sufficient enantiomeric excess of the desired amine product. In **Scheme 2.2**, an exemplary overview of the latest developments for the chemical reductive asymmetric synthesis of (*R*)-sitagliptin, an anti-diabetic drug, is depicted to demonstrate some selected chiral catalysts and parameters influencing yield and enantiomeric excess.

Although there are diverse and efficient methods to access many chiral amines, a lot of challenges remain for instance maximizing reaction step efficiency and functional group compatibility, as well as furthering access to remaining chiral amine structural classes.^[9] Major drawback of the majority of these traditional methods for the preparation of chiral primary amines is that the reaction itself or an inevitable hydrogenolysis deprotection step after the conversion of the afore activated precursors is supposed to be conducted at pressures of at least 15-20 bar H₂ and 50-60°C.^[9] This contributes to high production costs, aside from heavy metal waste disposal and application of chiral ligands. Thus, alternative environmentally benign and cost-efficient routes to access chiral amines with high enantiomeric excess are of great interest.

2.2 Alternative Biocatalytic Approaches

Enzymes intrinsically exhibit the capability to discriminate enantiomers or the different faces of prochiral compounds and thus represent attractive alternatives for the preparation of chiral compounds. Research endeavors of the past decades made a truly impressive variety of different type of enzymes accessible for chiral amine synthesis. By now, this tool-box^[16] comprises among others: Imine reductases, monoamine oxidases, hydrolases such as lipases or amidases, amine



Scheme 2.2: Overview on synthetic reductive approaches for the asymmetric synthesis of the anti-diabetic drug Sitagliptin (17). Reproduced from reference [10] with permission of The Royal Society of Chemistry. Different chiral catalysts and additives influence yield and enantiomeric excess. (S/C: molar ratio of substrate load and catalyst load, 435 psi \approx 35 bar) **a)**: Ru catalyzed enantioselective hydrogenation of the enamine. **b)**: Ru and Rh catalyzed enantioselective reduction of the di-ketone via imine formation and cleavage using different catalysts and additives.

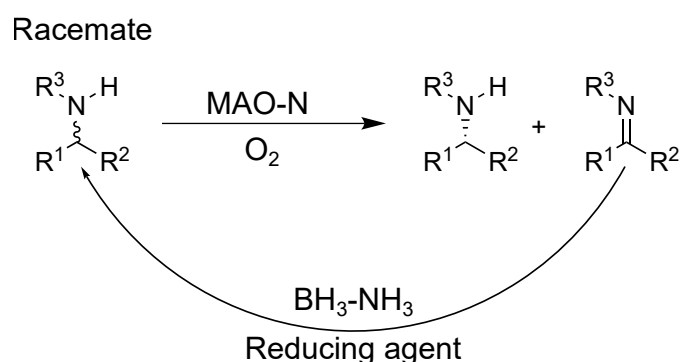
dehydrogenases, ammonia lyases, Pickett-Spenglerases, opine dehydrogenases, berberine bridge enzymes and transaminases.^[16–22]

Despite the use of enzymes for chiral catalysis seems obvious, the necessary development process for their actual application as industrial catalysts is elaborate and usually encompasses three different phases: Discovery of suitable enzymes or activities, further development, for instance substrate scope expansion, and finally maturation of the biocatalysts to fit the industrial manufacturing conditions.^[16] In case of transaminases their first records date back more than 50 years,^[21, 23, 24] but it took until the end of the 20th century until they came into focus as possible catalysts for chiral amine synthesis,^[25] and almost another ten years before further examples for their application at industrial scale were published.

2.2.1 Monoamine Oxidases (MAOs)

Monoamine oxidases (MAOs) represent very versatile and attractive enzymes for chiral amine preparation, as they can be applied for deracemization of racemic amines allowing yields up to 100 % and excellent enantiomeric purities. This is feasible by combining a chemical reducing agent with a MAO, which enantioselectively oxidizes one enantiomer of a racemic amine to an imine. The reducing agent in turn reduces the previously formed imine, which eventually enriches the desired enantiomer (**Scheme 2.3**). This approach provides several advantages, most importantly up to quantitative yields with excellent enantiomeric purities, but as well no impairment by equilibrium issues, as the oxidation of amines to imines with molecular oxygen is irreversible.

Major constraints for their application as industrial catalysts exhibit their restricted substrate scope and the desired enantiopreference. However, MAOs are currently subjected to protein engineering studies^[26, 27] and shortly before our project started MAO variants from *Aspergillus niger* were reported to be capable to deracemize structurally demanding amines, among them a variant for the preparation of the (*R*)-enantiomer of amine **I.1a** targeted in this study (see **Scheme 4.1**).^[17]



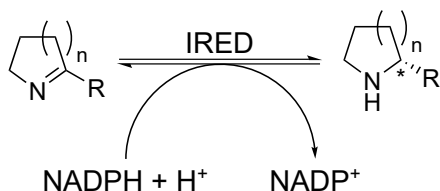
Scheme 2.3: Deracemization of racemic primary-, secondary- or tertiary amines by application of an enantioselective amine oxidase (MAO) and a chemical reducing agent. The desired enantiomer is enriched with yields up to 100 %. When a tertiary amine is oxidized by the MAO, an iminium ion is formed.

2.2.2 Imine Reductases (IREDs) and Reductive Aminases

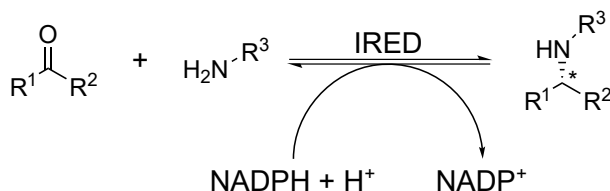
Imine reductases (IREDs) were newly discovered in 2010^[28] and since then they are emerging as new biocatalytic alternative for chiral amine synthesis, particularly for the preparation of chiral secondary amines by catalyzing the NADPH-dependent reduction of imines to amines (**Scheme 2.4**).^[29] Although, IREDs are most efficient in reducing endocyclic and thus stable imines, they have as well been shown to be applicable for the reduction of unstable and transient acyclic imines for the preparation of chiral secondary or tertiary amines. In some cases, even ammonia could serve as amine substrate to perform asymmetric reductive aminations, which in principal makes IREDs even accessible for the preparation of chiral primary amines, albeit with lower conversions so far.^[29, 30] There are IREDs with (*S*)- or (*R*)-selectivity and certain motifs were suggested to determine their selectivity, but so far no systematical sub-categorization seems to be consistent.^[29] The restricted substrate scope in terms of ketone and amine pairings represents one of the most important constraints for their industrial application. However, future research is likely to identify more IREDs and variants thereof for their application at industrial scale.

Very recently, a reductive aminase from *Aspergillus oryzae* was identified to catalyze both imine formation and reduction, even at low amine:ketone ratios of 1:1 at high yields (up to 94 % conversion) and excellent optical purities (>98% ee).^[31] These reductive aminases represent an important sub-group of IREDs with unique properties for the biocatalytic preparation of chiral amines.

a) Endocyclic Imine Reduction



b) Acyclic Imine Reduction



Scheme 2.4: NADPH-dependent reduction of endocyclic - a) and acyclic imines b) catalyzed by imine reductases (IREDs). IREDs allow up to 100 % yield with high to excellent optical purities. In case of performing reductive aminations of ketone and amine pairings, the transient imine intermediate is reduced, affording primary, secondary or tertiary chiral amines, albeit with restricted scope of amine and ketone substrates. Reductive aminases represent an important sub-group of IREDs and catalyze both imine formation and reduction, which allows the reductive amination of ketones with amines at low ketone:amine ratios at quantitative yields.^[31]

2.2.3 Amine Dehydrogenases (AmDHs)

Amine dehydrogenases (AmDHs) were recently identified via engineering amino acid dehydrogenases (AADHs) for expanding their restricted substrate scope from keto acids to ketones. AmDHs and AADHs catalyze the NAD(P)H-dependent reductive amination of ketones or keto acids to amines or amino acids using ammonia as amine substrate. Search of sequence databases for motifs that had been defined on the basis of the key mutations for ketone acceptance in AADHs, revealed as well existing wild-type AmDHs.^[32] As until now all AmDHs are derived

from AADHs, there is only one type of selectivity available and the substrate scope can be expected to be restricted to compounds resembling amino acid structures.

2.2.4 Transaminases (TAs)

Transaminases (EC 2.6.1.) belong to the largest group of pyridoxal 5'-phosphate (PLP)-cofactor dependent enzymes^[33] that aside from transamination, catalyze a lot more entirely different reactions, such as decarboxylation-, aldol-, elimination- and racemization reactions.^[34] For instance, even unactivated carbon-carbon bonds can be oxidized by PLP-dependent enzymes, as shown recently.^[35] A systematic sub-categorization of PLP-dependent enzymes based on their sequence similarities or their catalyzed type of reaction was not stringently feasible. Instead, analysis of protein structures revealed that enzymes of the same type of three-dimensional structure catalyze different reactions at different carbon atoms of their substrates. Thus, sub-division of PLP-dependent enzymes was eventually based on five different fold types instead of chemistry (Figure 2.2).^[36, 37]

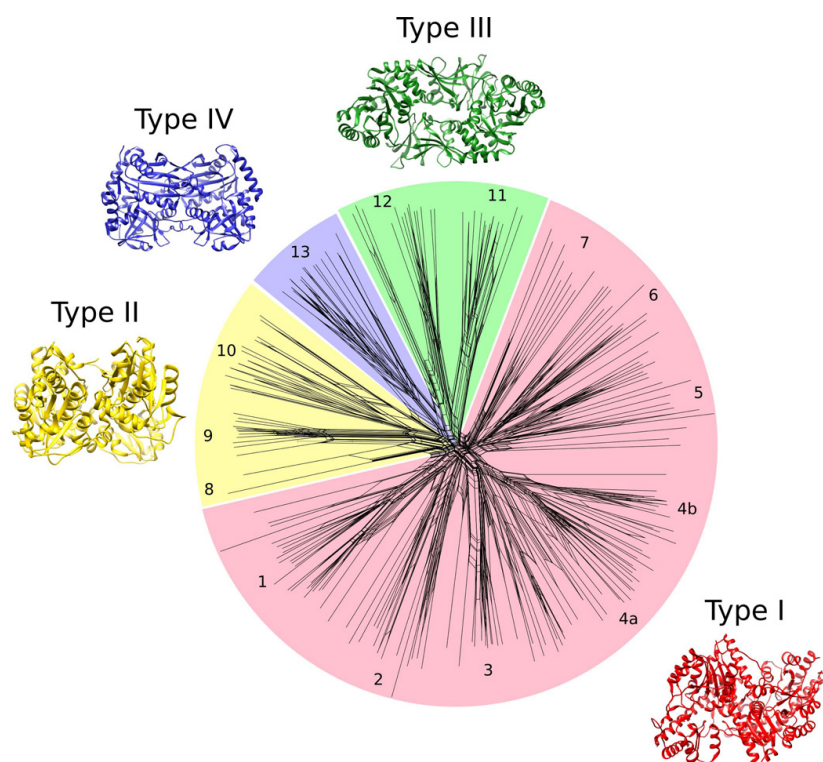


Figure 2.2: PLP-dependent enzymes exhibit different protein folds and are subcategorized based on these different fold types. Phylogenetic analysis of 204 PLP-dependent enzymes of four exemplary superfamilies. Each fold type originates from separate evolutionary ancestries resulting in entirely different protein structures. Amine transaminases are present in fold type I (commonly denoted as (*S*)-selective) amine transaminases and in fold type IV (commonly denoted as (*R*)-selective) amine transaminases. Protein engineering results from fold type IV amine transaminases are not directly transferable to fold type I transaminases and *vice versa* due to their structural differences. The figure was taken from reference [38] and was reproduced with permission from John Wiley and Sons. The red, yellow, green, and blue colored areas and protein structures belong to fold types I-IV. The small numbers 1-13 indicate individual clusters within the folds and represent groups of function specific enzymes.

There are two structurally different types of amine transaminases, fold type I (commonly denoted as (*S*)-selective) amine transaminases and fold type IV (commonly denoted as (*R*)-selective) amine transaminases.^[39] Despite their structural differences, both fold type I and IV amine transaminases possess quaternary structures most frequently composing of two homodimers. Each monomer consists of a smaller and a larger domain and possesses an active site with a covalently bound PLP-cofactor at the dimer's interface. Thus, each of the active sites at the interface of the dimers involve residues of both monomers for active site formation. The major difference of the two fold type transaminases is the fact that the site of cofactor binding is arranged in a near mirror-inverted way so that the active site lysine in fold type IV transaminases is positioned on the *re*-face and the *si*-face is exposed to the solvent and *vice versa* in fold type I enzymes.^[34]

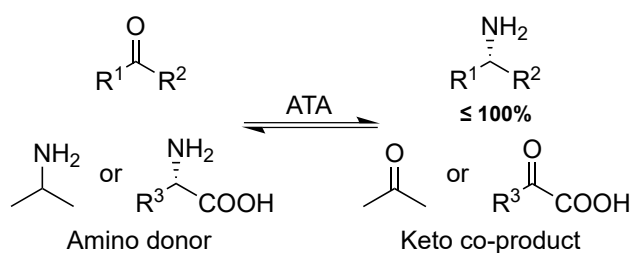
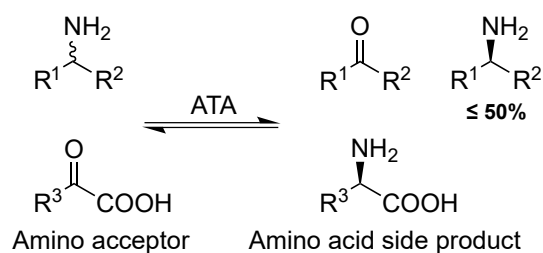
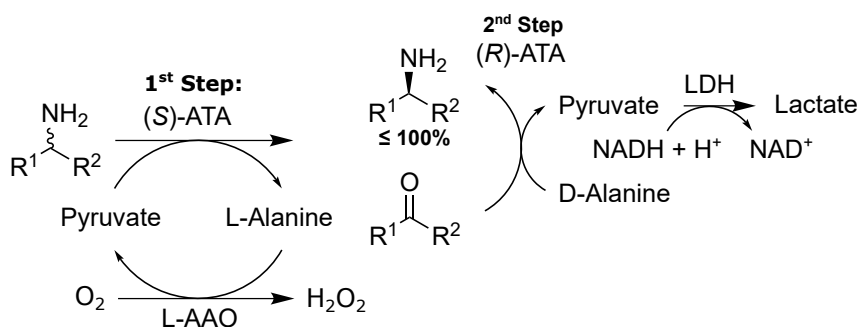
Synthesis Strategies Using Transaminases

Transaminases catalyze the transfer of an amino group of a donor amine to the carbonyl carbon atom of an α -keto acid, a ketone, or an aldehyde. This allows application of transaminases for the preparation of secondary α -chiral primary amines starting from prochiral keto-substrate synthons like it is the case for many chemical reductive approaches. However, in contrast to the chemical counterpart, the transaminase-catalyzed asymmetric amination (**Scheme 2.5a**), provides the desired chiral amine in a single step with up to 100 % yield without any need for high-pressure hydrogen supply, without need for increased temperatures and without reactive group incompatibilities except for the need for aqueous reaction conditions in most of the cases.

Apart from this asymmetric synthesis mode, transaminases are as well suitable to be used for kinetic resolution of racemic amines (**Scheme 2.5b**), by deaminating the undesired enantiomer and enriching the other one, with an inherently restricted maximum yield of 50 %, as only one enantiomer is sustained. Combination of the two aforementioned strategies in a one-pot, two-step process allows deracemization of a racemic amine with up to 100 % yield (**Scheme 2.5c**), which is in particular interesting, if the precursor keto-substrate is more difficult to access than the racemic amine and if two enantio-complementary transaminases for the desired substrate are available.

Chemo-enzymatic Processes Involving Transaminases

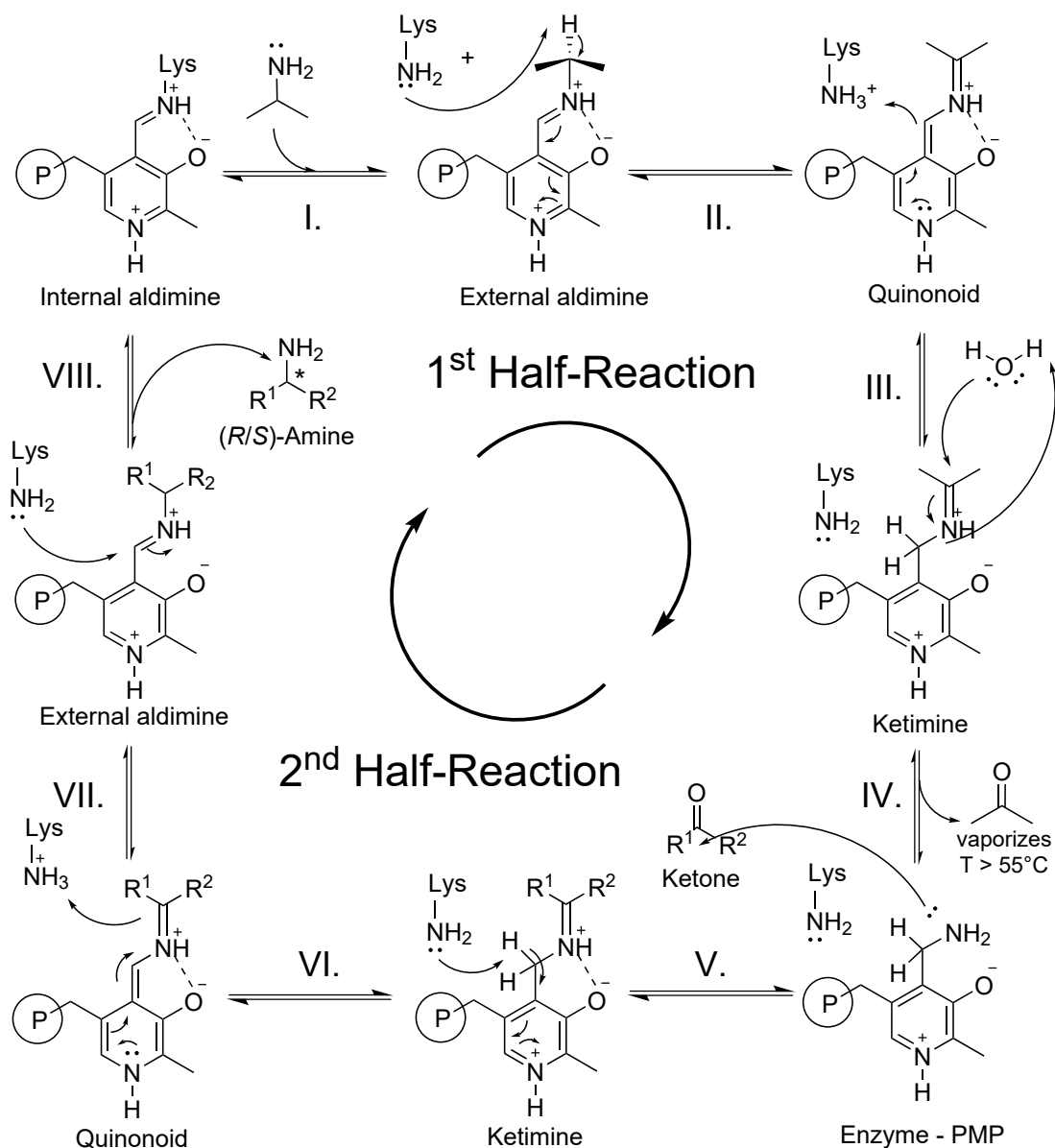
Although in the last decade many alternative enzymatic options for chiral amine synthesis were discovered that may rival transaminases in the future, transaminases will still remain attractive for industrial process applications, especially using isopropylamine as cheap amine donor substrate. Until now, transaminases represent the most mature biocatalysts for asymmetric chiral primary amine synthesis, which comes along with invaluable industrial experiences and know-how for their application at industrial scale. These findings were extensively reviewed, but go beyond the scope of this thesis.^[21, 40]

a) Asymmetric Synthesis**b) Kinetic Resolution****c) One-Pot, Two-Step Deracemization**

Scheme 2.5: Different synthesis strategies using transaminases for the preparation of α -secondary chiral primary amines. **a)** Asymmetric synthesis: The amino group of a donor amine such as isopropylamine or alanine is transferred to a prochiral keto-substrate affording the desired chiral amine with up to 100 % yield. **b)** Kinetic resolution: The desired opposite enantiomer is enriched by deaminating the undesired enantiomer using e.g. pyruvate as amino acceptor. **c)** Combination of the two aforementioned methods allows deracemization of a racemate with up to 100 % yield using two enantio-complementary transaminases in a one-pot, two-step process.

Mechanism of Transamination and Shift of the Equilibrium

Transaminases operate in two reversible half-reactions, each involving two different pairs of educts and products but comprising identical steps exhibiting ping-pong-bi-bi kinetics. In (**Scheme 2.6**) an exemplary reaction cycle of an (*R*)- or (*S*)-selective amine transaminase using isopropylamine as amine donor in asymmetric synthesis is depicted. A disquisition on the detailed reaction mechanism can be retrieved from references [34, 41] but also from [39, 42]. In the past three years, the reaction mechanism of transaminases and the mechanism of dual substrate recognition were further supported by means of density functional theory calculations.^[43, 44]



Scheme 2.6: Exemplary reaction mechanism of an engineered transaminase variant catalyzing the asymmetric synthesis using isopropylamine as amine donor. The co-product acetone is removed by reduced pressure and elevated temperatures to shift the equilibrium in the desired direction. The symbol $\textcircled{\text{P}}$ represents the phosphate group of PLP.

As can be seen from the scheme above, the transamination reaction represents an equilibrium reaction, which is relevant for its application for industrial purposes to achieve high or full conversions. Many methods were developed to displace the equilibrium to the side of the products, such as the application of the amine donor in excess, removal of the desired product or the co-product by extraction, vaporization or by degrading the co-product in biochemical cascade reactions.^[40]

The most prominent amine donors are alanine and isopropylamine. The former one inevitably requires application of pyruvate-degrading enzymes due to the unfavorable equilibrium situation, which is in most of the cases achieved by combination with a lactate dehydrogenase (LDH) and an NADH-cofactor recycling system, for instance a glucose dehydrogenase (GDH).^[45] The application of isopropylamine as amine donor is very attractive, as it is cheap and can be applied in large excess without the need for expensive co-enzymes. Additionally, the application of isopropylamine as amine donor facilitates the downstream process, as the reaction side-product is acetone, which can be easily removed by vaporization. Removal of acetone is as well feasible by nitrogen gas-flow or reduced pressure,^[40, 46] which was recently rationalized.^[47] The authors identified the specific thermodynamic equilibrium constant of the reaction of interest, as well as the volatility of the keto-substrates as critical parameters for the efficiency of *in-situ* acetone removal.^[40, 47] However, the major limitation for the application of isopropylamine remains the suitability of the biocatalysts regarding their stability and their sufficient activity for the amine donor.

Substrate Scope Limitation of Wild-Type Transaminases

The natural substrate scope of transaminases constitutes a major constraint for the synthesis of structurally diverse chiral amines. Especially, the accommodation of substrates with two large substituents encompassing the carbonyl carbon atom is generally not feasible for any wild-type transaminase known until now. In 2002, Shin *et al.* investigated the active site of the fold type I *Vibrio fluvialis* JS17 transaminase and finally proposed a binding model consisting of a small and a large binding pocket (indicated by L and S, respectively), that was conform to their experiments (**Figure 2.3**).^[48, 49] While the large binding pocket shows dual recognition for both the accommodation of hydrophobic groups up to n-hexyl and a carboxylate functionality, the small binding pocket was found to be strictly restricted to substituents no longer than an ethyl group.^[48, 49]

Although, it is actually questionable, if this binding model can be directly transferred to all fold type I and fold type IV amine transaminases, it has been widely accepted as general binding model for all transaminases.^[21] In fact, there are only rare exceptional literature reports of wild-type transaminases that have detectable activities against substrates with propyl moieties to be accommodated in the small binding pocket.^[50] Nevertheless, even the acceptance of propyl moieties does not allow the synthesis of many pharmacologically interesting but larger amines by application of transaminases.

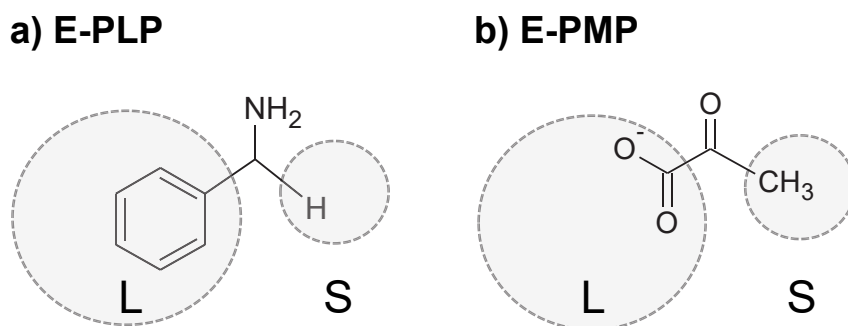


Figure 2.3: Substrate binding model of two binding pockets proposed by Shin *et al.*^[48] for the fold type I transaminase of *Vibrio fluvialis*.^[48] The large binding pocket (L) provides dual substrate recognition for the accommodation of both carboxylic groups and hydrophobic groups of the size of up to n-hexyl moieties, while the small binding pocket (S) is restricted to accommodate moieties no longer than an ethyl-group. Adapted from reference [49], with permission from Elsevier.

Protein-Engineering of Transaminases for Substrate Scope Extension

Protein Engineering is a large scientific research field that is engaged in the development and optimization of new biocatalysts by directed evolution or rational bioinformatic means.^[51] Aside from enhancing the thermostability, the enantioselectivity and the stability against organic solvents, particularly the extension of the natural substrate scope to afford tailor-made biocatalysts are central intentions of protein engineering.

In case of fold type IV transaminases there is an ultimate example of successful protein engineering that finally provided an efficient catalyst for the industrial scale production of the above-mentioned antidiabetic drug sitagliptin at 45 °C, 1 M isopropylamine, 0.5 M ketone, 50 % DMSO yielding 92 % conversion and 99.95 % e.e., demonstrating the synthetic potential of transaminases.^[52] The resulting biotechnological process eliminated the dependency on heavy metal catalysis, made high-pressure hydrogenation equipment dispensable and thus allowed to decrease the total manufacturing costs due to a 10 – 13 % increased overall yield and a 53 % increased overall productivity compared to the chemical asymmetric hydrogenation process.^[52, 53] The protein engineering effort to do so was tremendous and involved a substrate walking modeling approach with a truncated substrate, in which the large trifluorobenzyl group was substituted by a methyl group (**Figure 2.4**), followed by ten iterative rounds of directed evolution under successively increased demanding conditions. In total, 36 480 variants were screened, by analyzing each reaction with liquid chromatography-mass spectroscopy (LC/MS) or achiral HPLC. The final transaminase variant of the (*R*)-selective ATA-117 from *Arthrobacter* sp. for the synthesis of sitagliptin contained 27 mutations,^[52] which equals 8 % of its entire sequence.^[54]

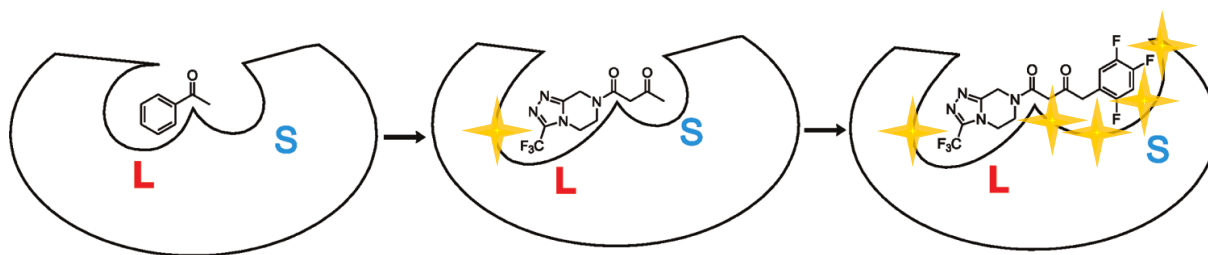


Figure 2.4: Substrate walking approach for opening the active site for prositagliptin. A truncated precursor substrate in which the large trifluorobenzyl group had been substituted by a methyl group to subsequently enlarge the large binding (L) pocket was applied, before enlarging the small binding pocket (S) by screening against the entire, actually desired substrate. The figure was adapted from Mathew and Yun^[55] with clearance from ACS Publications.

In contrast to this outstanding example for fold type IV transaminases, only few reports about successful protein engineering for bulky substrate acceptance of fold type I transaminases (commonly denoted as (*S*)-selective) were published until this project started. All of these endeavors were based on *Vibrio fluvialis* transaminase to expand its small binding pocket for the accommodation of propyl moieties,^[56, 57] methyl alcohols for the synthesis of phenylglycinol^[56] or *sec*-pentyl moieties for the synthesis of imagabalin.^[58] However, until then no general solution for the conversion of bulky substrates, such as sitagliptin, was available for fold type I transaminases.

3 Enzyme Screening Assays *versus* Instrumental Analytics

In-depth investigation of each single enzyme variant by determining reaction conversions via conventional analytical methods including HPLC or GC-MS analysis as conducted by Savile *et al.*^[52] is extremely laborious, time consuming and expensive and thus hampers the productivity in protein engineering, not to mention the extraordinarily high demand for HPLC and GC laboratory equipment.^[59] Therefore, screening assays are applied to convert enzyme activities into a detectable signal such as temperature changes, spectral changes, change of turbidity, change of electrochemical properties or microbial growth, in order to estimate the enzyme's activity without entire analytics. Depending on the time effort for screening an individual mutant, assays are categorized in low- to high-throughput assays. Apart from the time effort, also screening cost and the amount of volume in the assay reaction that is necessary for screening plays an important role for their categorization as high-throughput assay. Particularly when directed evolution^[60, 61] is applied, library sizes increase exponentially. For instance substitution of one, two or three random amino acids in a 100 residues-protein results in about $1.9 \cdot 10^3$ (for one substitution), $2.0 \cdot 10^6$ (for two substitutions), $1.3 \cdot 10^9$ (for three substitutions) unique protein-sequences without consideration of redundant or truncated sequences.^[60] Simultaneous saturation of three amino acid positions at once by NNK codon usage, results in about $3.3 \cdot 10^4$ possible DNA-sequences.^[62] For screening 95 % of all these individuals an oversampling factor of three has to be multiplied with the number of possible combinations,^[62] provided the composition of the library is equally distributed, which leads to even bigger library sizes. All these aspects emphasize the need of fast and facile screening methods.

Until now, many different types of screening methods, all entailing different advantages, disadvantages and requirements, were developed. Most of them, require inoculation, cell growth, cell-lysis and removal of cell debris in subsequent steps in microtiter plates, which allows screening of up to 96 different variants per plate. However, this type of screening assay provides only moderate throughput compared to high-throughput assays, such as selection-based assays, which are virtually restricted by transformation efficiency and library generation methods, as only variants possessing the desired feature are able to survive and breed. Methods such as in vitro compartmentalization, or strategies involving cell surface displays, allow handling library sizes of approximately 10^9 individual mutants,^[61] but require microfluidic or fluorescence-activated cell sorting (FACS) equipment and fluorogenic enzyme products for detection. Agar plate-based assays allow at least one order of magnitude higher throughput than microtiter plate-based assays, as the colonies can be directly screened on the agar plate or on nitrocellulose membranes,

respectively. Thus, many time-consuming steps such as inoculation or removal of cell debris are not applicable, which increases the throughput.

3.1 Principle Screening Options for Transaminases

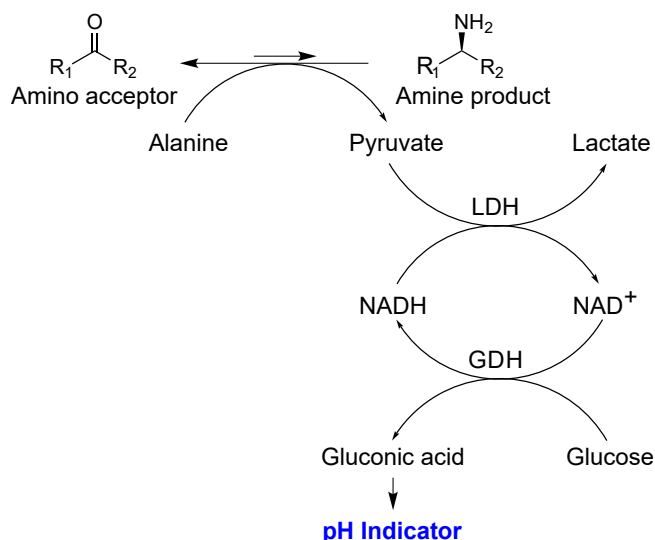
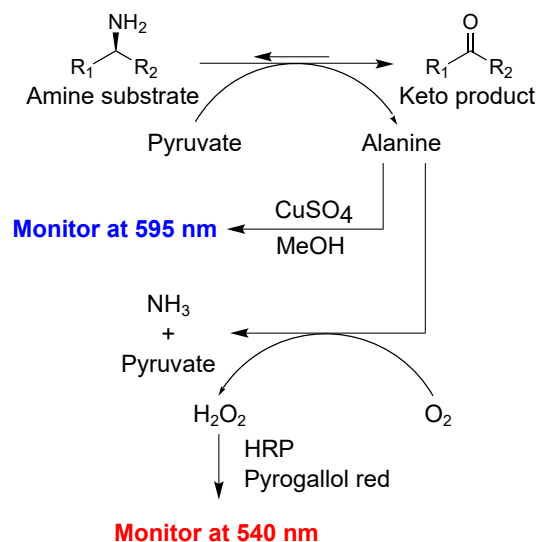
In general, assays for transaminases detect the conversion of one of the two substrate pairs, which is in most of the cases alanine or pyruvate. Alternatively, there are assays that allow the detection of the conversion of certain other substrate pairs that are not keto-acids or amino acids. However, these assays usually make specific demands on these substrates or products, which prohibits to freely select both substrates simultaneously for screening. Accordingly, an independent simultaneous selection of two desired substrates is only feasible if an assay for one of the two substrates is available or conventional analytics are applied. Until the start of this project the vast majority of assays for transaminases were only available as microtiter plate (MTP) assays with the exception of very few assays with higher throughput but restricted applicability.^[63] The following paragraph demonstrates what type of screening options are available for transaminases.

3.1.1 Transaminase Assay Principles

Assaying Keto-Acids or Amino Acids

Several assay methods for transaminases are available for the detection of keto-acids or amino acids formed upon transamination in asymmetric synthesis or kinetic resolution, respectively. For the asymmetric synthesis with transaminases using alanine as amino donor substrate coupled assays were developed to detect pyruvate formation (**Scheme 3.1 a**). This was realized for instance by converting pyruvate to lactate using a lactate dehydrogenase (LDH) combined with a glucose dehydrogenase (GDH) for NADH recycling, which eventually causes a decreasing pH upon gluconic acid formation. A suitable pH-indicator allows a spectrophotometric read-out.^[64]

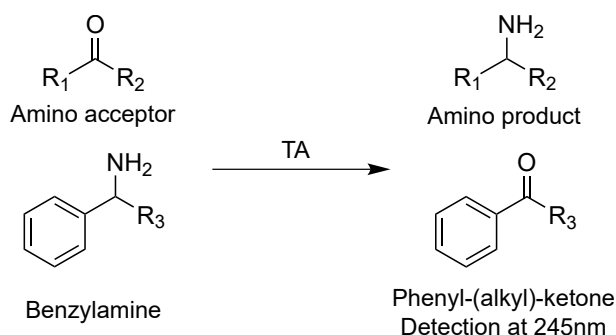
For kinetic resolution using pyruvate or other keto acids as amino acceptor substrates, assays were developed to monitor amino acid formation. One of the first assays available for transaminases features the detection of α -amino acids by formation of blue copper complexes (**Scheme 3.1 b**)^[65] with the drawback of a relatively high background signal in crude lysate applications caused by cellular amino acids.^[40] Similarly, amino acid oxidase coupled assays were developed for the detection of primarily alanine formed upon transaminase-catalyzed kinetic resolution of a racemic amine of interest by detecting hydrogen peroxide formation using a horseradish peroxidase in combination with a suitable chromogenic substrate (**Scheme 3.1 b**)^[66] Major disadvantage of this type of assay is that for L- or D-alanine separate enzymes with respective selectivities have to be applied. Both of them increase the screening cost, as particularly L-amino acid oxidases are challenging to be heterologously over-expressed.^[67, 68]

a) Asymmetric Synthesis**b) Kinetic Resolution**

Scheme 3.1: Selected assays for screening transaminase-catalyzed reactions using alanine as amine donor a) or pyruvate as amino acceptor b).

Direct Assays

Direct assays provide several major advantages compared to coupled assays, as one of the educts or products can be directly monitored without additional assay enzymes or ingredients, which simplifies the screening and is much more cost efficient. The most prominent direct assay for transaminases represents the acetophenone assay, which allows to screen for activity against amines having an aromatic group in α -position and thus have significantly different spectrophotometric properties in the UV range compared to the resulting keto-products (Scheme 3.2).^[69]



Scheme 3.2: The acetophenone assays allows screening of transaminases in kinetic resolution mode by spectrophotometrically detecting the formation of the phenone product in the UV range at around 245 nm.

3.1.2 Towards High-throughput Options for Transaminases

For screening applications of transaminase libraries comprising several thousands or even more individual transaminase variants assay methods with significantly higher throughput than MTP-based assays are of great interest. However, until this research project started, the only example for a high-throughput transaminase screening method was not applicable for other targeted substrates[†], as a screening in kinetic resolution was only feasible due to the fact that the keto product (substituted tetralone) forms a colored dye upon air exposure (**Scheme 3.3**). Thus, cell colonies could be directly transferred from petri dishes to nitrocellulose membranes for screening in solid phase leading to a thermostable transaminase from *Arthrobacter citreus* for aminotetraline synthesis.^[63]



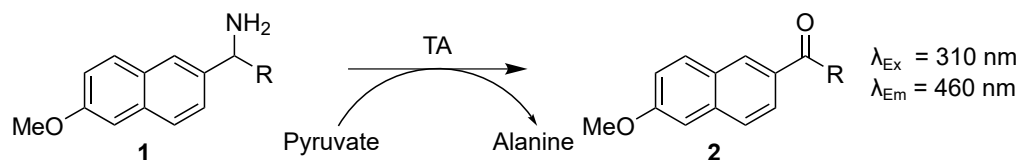
Scheme 3.3: The tetralone assay can be used for high-throughput screening of transaminases variants on nitrocellulose membranes (solid phase assay) for activity against substituted aminotetraline. The resulting tetralone product forms a dye when exposed to air. The assay is restricted to aminotetraline and can not be simply applied for protein engineering against other target ketones. The scheme was adapted from reference [63].

Further assays, that rely on the same principle where published later, when this project was already in progress: O'Reilly and co-workers reported on the application of *ortho*-xylenediamine dihydrochlorid as amine donor substrate that forms a colored precipitate via spontaneous polymerization of the aromatic isoindole formed upon transamination.^[70] Similarly, Hailes and co-workers reported on the application of 2-(4-nitrophenyl)ethan-1-amine as amine donor that forms a red precipitate upon transamination.^[71] Both methods are suggested as a solid phase assay screening option on nitrocellulose membranes, however with two major disadvantages: The amine donors are no natural substrates for transaminases and have to be compatible with the screening scaffold. Particularly, if the target substrate is structurally very different from the amine donors, it is unclear if mutations will be found that provide activity for both the amine donor and the targeted keto substrate. Additionally, there is a false positive staining visible in controls without keto substrate of interest, indicating that the amine group is transferred also on other cell contained keto compounds than the actually targeted substrate.^[71]

This gap in existing high-throughput assays for transaminases was intended to be closed with our further below introduced glycine oxidase assay. In contrast to the above described assays, the glycine oxidase assay involves glyoxylate as natural and small transaminase substrate that is converted to glycine using any amino donor of interest without significant false positive signal and is as well available for screening colonies on nitrocellulose membranes.

[†]Theoretically, aminotetraline could serve as amine donor for screening against other keto substrates of interest. However, aminotetraline is not a natural substrate for transaminases, which hampers its application for other screening purposes. In addition to that, a background signal can not be excluded, when the amino group is transferred to other cell contained ketones or keto acids instead on the desired keto substrate of interest.

A different approach was reported in March 2015 by Fessner and co-workers that is based on the conversion of 1-(6-methoxynaphth-2-yl)alkylamines with variable moieties that is suitable for a substrate walking approach for increasing the size of the small binding pocket of transaminases.^[72] Upon transamination the fluorophore acetonaphthone is released (**Scheme 3.4**), similar to the acetophenone assay, but with higher sensitivity and further possible high-throughput options. Additionally, several wild-type transaminases were shown to be active against the amine donor.^[72] Nevertheless, the assay is substrate dependent and to the best of our knowledge, no FACS or microfluidic based screening procedure has been elaborated and applied for transaminases, yet.



Scheme 3.4: Fluorometric assay for transaminases. As amine donor 1-(6-methoxynaphth-2-yl)alkylamines (**1**) are applied. These are converted into the fluorophore acetonaphthone (**2**) upon transamination. The assay provides higher sensitivity than the acetophenone assay and is suitable to expand the small binding pocket by enlarging the alkyl substituent and application of a substrate walking approach. The assay principle is amenable for FACS or microfluidic based screening procedure, which to the best of our knowledge has not yet been elaborated for transaminases. The scheme was adapted from reference [72].

4 Protein-Engineering of *Ruegeria* sp. TM1040 Transaminase

4.1 Requisite Substrates and Project Strategy

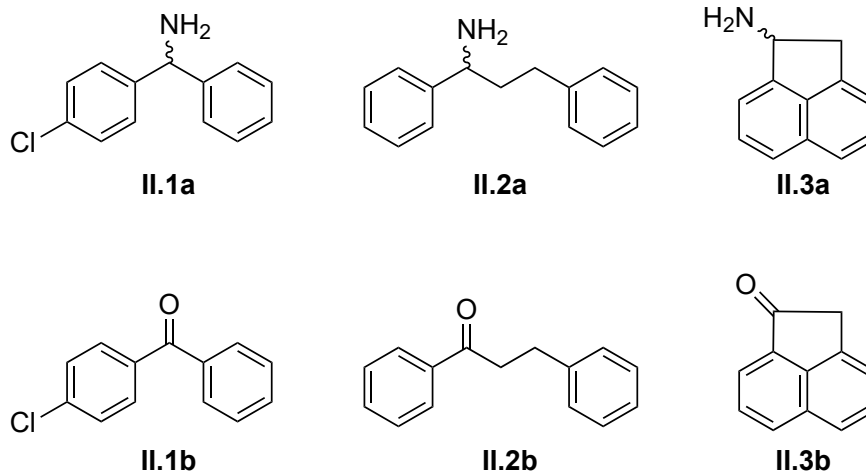
In this thesis the objective was to develop transaminases, in particular transaminases of fold type I, that allow the conversion of substrates with two bulky substituents next to the chiral center. In order to evaluate and to evolve the ability of potential transaminase candidates to do so, five structurally different test substrate pairs were conceived by the company of Roche (**Figure 4.1**).

Based on their structure, the compounds can be divided into three different groups and the corresponding results were accordingly published in three publications. The first three amine/ketone substrate pairs (**II.1-II.3**) predominantly consist of aromatic groups: Two phenyl rings adjacent to the carbonyl carbon atom, one of them *para*-substituted with a chlorine atom (**II.1**), two phenyl rings adjacent to the carbonyl carbon atom, one of these phenyl rings is separated from the carbonyl carbon atom by a flexible aliphatic linker consisting of two carbon atoms (-CH₂-CH₂-) (**II.2**) and the last compound consisting of two fused benzene rings (naphthalene), where C1 and C8 are connected via two aliphatic carbon atoms, one of them carrying the amino group or the carbonyl oxygen, respectively (**II.3**). All of these three compounds are relatively planar. The latter one is definitely most planar, while the middle one is most flexible and thus can as well adopt non-planar conformations. The two phenyl rings of the first amine substrate are able to rotate as well.

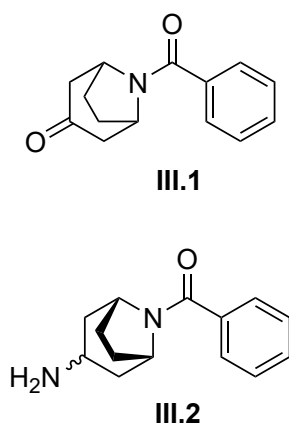
The other two substrate pairs differ significantly from the aforementioned substrates. Compound (**IV**) carries only one phenyl ring on one side, but having a spatially bulky, aliphatic tert-butyl moiety on the other side. Compound (**III**) is a bicyclic bridged compound of significant three-dimensional bulkiness. The corresponding amine can be endo or exo relative to the smallest bridge.

Due to the structural differences of the model substrates, it was expected that different solutions would be necessary to accommodate the substrates in the active-site, which might lead to a set of versatile enzyme variants for the conversion of other bulky and structurally diverse pharmaceutically interesting compounds.

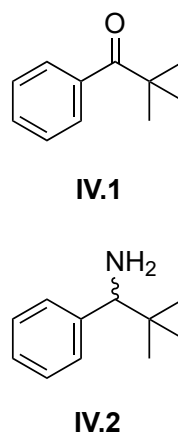
Article II



Article III



Article IV



Scheme 4.1: Target chiral amine products and their corresponding precursor keto substrates addressed in this thesis. The numeration of the compounds is based on the numbering of the respective articles:

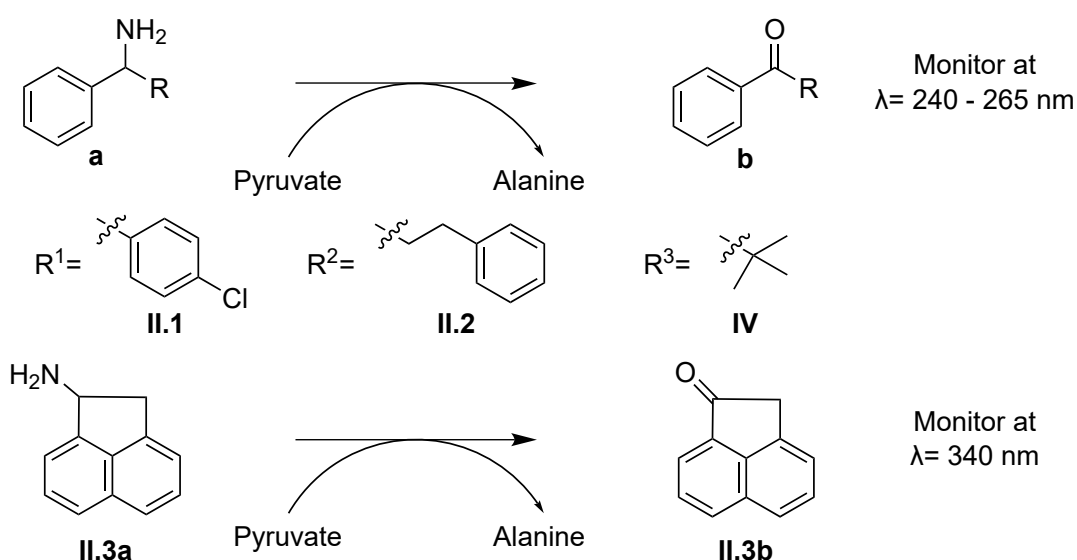
- | | |
|--|--|
| II.1 a) 1-(4-chlorophenyl)-1-phenyl-1-aminomethane, | II.1 b) (4-chlorophenyl)-phenyl-methanone, |
| II.2 a) 1,3-diphenyl-1-aminopropane, | II.2 b) 1,3-diphenylpropan-1-one, |
| II.3 a) 1,2-dihydroacenaphthylen-1-amine, | II.3 b) 2H-acenaphthylen-1-one, |
| III.1) 8-benzoyl-8-azabicyclo[3.2.1]octan-3-one, | III.2) 3-amino-8-benzoyl-8-azabicyclo[3.2.1]octane, |
| IV.1) 2,2-dimethyl-1-phenyl-propan-1-one, | IV.2) 2,2-Dimethyl-1-phenylpropan-1-amine. |

4.2 Screening Assays for the Target Substrates

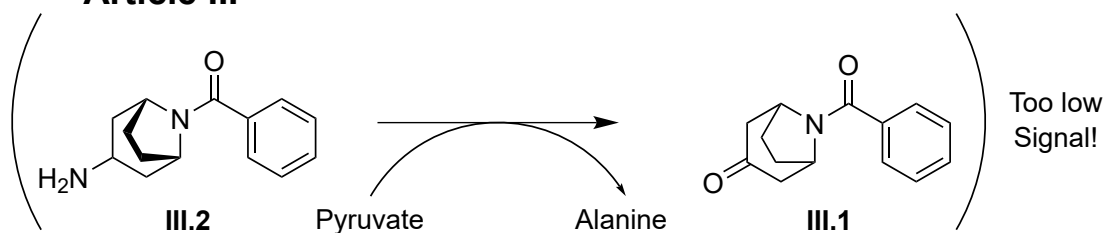
Before any protein engineering experiments could be carried out, it was important to have suitable screening assays available. These assays were not only supposed to allow quick evaluation of single point mutations and site-saturation mutagenesis experiments, but were also supposed to be utilized for substrate profiling to identify suitable starting transaminase scaffolds.

As four of the five requisite substrates carry aromatic substituents next to the carbon atom with the targeted amino group, a direct assay for kinetic resolution of the corresponding racemic amines based on different absorbance spectra of the amines and their corresponding ketones in the UV range could be established (**Scheme 4.2**). Preparation of calibration curves and determination of absorption coefficients allowed to determine specific activities in kinetic resolution for four of the five reactions. (These experiments had been assigned to the area of responsibility of I.V.P.).

Article II & IV



Article III

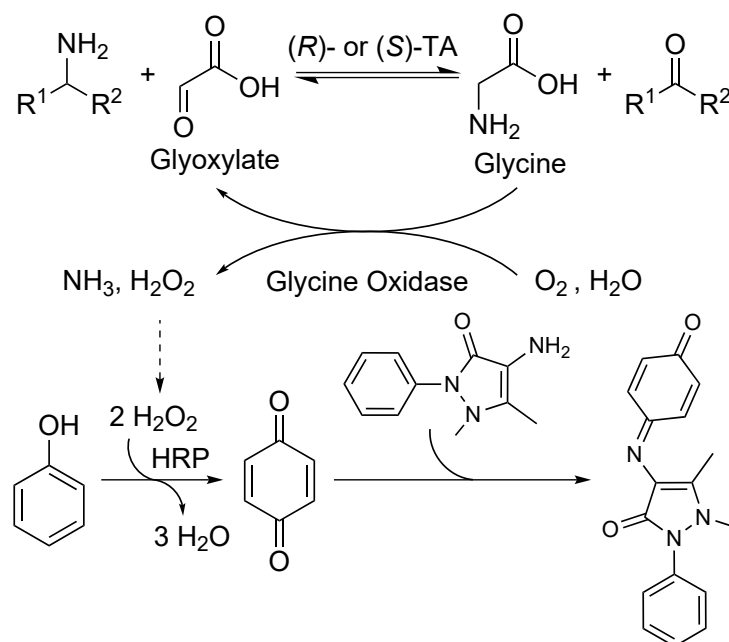


Scheme 4.2: Direct microtiter plate-based assays for screening in kinetic resolution are available for four out of five target substrates. The last substrate pair had a too low difference of their spectra of absorbance, so that a different type of assay had to be adapted.

For compounds **III.1** and **III.2** no sufficient difference in absorbance was found, which required us to establish another type of assay for these substrates. Furthermore, the direct assays are as denoted above restricted to microtiter plate-based throughput formats. For directed evolution of our transaminase scaffolds an assay with higher throughput was of great interest to screen higher library sizes.

4.2.1 Adaption of the Glycine Oxidase Assay

During my master-thesis an alternative assay for transaminases amenable to high-throughput screening on nitrocellulose membranes was developed and a prove of principle for the agar plate assay was demonstrated. This assay allows screening either (*R*)- or (*S*)-selective transaminases for activity against variable amine substrates in kinetic resolution. Instead of pyruvate, the one carbon atom smaller aldehyde acid glyoxylate is applied as amino acceptor. This is advantageous, as the amino side-product glycine is non-chiral and thus no separate L- or D-amino acid oxidases are required. Glycine will be detected by a glycine oxidase, producing hydrogen peroxide that in turn is used to synthesize a quinone imine dye (**Scheme 4.3**). This way, also substrate pairs without different absorbance spectra can be assayed with two additionally coupled enzymes. As glycine represents a natural substrate for most transaminases, the amine acceptor is applicable in many cases and due to its small size incompatibilities with the targeted substrate seem to be unlikely. Further detailed information on the choice of the horseradish peroxidase substrate are given in our book chapter and in **Article I**.



Scheme 4.3: Glycine oxidase assay: Application of glyoxylate as natural amino acceptor substrate allows screening either (*R*)- or (*S*)- selective transaminases for activity against different variable amine substrates. Production of achiral glycine is then followed by oxidation and hydrogen peroxide formation leading to the formation of a red quinone imine dye. Toxic phenol can be substituted by vanillic acid as demonstrated in the supporting information of **Article I**. The scheme was reproduced from our article reference [73] with permission from ACS. The article is available under ACS AuthorChoice license <http://pubs.acs.org/doi/full/10.1021/ac503445y>.

Although the assay principle was already shown in solid phase, the transformation efficiency was too low for directed evolution, as the glycine oxidase gene was not available in a plasmid that is compatible with the other plasmids containing the genes for our in-house transaminases.* Thus, for application of the solid phase assay in directed evolution experiments the glycine oxidase gene was subcloned into a compatible plasmid. Furthermore, the glycine oxidase assay was supposed to be applied for microtiter plate-based monitoring of activities against substrate (**III**) for that no direct assay was feasible. In order to do so, the liquid phase assay had to be elaborated for substrate profiling and later as well for quantification of the amount of glycine formed, which even allowed the determination of specific activities in liquid phase (**Article III**). Furthermore, the screening protocol of the agar plate high-throughput assay had to be finalized to make it more robust to evolve future transaminase variants for increased activity. All experiments to demonstrate the applicability of the assay both in liquid phase and solid phase described in (**Article I**) were designed and conducted within the scope of this PhD-project.

Microtiter Plate Assay Elaboration

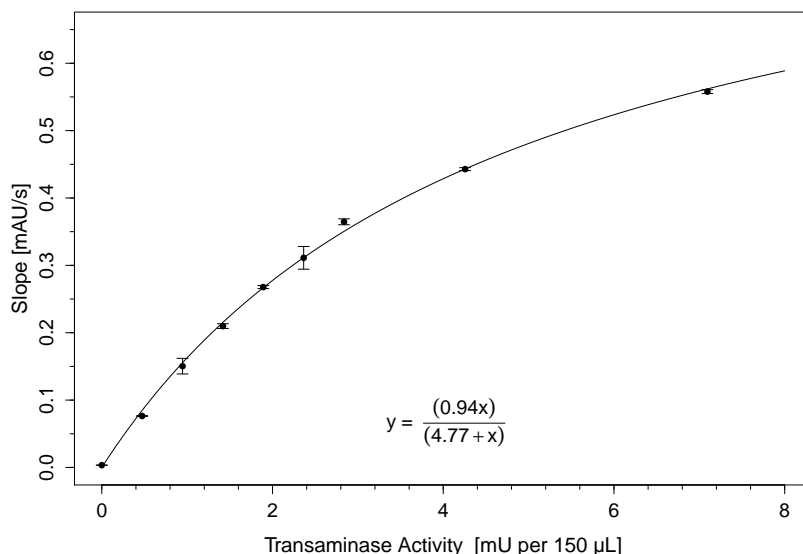
The microtiter plate assay was calibrated by application of glycine standards and end point measurements of absorbance at 498 nm, which revealed a linear range up to 0.67 mM (Supporting Information of **Article I**). To investigate the dynamic range of the assay involving continuous glycine formation, sequential dilutions of a purified (*R*)-selective transaminase were applied and screened against racemic α -phenylethylamine by following the increase of absorbance at 498 nm (**Scheme 4.4**).

For low transaminase activities a nearly linear relationship between the observed initial rate and the amount of transaminase activity in the assay has been found. The nonlinear relationship for higher transaminase activities can be explained by the fact that the transamination reaction is no longer the rate-determining step and the amount of assay enzymes has to be increased in turn to guarantee a faster downstream conversion of glycine to form the quinone imine. Thus, it was demonstrated that the assay distinguishes different transaminase activities, provided the amount of assay enzymes is adapted. Controls without transaminase gave a negligible slope, which may be explained by autocatalytic quinone imine dye formation.

Later in the project, the linear range of the assay was expanded by increasing the amount of glycine oxidase and for determination of specific activities always two dilutions of the same variant were applied to certify that at least the lower transaminase concentration is in the linear range.

As a next step, it was demonstrated that the glycine oxidase assay is suitable to screen different transaminases in crude lysate for the acceptance of different amines by screening 15 different wild-type transaminases (supporting information of **Article I**) by application of the glycine oxidase assay and comparison of the results with the data derived by screening using the direct acetophenone assay under identical conditions. After expression, lysis and screening for activity for (*R*)- and (*S*)- α -phenylethylamine using the two assays under identical conditions, volumetric

*Compatible plasmids have independently regulated origins of replications, which is crucial to achieve high enough transformation efficiencies transforming the ep-PCR libraries.



Scheme 4.4: Relation between the observed initial rate in the glycine oxidase assay and the actual transaminase activity applied. A purified (*R*)-selective transaminase was sequentially diluted and screened against racemic α -phenylethylamine. As long as the transaminase activity is low enough, which is realized by corresponding dilutions of the sample, the assay signal is almost linear to the activity. The scheme was reproduced from our article reference [73] with permission from ACS. The article is available under ACS AuthorChoice license <http://pubs.acs.org/doi/full/10.1021/ac503445y>.

activities for each transaminase duplicate were calculated based on the direct acetophenone assay and were compared with the slopes derived from the glycine oxidase assay. All transaminases that have been found active against (*R*)- or (*S*)- α -phenylethylamine in the direct photometric assay were also found active in the glycine oxidase assay, which showed that the liquid phase assay was applicable for screening libraries in crude lysate. As screening in crude lysate causes high deviations, only rough comparison between the data and no quantitative correlation was made (**Figure 4.1**).

		Acetophenone-	GO-Assay	
(R)-Selective	AspFum	+	++	(R)-PEA
	AspOry	+	++	
	AspTer	+	+	
	ATA117	+	++	
	GamPro	+	+	
	JanSp	+++	+++	
	LabAle	+	++	
	MycVan	+	+++	
	NeoFis	+	++	
	RhiEtl	+++	++++	
(S)-Selective	3I5T	0	0	(S)-PEA
	3FCR	0	0	
	Cvi	0	0	
	Vfi	0	+	
	3HMU	+	+	
(R)-Selective	AspFum	0	0	(S)-PEA
	AspOry	0	0	
	AspTer	0	0	
	ATA117	0	0	
	GamPro	0	0	
	JanSp	0	0	
	LabAle	0	0	
	MycVan	0	0	
	NeoFis	0	0	
	RhiEtl	0	0	
(S)-Selective	3I5T	++	++	(S)-PEA
	3FCR	+	++	
	Cvi	+++	+++	
	Vfi	++++	++++	
	3HMU	++++	++++	
		Activity	Activity	

Figure 4.1: Substrate profiling results of 15 different transaminases (supporting information of Article I) that were screened for the acceptance of (R)- and (S)- α -phenylethylamine (PEA) in crude lysate using the glycine oxidase assay opposed to results obtained by screening with the acetophenone assay under identical conditions. The symbols 0 (no activity), +, ++, +++ and ++++ (very high activity) exemplify the amount of activity that was detected by the respective assays. The figure was reproduced from our article reference [73] with permission from ACS. The article is available under ACS AuthorChoice license <http://pubs.acs.org/doi/full/10.1021/ac503445y>.

Solid-Phase-Screening

The idea of an agar plate assay is to directly apply the whole cell colonies for growth, expression, lysis and screening on a solid-support after transformation instead of picking colonies for inoculation in microtiter plates, which facilitates the screening procedure and increases the throughput. A detailed disquisition on the procedure of the agar plate assay can be found in **Article I** and in our book chapter.

To demonstrate that the solid phase assay is applicable under realistic screening conditions, several experiments are reported in **Article I**. Among those, there are experiments with mixtures of cells containing genes coding for different transaminases that were plated out for colony growth and screening on nitrocellulose membranes. For these transaminases the following different volumetric activities had been determined in the prior microtiter plate screening using the acetophenone assay: 3HMU-transaminase (16 U/mL), 3FCR-transaminase (0.4 U/mL) and 3GJU, which was not active or below detection limit. In the agar plate screening experiments the different activities could be discriminated as expected by two different staining intensities of colony mixtures having expressed 3FCR or 3HMU transaminases and slightly colored colonies *versus* uncolored colonies for mixtures of 3FCR and 3GJU (**Figure 4.2**).

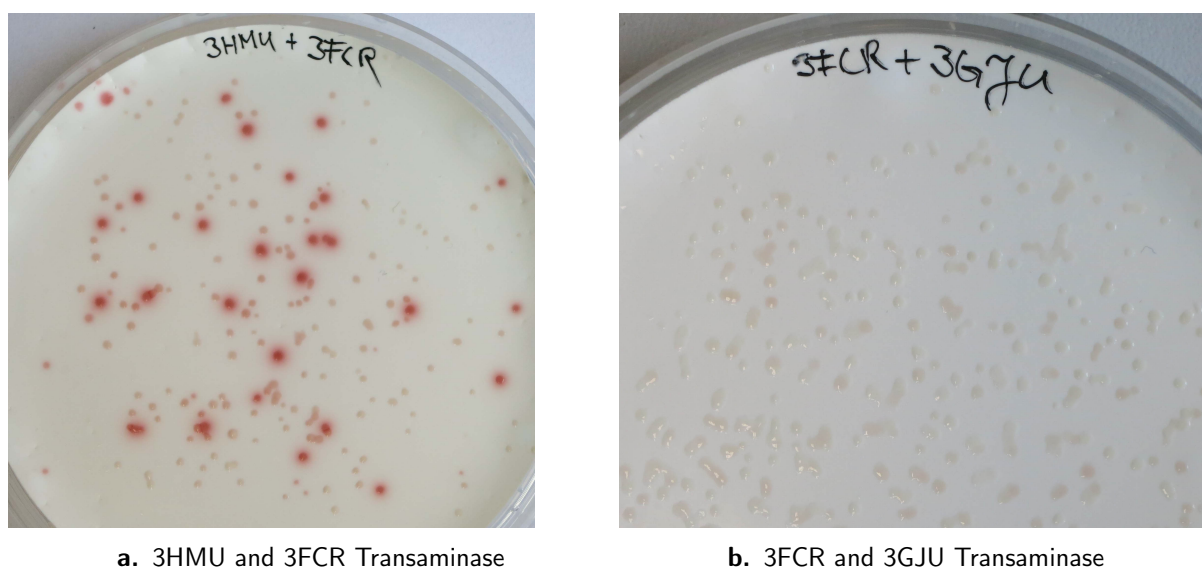


Figure 4.2: Proof of principle of the agar plate assay to demonstrate discrimination of different transaminase activities. The figure was reproduced from our article reference [73] with permission from ACS. The article is available under ACS AuthorChoice license <http://pubs.acs.org/doi/full/10.1021/ac503445y>. In the prior liquid phase screening volumetric activities for (*S*)- α -phenylethylamine were determined for 3HMU (16 U/mL), 3FCR (0.4 U/mL) and 3GJU (not active or below detection limit) by the direct acetophenone assay. After incubation of the membranes with colonies having expressed 3HMU and 3FCR (a.) showed two different staining intensities, while in case of 3FCR and 3GJU transaminase (b.) only slightly colored and uncolored colonies were found.

Importantly, negative controls were included as well: Active transaminases were screened on assay plates containing all necessary ingredients but without amine substrate and inactive variants screened on assay plates with α -phenylethylamine, which resulted in both cases in no staining of the colonies (**Article I**, and supporting information).

Furthermore, in (**Article I**) insights into ongoing directed evolution experiments were granted. Screening an ep-PCR library of the 3HMU transaminase against (*S*)- α -phenylpropylamine in solid phase allowed discrimination of active from inactive colonies, which was certified by a microtiter plate screening using the direct acetophenone assay. However, in this project a different scaffold was in our focus for protein engineering for the acceptance of our requisite substrates. Thus, the variants of 3HMU were not further investigated. Instead, experiments for the validation of the quality of an ep-PCR library based on the 3FCR_59W_87F_152F_231A variant were shown in the supporting information of (**Article I**). The library was screened against the standard transaminase substrate (*S*)- α -phenylethylamine to investigate how many variants are active or inactive in the library, which resulted in various different staining intensities depending on the duration of incubation of the membranes on the assay plates (**Figure 4.3**). These experiments implied that the glycine oxidase agar plate assay, is applicable as a prescreening method in our project for directed evolution.

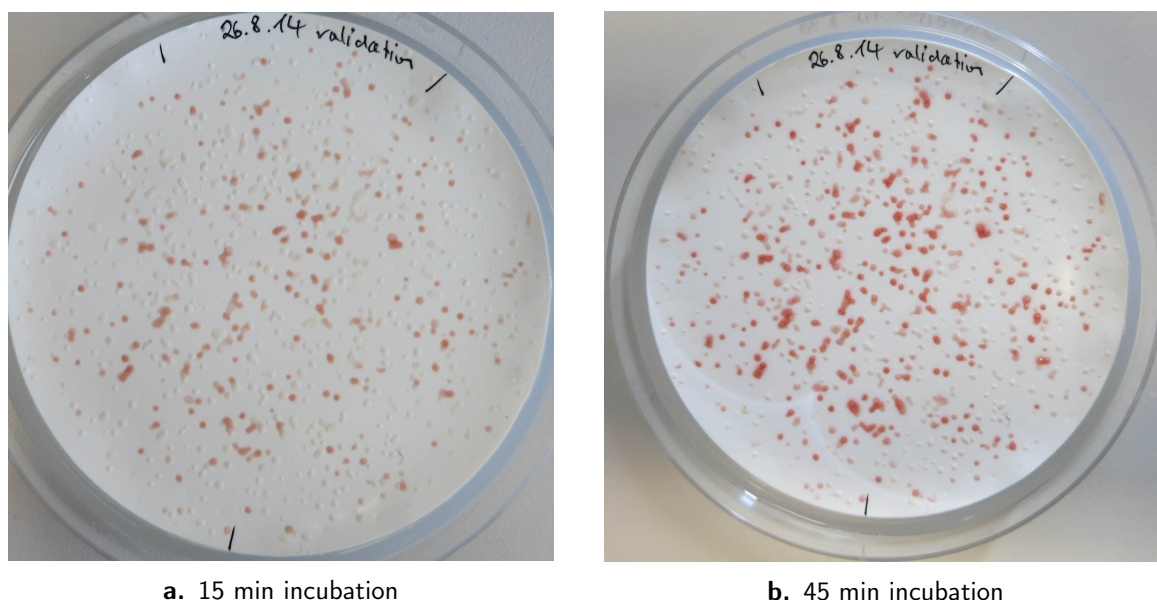


Figure 4.3: Validation of an epPCR-library of the 3FCR transaminase variant (Y59W_Y87F_Y152F_T231A) by screening against the standard substrate (S)- α -phenylethylamine. The figure was reproduced from our article reference [73] with permission from ACS. The article is available under ACS AuthorChoice license <http://pubs.acs.org/doi/full/10.1021/ac503445y>. Pictures after 15 minutes (a.) and after 45 minutes (b.) of incubation on assay plates show different staining intensities and different staining velocities of the colonies.

4.3 Identification of a Starting Scaffold and Bioinformatic Analysis

After reliable screening assays for the requisite substrates were elaborated, the first aim was to select a suitable enzyme scaffold for protein engineering. Ideally, one of the in-house transaminase variants of previous projects,^[74] or one of the wild-type transaminases^[75, 76] that were discovered previously by our group, would exhibit initial activity towards one of the desired substrates. Thus, all wild-type in-house transaminases from fold type I and IV and some of the mutants from previous projects were screened in microtiter-plate format against the racemic amines (**Scheme 4.1**).

Surprisingly, several of them exhibited marginal activity towards amine **II.2a**, **II.3a** and **III.2** but no activity against amine **II.1a** or **IV.2** was detectable in crude lysate. All interesting transaminases were purified to certify their activity with higher protein-concentration (all kinetic resolution assays were certified by analytical scale reactions and HPLC analysis).

These in-depth investigations revealed that one of the transaminase variants based on the *Ruegeria* sp. TM1040 Transaminase (abbreviated as 3FCR from its pdb code) exhibited even a marginal initial activity against amine **II.1a** and **III.2**, which immediately brought it into our focus for investigation by further structural analysis and protein engineering. None of our active site focused rational mutagenesis efforts in the other transaminase scaffolds led to significantly increased activities or generated new activities. Thus, we eventually restricted all of our efforts on the 3FCR-transaminase scaffold with mutations Y59W and T231A that was identified in the initial substrate screening and that seemed to be quite evolvable.

4.3.1 Quinonoid Analysis and Rational Mutagenesis

As during catalysis of transamination (**Scheme 2.6**) the formation of the quinonoid intermediate is considered to be the energetically most demanding and spatially bulky reaction step, all requisite substrates were modeled in their quinonoid form bound to the PLP-cofactor in the active site of the 3FCR-transaminase for further analysis (supporting information of **Article II**, the bioinformatics were assigned to the responsibility of I.V.P.). These subsequently energy-minimized complexes were applied to study the possible interactions of the neighboring amino acid positions of the enzyme scaffold with the quinonoids (**Figure 4.4**).

Thus, additionally to position 59 and 231, three further amino acid positions were identified to directly interfere in the accommodation of the substrates. Tyrosine in position 87 seemed to be interacting with the moiety of the substrate in the small binding pocket and the hydroxyl group of that tyrosine was suspected to pose a steric hindrance for large moieties there. However, as most of the substrates provide an aromatic residue to be accommodated in the active site, it was expected that π - π -interactions of a phenylalanine in this position 87 would lead to favorable interactions. In fact, mutation Y87F significantly increased the specific activity for all aromatic amine substrates (**Table 4.1**), while smaller amino acids such as valine or glutamine provided drastically decreased activity up to a decrease of up to 97 % (data not shown). The second amino acid position of interest was tyrosine in position 152, which is supposed to coordinate the PLP-cofactor by the aromatic hydroxy phenyl ring. Thus, in this position it was clear to keep an aromatic residue. In order to prevent any negative effect of the hydroxyl group, which points towards the PLP-phosphate group and the bound substrates, a phenylalanine substitution was selected in this position 152. The experimental data indeed demonstrated a beneficial effect of mutation 152F on the stability of the scaffold (supporting information of **Article II**), which resulted in an overall improved catalytic behavior, probably due to the stabilization of the PLP-cofactor in the active site. In addition to that, the specific activity for amine **II.1a** and **II.3a** was significantly increased by mutation 152F (**Table 4.1**). The third amino acid position was proline in position 423, which was replaced by a histidine in this study, as it was assumed to facilitate the diffusion of substrates in the active site by providing more flexibility at the entrance loop. However, despite an increase of the specific activity was evident (**Table 4.1**), this mutation has been discarded, due to its destabilizing effect.

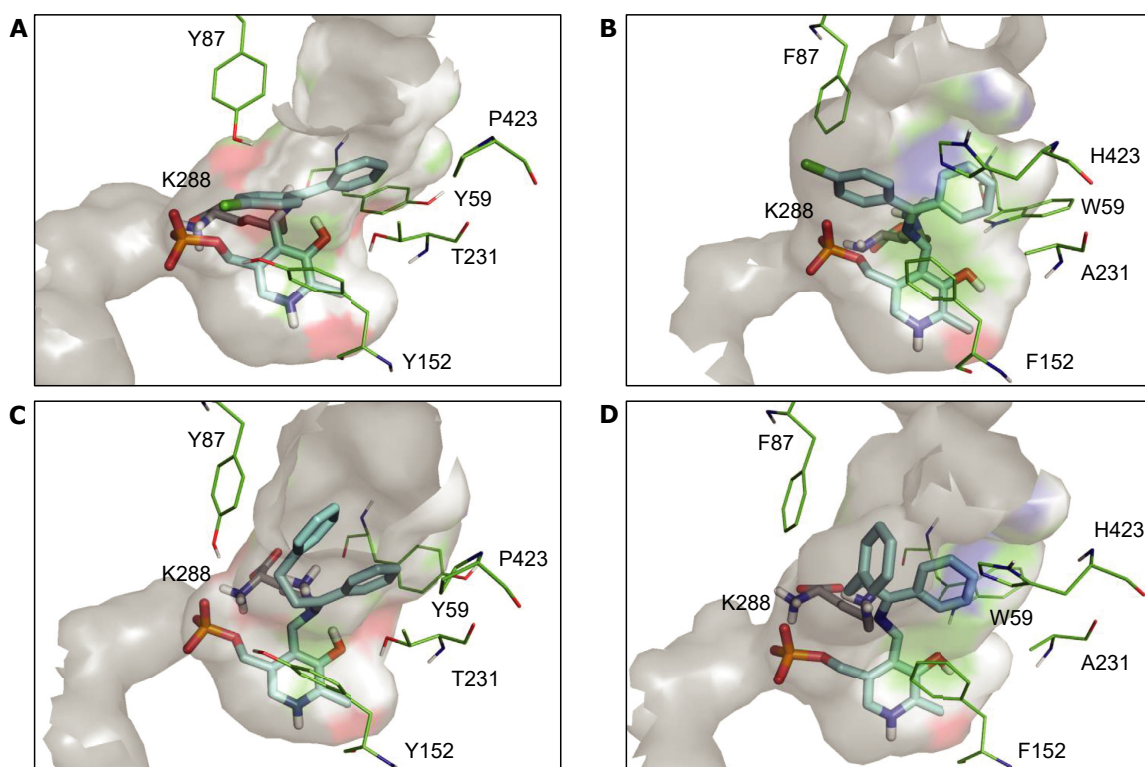


Figure 4.4: Quinonoid of compounds II.1 and II.2 accommodated in the active site of 3FCR. A–D: The quinonoid (cyan sticks) of II.1 (A,B) and II.2 (C,D) was modelled and energy-minimized in silico into the active site of wild-type 3FCR (A,C) and the variant exhibiting the highest activity (3FCR Y59W/Y87F/Y152F/T231A/P423H) (B,D). The bulky substrates cannot be accommodated in the binding pockets of wild-type 3FCR and thus the quinonoid cannot be planar (A,C). When the five mutations are implemented in the scaffold, the quinonoid is accommodated much better within the engineered active site. The catalytic lysine K288 (grey stick) is located behind PLP, the residues of interest are shown as green lines, and the surface of the residues 5 Å around the quinonoid is represented in grey (40% transparency). Non-polar electrons are hidden for clarity. The bioinformatic analysis was assigned to the responsibility of I.V.P, who prepared this figure (as taken from reference [54]).

Table 4.1: Specific activity [U mg^{-1}] of purified 3FCR and 3GJU mutants as determined in kinetic resolution mode using pyruvate as amine acceptor. Assay conditions: 50 mM CHES buffer pH 9.0, 0.1 mM PLP, 1 mM *rac*-amine, 2mM pyruvate, 5 % (vol/vol) DMSO, 0.002-0.8 mg mL⁻¹ purified transaminase, 30°C.

Variant	<i>rac</i> -II.1a	<i>rac</i> -II.2a	<i>rac</i> -II.3a
3FCR wild-type	NA ^a	0.001 ± 0.000	0.014 ± 0.000
3FCR_Y59W	0.002 ± 0.000	0.50 ± 0.02	0.27 ± 0.01
3FCR_T231A	NA	0.019 ± 0.001	0.065 ± 0.001
3FCR_Y59W_T231A	0.005 ± 0.000	0.92 ± 0.03	0.075 ± 0.005
3FCR_Y59W_Y87F_T231A	0.32 ± 0.01	3.3 ± 0.4	0.51 ± 0.01
3FCR_Y59W_Y87F_Y152F_T231A	0.54 ± 0.01	2.9 ± 0.1	0.66 ± 0.08
3FCR_Y59W_Y87F_Y152F_T231A_P423H	0.62 ± 0.04	8.9 ± 1.1	1.38 ± 0.01
3GJU wild-type	NA	0.003 ± 0.000	ND ^b
3GJU_Y60W_T232A	0.003 ± 0.000	0.66 ± 0.02	0.11 ± 0.01
3GJU_Y60W_Y88F_Y153F_T232A_P423H	0.22 ± 0.02	0.92 ± 0.07	0.90 ± 0.08

^aNA, not active or below detection limit

^bND, not determined

Remarkably, all of the four core mutations 59W, 87F, 152F, 231A that were identified to increase the activity against bulky aromatic substrates in the 3FCR transaminase (**Table 4.1**), have been described before. For instance, the single mutations 59W, 87F and 231A were introduced into the 3FCR-transaminase to increase its activity against the standard benchmark substrate 1-phenylethylamine in previous work by our group, but no determination of activities for larger compounds were conducted.^[74] The latter three mutations were originally derived from a multiple sequence alignment of the 3FCR transaminase with the *Vibrio fluvialis* (VibFlu)- and the *Chromobacterium violaceum* (Cv)-transaminase, that both already have these amino acids in the respective positions in their wild-type sequence. However, both of them are most strikingly no efficient catalysts for the desired compounds addressed in this study. The aforementioned positions of our mutation motif are as well reported in literature to be part of investigations in different transaminases,^[58, 77, 78] but eventually other specific mutations were chosen or the focus was directed to other positions in these transaminase scaffolds, without combining these mutations to determine their influence on the acceptance of bulky substrates and eventually without succeeding to convert as bulky substrates as investigated in this study.

However, combining all four mutations in a suitable scaffold such as the 3FCR-transaminase, enabled us to create a transaminase with significant activity towards the very bulky substrates **II.1**, **II.2** and **II.3** (as well compound **III**), which directly implies that both is crucial: The right amine transaminase and the motif consisting of the mutations 59W, 87F, 152F and 231A equivalently!

4.4 Validation of the Identified Sequence Motif

The actual goal of this study was not only to create a single transaminase with activity against various bulky substrates, but rather to provide a more general solution that would allow to acquire versatile catalysts from the entire sequence space by incorporating our motif into other further specified scaffolds.

To approach this goal we first of all investigated, whether transferring our sequence motif would have the same desired effect in other transaminases. As we knew from previous experiments that the VF-transaminase and the Cv-transaminase with sequence identities of about 33 % and 37 % were too remote, we selected the (*S*)-selective transaminase from *Mesorhizobium loti* maff303099 (abbreviated as 3GJU from its PDB code), which exhibits a 71.5% amino acid sequence identity to 3FCR, for initial studies. Similar to the 3FCR-scaffold, the 3GJU-transaminase exhibits negligible activity against amine **II.2a** but notably no activity against amine **II.1a** (**Table 4.1**).

In fact, incorporating the two mutations 59W and 231A in the corresponding positions of the 3GJU transaminase expanded as well its substrate scope for amine **II.1a**, similarly as the two mutations did in the 3FCR-scaffold (**Table 4.1**). Incorporation of all five former identified mutations in the corresponding positions of the 3GJU transaminase, generated even significant activity for all aromatic amines **II.1a - II.3a** (**Table 4.1**).

These results indicated that the identified motif seemed to be transferable to other transaminases with sequence identities at least as low as about 70 % to the 3FCR-transaminase, yielding

variants with considerable activity against the aforementioned bulky substrates. To further support this finding, we decided to search our M5nr^[79] database* for putative transaminases with sufficient sequence identity to the 3FCR-transaminase scaffold for further investigation (The database search was assigned to the responsibility of I.V.P.). This *in silico* screening using the 3FCR_59W_87F_152F_231A as reference sequence returned 100 matches. Despite the sequence identity was as low as 69.2 %, all residues in the four targeted motif positions were conserved regarding to the 3FCR transaminase wild-type amino acid sequence. We selected seven sequences exhibiting sequence identities between 69 and 91 % to the wild-type sequence of 3FCR to be ordered as synthetic genes already having the four suggested mutations of our motif incorporated. Mutation P423H was excluded as this mutation exhibited reduced stability, while having only a limited effect on activity. Remarkably, none of these seven proteins had ever been biochemically characterized and some of them have not even been annotated as putative transaminase.

Six of these synthetic genes could be expressed in *Escherichia coli* BL21 (DE3) according to our standard protocols for transaminase expression and every six expressible proteins possessed considerable activity towards all bulky aromatic amines in kinetic resolution (**Table 4.2**). Further evaluation of small scale asymmetric synthesis reactions revealed that all of them were as well selective catalysts (**Table 4.2**), albeit all of them were significantly less efficient in terms of conversions achieved in asymmetric synthesis compared to the 3FCR_59W_87F_152F_231A-variant (data not shown), which might be possibly due to lower stability of the variants.

Table 4.2: Specific activity and enantiomeric excess of the purified transaminases identified by the sequence similarity database research and incorporation of the four amino acid substitutions of our motif measured in kinetic resolution using pyruvate as amine acceptor. Assay conditions for kinetic resolution: 50 mM CHES buffer pH 9.0, 0.1 mM PLP, 1 mM *rac*-amine, 2mM pyruvate, 5 % (vol/vol) DMSO, 0.002-0.8 mg mL⁻¹ purified transaminase, 30°C. Assay conditions for a symmetric synthesis: 50 mM HEPES-NaOH buffer pH 8.0, 1 mM PLP, 8 mM ketone, 200 mM D,L-alanine, 2-3 mM NAD⁺, GDH (15 U mL⁻¹), D-glucose (220 mM) and LDH (50 U mL⁻¹), 20% DMSO, 0.3-1.4 mg mL⁻¹ purified enzyme, 30°C and 600 r.p.m. The enantiomeric excess was determined by analyzing analytical scale asymmetric synthesis reactions using racemic alanine as amine donor. Note that the absolute configuration given refers to the preferentially converted enantiomer, but not the enantiomer that is enriched in kinetic resolution.

Variant	Specific activity [U mg ⁻¹] (Enantiomeric excess [%])		
	<i>rac</i> -II.1a	<i>rac</i> -II.2a	<i>rac</i> -II.3a
TA-3	0.071 ± 0.001 (>99% (<i>R</i>))	1.0 ± 0.1 (>99% (<i>S</i>))	0.16 ± 0.03 (79% (<i>S</i>))
TA-5	0.16 ± 0.01 (>99% (<i>R</i>))	0.4 ± 0.1 (>99% (<i>S</i>))	0.18 ± 0.02 (56% (<i>S</i>))
TA-6	0.117 ± 0.003 (>99% (<i>R</i>))	0.6 ± 0.1 (>99% (<i>S</i>))	0.058 ± 0.005 (58% (<i>S</i>))
TA-7	0.17 ± 0.03 (>99% (<i>R</i>))	0.9 ± 0.2 (>99% (<i>S</i>))	0.40 ± 0.03 (76% (<i>S</i>))
TA-8	0.40 ± 0.05 (>97% (<i>R</i>))	1.9 ± 0.1 (>99% (<i>S</i>))	0.54 ± 0.02 (63% (<i>S</i>))
TA-9	0.35 ± 0.03 (>99% (<i>R</i>))	4.3 ± 0.2 (>99% (<i>S</i>))	0.50 ± 0.02 (82% (<i>S</i>))

*M5nr database: The M5nr database is a non-redundant joint database, which logically consists of sequence data and metadata (including annotations in various different formats). The sequence data are raw sequences and each sequence is supplied to the MD5 algorithm to generate a unique hexadecimal sequence identifier to link the metadata for a unique sequence to this "MD5 ID". This principle allows to import other databases with different annotation formats and just to append the metadata in case of redundant sequence entries instead of opening a new entry, which allows cost efficient (memory and CPU power) sequence similarity queries involving several different databases.

Furthermore, the substrate scope of all expressible transaminases from the database research, including the 3FCR-template with the mutations of the motif were characterized against three additional compounds, namely 1-phenylpropylamine, 1-phenylbutylamine and 2-phenylglycinol that are not of apparent pharmaceutical interest but that had been investigated in several studies^[50, 56, 57, 77, 80] focusing on the expansion and the investigation of the substrate scope of transaminases and thus can be considered as common benchmark substrates for transaminases. All of our aforementioned transaminase variants were considerably active and highly selective as well for these bulky substrates (**Article II**) having up to a propyl moiety or a methyl alcohol connected to the benzylamine group.

These results demonstrate that the implementation of the suggested motif in appropriate putative transaminases with sufficient homology to the 3FCR-transaminase scaffold provides access to fold type I transaminases exhibiting a novel and expanded substrate scope for various bulky substrates. Importantly, the defined sequence motif alone, is not sufficient to evolve activity for various bulky substrates: For instance the VibFlu- and Cv-transaminases, that exhibit sequence identities of less than 40 % to the 3FCR-transaminase, already have three of the required amino acids in the defined positions (59W, 87F and 231A), but do not exhibit considerable activity towards the substrates of interest.

4.4.1 Preparative Scale Synthesis of Chiral Amines I.1 – I.3

As detailed above, the motif incorporated in a suitable scaffold, generates transaminase variants capable to perform the chiral resolution of racemic bulky amines. However, only starting from the prochiral keto-substrates using asymmetric synthesis would afford the chiral amine with up to quantitative yield, which was indeed the actual intention of this study.

Hence, we applied the best scaffold the 3FCR_59W_87F_152F_231A for preparative-scale asymmetric synthesis of the chiral amines **II.1 – II.3** starting from the corresponding prochiral keto-substrates (100 mg ketone) using alanine as amine donor including the LDH and GDH system to shift the equilibrium in the desired reaction (The asymmetric synthesis experiments and product characterization were conducted by I.V.P and Roche). For each compound high conversions were achieved in reasonable reaction times (**Table 4.3**), which emphasizes the synthetic potential of the 3FCR_59W_87F_152F_231A transaminase variant also for industrial processes.

Table 4.3: Specific activity [U mg⁻¹] of purified 3FCR and 3GJU mutants as determined in kinetic resolution mode using pyruvate as amine acceptor. Assay conditions: 50 mM CHES buffer pH 9.0, 0.1 mM PLP, 1 mM *rac*-amine, 2mM pyruvate, 5 % (vol/vol) DMSO, 0.002-0.8 mg mL⁻¹ purified transaminase, 30°C.

Product:	(<i>R</i>)-II.1a	(<i>S</i>)-II.2a	(<i>S</i>)-II.3a
Reaction Time [h]:	24	24	46
Ratio of Substrate to Enzyme [wt/wt]:	2	5	2.5
Conversion [%]:	> 98	> 99	> 97
Isolated Yield [%]:	82 (HCl Salt)	71 (HCl Salt)	69 (HCl Salt)
Enantiomeric Excess [%]:	94.2	> 99.9	63.0

The enantioselectivity of this transaminase variant was perfect in case of reaction **II.2** resulting an enantiomeric excess of more than 99 %, very high for reaction **II.1** (94.2 % ee) and still moderate for reaction **II.3** (63 % ee), which clearly correlates with the structural difference of the two moieties adjacent to the keto group. Furthermore, preparative synthesis was demonstrated for the other benchmark amines 1-phenylpropylamine, 1-phenylbutylamine and 2-phenylglycinol. All of these reactions reached very high conversions (> 95 %) and very high enantiomeric excess (> 95 %) within short reaction times (**Article II**).

4.5 Diversification of the Scaffolds

For the other two structurally different requisite substrate pairs (**III & IV**) the suggested motif was not sufficient for useful catalysis. In case of compound **IV** no activity was detectable with any of the variants having different combinations of the four motif mutations incorporated, while for compound **III** activity was found in kinetic resolution but no sufficient amine synthesis using asymmetric synthesis was feasible. Thus, we had to address these substrates by a different protein engineering approach.

Indeed, any mutations that turned out to facilitate the conversion of one of the latter substrates, reduced the activity for the other aromatic substrates (data not shown). The aforementioned 3FCR_59W_231A and the 3FCR_59W_87F_152F_231A variants, were applied as starting point for further protein engineering for the remaining substrates. The amino acid positions 59, 152 and 231 were saturated and several single mutations in position 87 were investigated. None, of the mutations improved the activity against the aromatic amines **II.1a – II.3a**, but the results were the basis for further diversification of our 3FCR-scaffold for structurally different substrates.

4.5.1 Mutating Position 59 and Neighboring Residues Enhances the Activity Against the Bicyclic-bridged Substrate

The saturation mutagenesis experiments for amine **III.2** clearly pointed out a leucine mutation in position 59, which increased the activity by a factor of three in the 3FCR_59W_87F_152F_-231A template (**Table 4.4**). Furthermore, the analysis of the single mutations 59W and 231A from the variant of the 3FCR-transaminase that was initially found to be active against some of the substrates, further supported that mutation 59W of our motive was not the optimal amino acid for the bicyclic-bridged substrate (**Table 4.4**). Interestingly, mutation 152F was found to improve the stereoselectivity, as all variants without mutation 152F had only moderate selectivity (< 40 % ee (exo), data not shown), while the 3FCR_59W_87F_152F_-231A exhibited perfect selectivity for the exo-isomer. As the saturation of position 231 and the mutations in position 87 did not result in any better variants, in three of the four positions the optimal amino acids were already incorporated.

At this point, any further rational mutagenesis was hindered by the three-dimensional nature of compound **III** that did not follow the typical transaminase design concepts of having one large and one smaller substituent to be accommodated the two binding pockets each. Accordingly, it was unclear how exactly the substrate is oriented in the active site. For this reason, parallel to the optimization of the four positions we evolved the 3FCR-scaffold using directed evolution (ep-PCR) in combination with our glycine oxidase plate assay with the intention to combine beneficial mutations with the resulting mutations from the saturation experiments.

Screening ep-PCR libraries based on the 3FCR_Y59W_T231A resulted in a variant having several mutations, among them mutation I234F, which was identified to be responsible for the increase of activity, by characterization of the respective single mutants in the 3FCR_Y59W_-T231A (data not shown). Further investigation of this position by saturation experiments revealed that both phenylalanine and methionine are the most promising amino acids in this position for the kinetic resolution of amine **III.2**. The beneficial effect of these two mutations was confirmed both in the 3FCR_Y59W_T231A- (data not shown) and the 3FCR_59W_-87F_152F_-231A-variant (**Table 4.4**).

These two variants with mutations I234M and I234F were also investigated regarding their ability to synthesize amine **III.2** starting from the keto-substrate **III.1** using alanine or isopropylamine as amine donor (**Table 4.5**) and both of them were proved to acquire higher conversions independently of the amine donor. Remarkably, mutation I234F decreased the expression yield for unknown reasons. Hence, we had to apply 8-fold lower amount of enzyme compared to the other variants for the experiments (**Table 4.5**). Despite the lower amount of enzyme, similar conversions of the variant with mutation I234F were achieved compared to the variant with I234M indicating a higher catalytic efficiency. However, we continued protein engineering with mutation I234M, as it did not affect the expression yield but increased activity.

Table 4.4: Specific activities of the purified transaminases variants in kinetic resolution of amine III.2 using glyoxylate as amine acceptor. Assay conditions for kinetic resolution: 50 mM CHES buffer pH 9.5, 1 mM *rac*-amine, 2mM glyoxylate and 0.002-0.8 mg mL⁻¹ purified transaminase at 37°C.

Variant	<i>rac</i> -III.2
	Specific activity [mU mg ⁻¹]
3FCR (wild-type)	70
3FCR_Y59W	35
3FCR_T231A	130
3FCR_Y59W_T231A	45
3FCR_Y59W_Y87F_Y152F_T231A	45
3FCR_Y59L_Y87F_Y152F_T231A	145
3FCR_Y59W_Y87F_Y152F_T231A_I234F	80
3FCR_Y59W_Y87F_Y152F_T231A_I234M	116

Table 4.5: Selective synthesis of *exo*-amine III.2 using alanine or isopropylamine as amine donors. Both mutations I234M and I234F increased conversions independently of the amine donor.

Variant	Conversion [%] (Enantiomeric excess [%, <i>exo</i>])	
	With IPA ^a	With alanine ^b
3FCR_Y59W_T231A	0 (ND ^c)	4 (ND ^c)
3FCR_Y59W_Y87F_Y152F_T231A	10 (>99)	35 (>99)
3FCR_Y59W_Y87F_Y152F_T231A_I234M	19 (>99)	66 (>99)
3FCR_Y59W_Y87F_Y152F_T231A_I234F ^d	8 (>99)	40 (>99)

^aConditions for isopropylamine experiments: 2 mM ketone **III.1**, 0.2 M IPA, HEPES buffer (pH 8.0, 50 mM), 1 mM PLP, 5 % DMSO, 30°C, 600 rpm and 20 h of incubation.

^bConditions for alanine experiments: 8 mM ketone **III.1**, 0.2 M L-alanine, HEPES buffer (pH 8.0, 50 mM), 1 mM PLP, 20 % DMSO, 5 mM NADH, 25 mM glucose, 0.05 mg mL⁻¹ GDH, 5 µL mL⁻¹ LDH, 30°C, 600 rpm and 20 h of incubation.

^cND, not determined

^dLower conversions as 8-fold less amount of enzyme was applied due to expression issues, see text.

The 3FCR_Y59W_Y87F_Y152F_T231A_I234M was subjected to another round of directed evolution revealing position 382 as a new hot spot. Subsequent saturation of the position identified mutation L382M as the most promising mutation resulting into the 3FCR_Y59W_Y87F_Y152F_T231A_I234M_L382M variant (**Table 4.6**). However, investigation of all interesting variants regarding their ability to catalyze the selective synthesis of the *exo*-amine **III.2** revealed that higher activity in kinetic resolution is not always directly correlated to higher activity in the selective synthesis and that mutation 59L seems to be the key mutation for efficiency, although all mutations (59L, I234M and L382M) were beneficial in kinetic resolution (**Table 4.6**). The other two mutations led to an improvement compared to the scaffold (3FCR_Y59W_Y87F_Y152F_T231A) but not to the same extent as mutation 59L does. All variants maintained perfect *exo*-selectivity.

Eventually, a non-optimized small scale preparative synthesis using the 3FCR_Y59W_Y87F_Y152F_T231A_I234M was carried out using isopropylamine as amine donor, which provided 75% conversion (60% isolated yield) and >99.5% selectivity for the *exo*-amine as determined by HPLC analysis.

Table 4.6: Comparison of all interesting variants in kinetic resolution and selective synthesis of *exo*-amine **III.2 using isopropylamine as amine donors.** For the selective synthesis, mutation 59L seems to be the key mutation for catalysis. The experimental conditions for kinetic resolution were identical as in **Table 4.4** and for selective synthesis identical as in **Table 4.5** with isopropylamine as amine donor.

Variant	Specific activity [mU mg ⁻¹]	Conversion [% , <i>exo</i>]
3FCR_Y59W_Y87F_Y152F_T231A	45	23 (>99)
3FCR_Y59L_Y87F_Y152F_T231A	175	96 (>99)
3FCR_Y59W_Y87F_Y152F_T231A_I234M	135	55 (>99)
3FCR_Y59W_Y87F_Y152F_T231A_I234M_L382M	200	60 (>99)
3FCR_Y59L_S86A_Y87F_Y152F_T231A_I234M_L382M	295	94 (>99)

Bioinformatic Analysis

Based on the preparative results demonstrating that the exo-amine is formed upon transamination, we modeled the substrate in the active site as described previously, to elucidate the underlying reasons for the improved activity. As seen in (**Figure 4.5**) positions 59, 87 and 152 directly interact with the quinonoid. Mutation of tyrosine or tryptophane to leucine in position 59 provides significantly more space and increases the hydrophobicity in the large binding pocket. An alanine mutation in position 231, clearly creates more space in the large binding pocket, as described for the other aromatic substrates. Potentially, a hydroxyl group in position 87 could interact with the keto-group of the substrate, which might explain the beneficial effect of the phenylalanine mutation in this position. In case of position 152 a mutation of tyrosine to phenylalanine increased the selectivity for the exo-amine, which might be explained by a potential interaction of the hydroxyl group with the nitrogen-atom of the substrate, which would support the formation of the endo-isomer.

The amino acid positions 234 and 382 that were found by directed evolution are located behind position 59 and do not directly interact with the quinonoid. Thus, their influence on the activity is difficult to elucidate, but may be presumed to be related with indirect interactions with the amino acids in position 59 and 231. For instance, these mutations might stabilize residue 59 in a catalytically more active orientation, while residue 234 could have an influence *via* the backbone on the orientation of the neighboring residue 231, which directly interacts with the quinonoid.

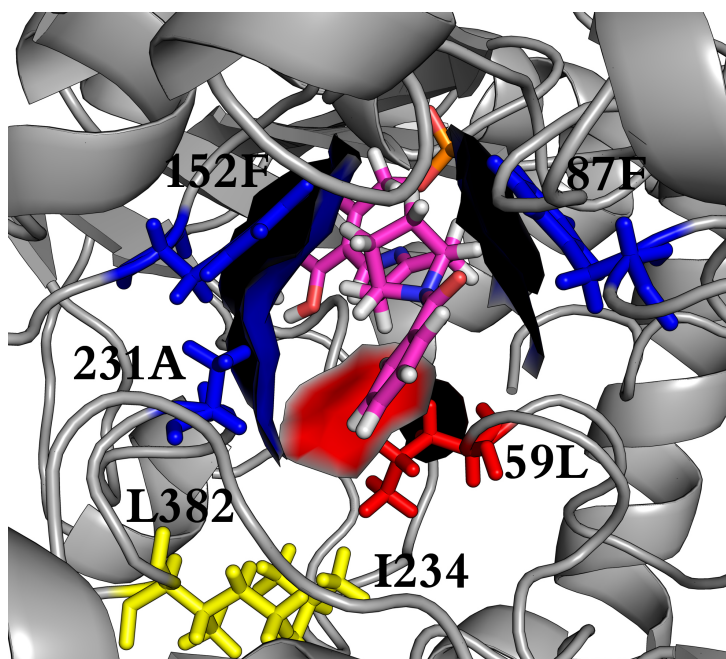


Figure 4.5: Quinonoid of compound III accommodated in the active site of the 3FCR_Y59L_Y87F_Y152F_T231A. The quinonoid (pink sticks) of III was modelled and energy-minimized in silico into the active site. The three amino acid mutations of the motif (87F, 152F and 231A) were depicted in blue and the key mutation 59L for activity against compound III is depicted in red. Furthermore, the surfaces of the residues directly interacting with the quinonoid forming the active site are represented as well. The amino acid positions 234 and 382 that were identified by directed evolution and that are located behind position 59 are depicted in yellow.

4.5.2 Aliphatic Amino Acids in Position 87 Enable Acceptance of the Spatially Bulky Substrate

The bioinformatic analysis for compound **IV** identified position 87 as promising position for mutagenesis, as it seemed obvious that no aromatic residue would be necessary to accommodate a spatially bulky tert-butyl moiety in the small binding pocket, as it was the case for the aromatic substrate moieties. Thus we selected aliphatic residues such as valine or leucine for incorporation in the 3FCR_59W_231A. The characterization results were interesting regarding two aspects. Firstly, these variants exhibited the first detectable activity against amine **IV.2**, while all other variants investigated in this project without aliphatic residues in position 87 of the 3FCR-transaminase were inactive. Secondly, it was remarkable that the variant with the larger leucine residue in position 87 was more active than the one with valine in this position, indicating that in this case the hydrophobicity might play a more important role than actually space for the accommodation of the sterically demanding substrate **IV** (Table 4.7).

Addition of mutation 152F to increase as well the stability of the scaffold, almost erased the activity and thus this mutation of the motif was not considered for now and we selected the 3FCR_59W_87L_231A to further proceed. As mutation 382M was beneficial for the aliphatic bicyclic-bridged compound **III**, we added this mutation for investigating its effect on activity against compound **IV**. In parallel, we subjected our starting scaffold to directed evolution using ep-PCR and the glycine oxidase plate assay for screening, which resulted in a more active variant with two additional mutations. Characterization of the respective single mutants identified G429A as beneficial for activity. A subsequent saturation of this position did not result in any more active mutations in this positions. As both mutation L382M and G429A were found to increase the activity in kinetic resolution, we combined the two mutations resulting in the 3FCR_59W_87L_231A_382M_429A (WLAMA) exhibiting seven-fold increased activity in kinetic resolution compared to the 3FCR_59W_87L_231A starting template (Table 4.7).

Table 4.7: Specific activity [U mg⁻¹] of purified 3FCR-transaminase variants as determined in kinetic resolution mode using pyruvate as amine acceptor. Assay conditions: 50 mM CHES buffer pH 9.0, 1 mM *rac*-amine **IV**, 2 mM pyruvate, 5 % (vol/vol) DMSO, 0.002-0.8 mg mL⁻¹ purified transaminase, 30°C.

Variant	<i>rac</i> - IV.2
3FCR wild-type	NA ^a
3FCR_Y59W_T231A	NA ^a
3FCR_Y59W_Y87F_T231A	NA ^a
3FCR_Y59W_Y87V_T231A	6.5 ± 0.4
3FCR_Y59W_Y87L_T231A	11.5 ± 0.8
3FCR_Y59W_Y87L_T231A_L382M	19.0 ± 1.9
3FCR_Y59W_Y87L_T231A_G429A	44.8 ± 0.9
3FCR_Y59W_Y87L_T231A_L382M_G429A (WLAMA)	77.1 ± 5.5

^aNA, not active or below detection limit

In parallel to these protein engineering endeavors, a preparative kinetic resolution experiment (100 mg racemic **IV.2**-amine) was conducted with the initially identified 3FCR_59W_87L_-231A-variant to investigate the synthetic potential of the identified variants and to certify the results from the direct screening assay. The results had a great impact on our protein engineering strategy, as the enriched and isolated enantiomer (38 mg) was found to be (*S*)-configured (96.2 % ee), which clearly implied that the opposite (*R*)-enantiomer was converted in contrast to our expectations! Thus, we needed to repeat the structural analysis, this time modeling the tert-butyl moiety in the large binding pocket and the phenyl ring in the other binding pocket, which is now conform with the observed catalytic behavior. In this orientation, the tert-butyl moiety directly interacts with the amino acids in positions 58, 59, 85, 231 and 422 (**Figure 4.6**).

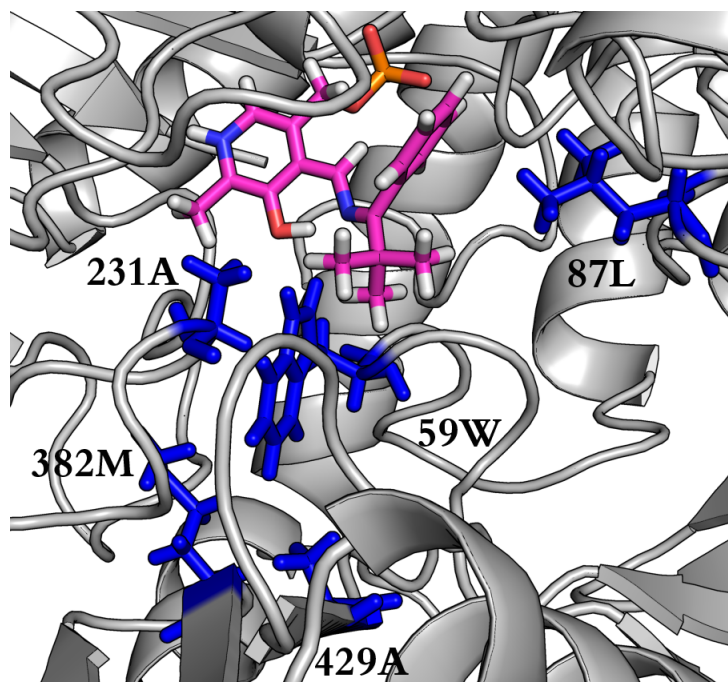


Figure 4.6: Quinonoid of compounds **IV** accommodated in the active site of the 3FCR_Y59W_Y87L_T231A_-L382M_G429A. The quinonoid of compound **IV** (depicted in pink) was modelled and energy-minimized in silico into the active site. The relevant residues with mutations Y59W, Y87L, T231A, L382M and G429A are represented in blue. Copyright Wiley-VCH Verlag GmbH & Co. KGaA. Reproduced from our article reference [81] with permission.

As the tert-butyl moiety was found to be accommodated in the large binding pocket, where usually the phenyl ring of the other investigated substrates is bound, we decided to further investigate these neighboring residues (positions 58, 59 and 85 were investigated, data not shown), but no further improvement of activity was detectable (Article IV).

Thus, all interesting variants were subjected to analytical scale asymmetric synthesis experiments using alanine and isopropylamine as amine donors. Despite the low activities in kinetic resolution, all variants provided full conversion after 42 hours using alanine as amine donor. Isopropylamine was accepted as well, albeit with lower efficiency (Table 4.8). Incorporation of mutation 152F from the sequence motif in the most active scaffold decreased its conversions in asymmetric synthesis (Table 4.8) and the stabilizing effect was only marginal, which was accounted from corresponding comparative experiments pre-incubating the variants at 30°C with and without isopropylamine (Article IV).

Table 4.8: Analytical scale asymmetric synthesis experiments to investigate all interesting variants that were active in kinetic resolution using alanine or isopropylamine as amine donors. Reaction conditions: 4mM ketone (IV.1), HEPES buffer (50 mM, pH 8.0), 5 % (v/v) DMSO, 1.35 mg mL⁻¹ purified transaminase, 1 mM PLP at 30°C, 600 rpm and 42 h of incubation. The amine donor was 200 mM isopropylamine or 200 mM L-alanine. In case of alanine 150 mM D-glucose, 45 U mg⁻¹ LDH, 15 U mg⁻¹ GDH and 1 mM NADH were supplied.

Variant	Conversion [%] (ee [%])	
	with L-Alanine	with IPA
3FCR_Y59W_Y87L_T231A	100 (>99)	22 ± 2.3 (n.d.)
3FCR_Y59W_Y87L_T231A_L382M	100 (>99)	38 ± 1.4 (>99)
3FCR_Y59W_Y87L_T231A_G429A	100 (>99)	45 ± 0.8 (>99)
3FCR_Y59W_Y87L_T231A_L382M_G429A (= WLAMA)	100 (>99)	71 ± 3.5 (>99)
3FCR_Y59W_Y87L_Y152F_T231A_L382M_G429A	100 (>99)	40 ± 2.8 (>99)

Direct Comparison with VibFlu-Transaminase

Recently, our group reported an alternative protein engineering solution to generate activity for compound **IV** in the transaminase of *Vibrio fluvialis*,^[82] which exhibits only 33 % sequence identity to the *Ruegeria* sp. TM1040 Transaminase of this study. Screening variants from a library with six simultaneously saturated positions in the active site of the VibFlu transaminase identified some variants with activity both in kinetic resolution and asymmetric synthesis. Thus, two different solutions were available in two different scaffolds and it seemed interesting to analyze in detail, which mutations lead to activity against the desired substrate in the two scaffolds.

Despite the low sequence identity, the two structures (PDB IDs: 3FCR and 4E3Q) are very similar. Their structural alignment results in an RMSD of only 1.154 Å, which implies a very high structural similarity. In addition to that, most residues in the active site* of the 3FCR_WLAMA-variant and the VibFlu transaminase were found to be conserved. Both wild-type transaminases are inactive against compound **IV**.

The best two VibFlu-transaminase variants had the following mutations: L56V, W57C, F85V, V153A (H3_RAV) and L56V, W57F, F85V, V153A, R415C (H1_A).^[82] The latter positions correspond to the following positions in the 3FCR_WLAMA scaffold: L58, W59, L87, S155, and R420. In general, the two transaminase scaffolds evolved almost entirely differently, despite their structural similarity. Notably, three out of five mutations (Y59W, T231A, and L382M) of our best variant are already present in the corresponding positions of the wild-type VibFlu-transaminase. Vice-versa, mutations L58V, (L58A) and S155A, that were present in the most active VibFlu transaminase variants, were found to drastically reduce the activity in the 3FCR_WLAMA scaffold for the substrate of interest. However, a final statement seems unfeasible, as no data were available for intermediate variants of the VibFlu-transaminase, such as VibFlu_F85V_V153A, which might be active but was not investigated. Nevertheless, no clear motif to acquire the desired activity could be identified, with one distinct and exceptional communality between the two enzymes. Exclusively, variants with aliphatic amino acids such as valine or leucine in position 87 were found to be active for the desired substrate in case of the 3FCR-transaminase scaffold, while variants with valine in the position corresponding to position 87 in the VibFlu transaminase were found to be the most active variants. Thus, the most important position represents position 87, as it was proven to be beneficial in both scaffolds underlining its potential role in the identification of other transaminases accepting substrates with tert-butyl moieties.

*Residues within a 10 Å radius from the enamine nitrogen atom of the external aldimine of PLP and the substrate were considered to form the active site

5 Conclusion

In this joint project, a fold type I transaminase from *Ruegeria* sp. TM1040 (3FCR-transaminase) was engineered for the conversion of a set of sterically demanding and structurally diverse model substrates for the synthesis of chiral amines and the kinetic resolution of racemates. It was demonstrated that implementation of the four identified core mutations (Y59W, Y87F, Y152F and T231A) in putative, partially uncharacterized transaminase sequences derived from database inquiries grants access to diverse transaminases with a novel and broad substrate spectrum including remarkably bulky and thus pharmaceutically interesting compounds. Furthermore, it was shown, that the sequence motif of the four mutations alone was not sufficient to generate the expanded substrate profile. The target transaminase sequences are required to possess at least 70 % sequence identity to the *Ruegeria* sp. TM1040 transaminase in order to attain the desired properties by implementation of the four mutations. These findings represent not only the first successful protein engineering endeavor of fold type I transaminases for highly bulky substrate acceptance, but also provide a more general solution for novel fold type I transaminases for the first time. In the long term, knowledge from this project is conceived to assist in the development of shorter, more economic and greener routes to chiral drugs and fine chemicals.

For the accommodation of compounds containing tert-butyl moieties or bi-cyclic bridged substrates, the sequence motif had to be refined by additional structure guided mutations, saturation mutagenesis and directed evolution using our novel high-throughput agar plate assay for transaminases. In this context, two key mutations could be assigned to be responsible for generating useful catalytic activity in the 3FCR transaminase for the aforementioned additional substrates. Mutation 59L seemed to be the key mutation aside from other beneficial mutations for the bi-cyclic bridged substrate, albeit we did not investigate its effect in other transaminases scaffolds. Mutation 87L generated activity for the tert-butyl moiety containing substrate, which was found to play as well an important role for the activity towards the same substrate in the VibFlu transaminase.

For the synthesis of the latter two amines (in analytical scale) the amino donor isopropylamine could be applied, which represents the most economic amine donor for transaminases, while all other amines could be synthesized using alanine as amine donor with high yields and good to perfect optical purities. For each of the five target model substrates a 100 mg preparative-scale experiment was conducted to prove the synthetic applicability of our variants.

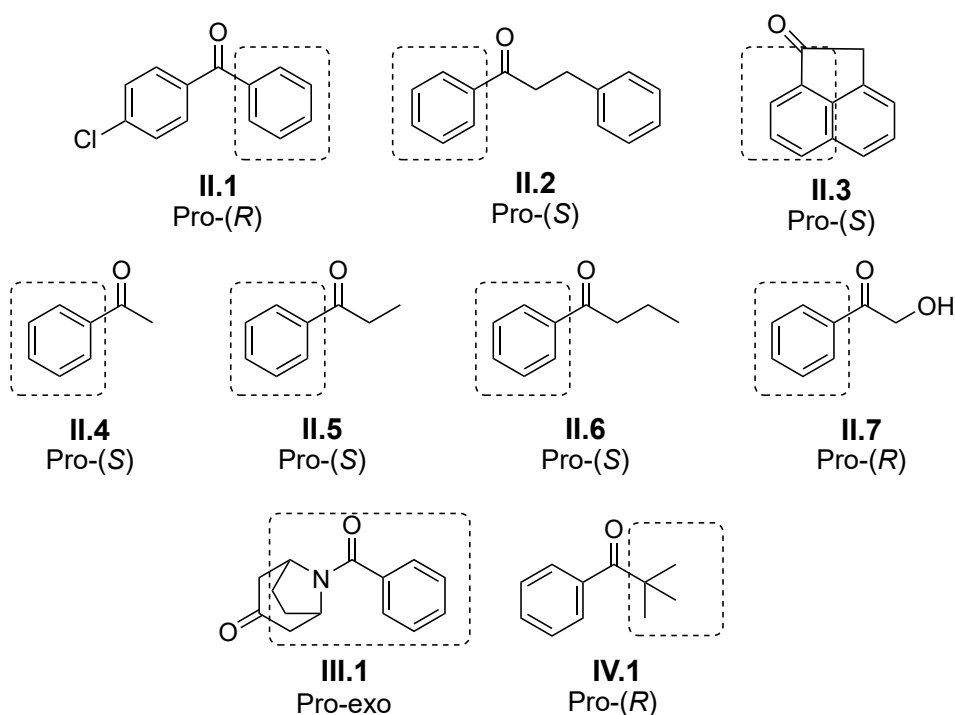


Figure 5.1: Substrate spectrum and selectivity of the novel transaminases identified in the present study. Compounds II.1 - II.3, compound III and compound IV were selected as primary target substrates, while compounds II.4 - II.7 were investigated to further demonstrate that the novel transaminases exhibit a generally extended and broad substrate scope. The regions surrounded by dashed boxes represent the moiety of each molecule that is accommodated in the large binding pocket of the transaminases, according to the experimental results. For compound IV, we observed an inverted selectivity, as the aliphatic moiety is bound in the large binding pocket instead of the aromatic ring. As observed, not always the larger or smaller moiety is consistently bound by one or the other binding pocket.

Remarkably, wild-type transaminases such as the transaminase from *Vibrio fluvialis* (VibFlu-transaminase) (33 % sequence identity to the 3FCR-transaminase) were found to have already three of the four core mutations of our motif in the corresponding positions in their protein structure, but do not possess significant activity towards the bulky substrates. These findings underline the importance to select the right transaminase for evolution and that the four core mutations alone are not sufficient to expand the substrate scope. Notably, the wild-type 3FCR-transaminase exhibits only miserable activity against standard benchmark substrates for transaminases such as α -phenylethylamine, which was likely the reason why it had not been previously selected for mutagenesis experiments for more bulky substrates. In contrast, the VibFlu-transaminase was frequently selected for protein engineering, most probably due to its high activity against standard benchmark substrates. Thus, despite the structural similarity of the 3FCR- and the VibFlu-transaminase, there must be essential and beneficial differences between transaminases with higher sequence identities to the 3FCR-scaffold and other distantly related scaffolds that allow the bulky substrate acceptance in the 3FCR-transaminase, when the four mutations are implemented. However, these differences could not be further specified within the scope of this project.

This implies, that modeling the quinonoid intermediates in the active site and analysis of possible repulsive or unfavorable interactions for according mutations will not alone and generally lead to success in any transaminase scaffold. Thus, the same protein engineering strategy alone, is not generally applicable for similar protein engineering questions, or one could also summarize: Not all enzymes are equally suitable to serve as starting scaffold for protein engineering. Hence, it seems to be interesting to recapitulate some of the crucial parameters that might have contributed to successfully identify novel transaminases with bulky substrate acceptance in the present study:

1. Screening for a set of model substrates and not only for one single target substrate,
2. venturing to select some ambitious target substrates for screening,
3. screening many different potential wild-type enzymes as possible starting scaffold for mutagenesis, including distantly related enzymes with unspectacular substrate scope regarding standard substrates compared to common scaffolds,
4. designing straight-forward single mutations in the active site of putative transaminase candidates after structural analysis and literature research to expand their substrate scopes from initial activity towards one of the target substrates and no activity for the other substrates to detectable activity for more than one of the target substrates to identify evolvable scaffolds.

All these elements should rather maximize the chances to identify a suitable generalist enzyme for specialization, than focusing on existing, well characterized and already specialized scaffolds for standard substrates. As observed, always screening closely related enzymes for the same standard substrates will most probably not render access to novel catalysts with novel substrate scopes. As proven in the present study, certain paradigms, such as the strict limitation of the small binding pocket of all transaminases to substrate moieties no larger than an ethyl group, in hindsight prove to be not correct – at least not for generally all transaminases (The 3FCR_59W_231A variant was active against most of the bulky substrates. Both mutations are located in the large binding pocket and do not increase the size of the small binding pocket. The wild-type of the 3FCR transaminase exhibits detectable activity against amines **II.2a**, **II.3a** and **III.2**). Thus, screening for activity towards multiple different but challenging substrates, will generally increase the probability to identify new starting scaffolds with initial activity for some of the desired substrates. These scaffolds should serve as a starting point by subjecting them to further analysis and mutagenesis to further broaden their substrate scope for the remaining test substrates. If available, the enzyme collection should consist of heterogeneous enzymes of various similarities from similar to entirely distantly related and mutants thereof to ensure novel enzymes with new properties are available for identification. All scaffolds identified to exhibit initial activity for some of the target screening substrates should be subjected to structural analysis, following straight-forward mutations in the active site to elaborate, which of the enzymes is actually evolvable. For instance, efforts were as well invested to generate the activity for the requisite substrates in other transaminase scaffolds, for instance by engineering the transaminase

from *Ruegeria pomeroyi* (abbreviated as 3HMU from its pdb code), which exhibits high specific activities for standard substrates and was identified to have little activity for compound **II.3** and **III**. However, none of the efforts improved its activity or extended the substrate scope causing us to switch to another scaffold.

To summarize in short, furthering the frontiers of science goes along with taking risks to question standard paradigms, considering new, maybe initially uninteresting scaffolds and challenging the until then seemingly impossible. Specifically for protein engineering, working on an evolvable template seems to be the key to success and sometimes presupposes a good portion of fortune.

References

- [1] E. J. Ariens, “Stereochemistry, a basis for sophisticated nonsense in pharmacokinetics and clinical pharmacology”, *European journal of clinical pharmacology* **1984**, *26*, 663–668.
- [2] H. Murakami in *Novel optical resolution technologies: From racemates to single enantiomers – chiral synthetic drugs over the last 20 years*, Vol. 269, (Eds.: K. Sakai, N. Hirayama, R. Tamura), Springer Berlin Heidelberg, Berlin, Heidelberg, **2006**, pp. 273–299.
- [3] M. Breuer, K. Ditrich, T. Habicher, B. Hauer, M. Keßeler, R. Stürmer, T. Zelinski, “Industrial methods for the production of optically active intermediates”, *Angewandte Chemie International Edition* **2004**, *43*, 788–824.
- [4] D. Ghislieri, N. J. Turner, “Biocatalytic approaches to the synthesis of enantiomerically pure chiral amines”, *Topics in Catalysis* **2014**, *57*, 284–300.
- [5] N. J. Turner, “Directed evolution drives the next generation of biocatalysts”, *Nature Chemical Biology* **2009**, *5*, 567–573.
- [6] H. W. Porter, “Resolution of chiral drugs”, *Pure and Applied Chemistry* **1991**, *63*, 1119–1122.
- [7] T. C. Nugent, *Chiral amine synthesis: Methods, developments and applications*, Wiley-VCH, Weinheim, **2010**.
- [8] T. Nugent, M. El-Shazly, “Chiral amine synthesis - recent developments and trends for enamide reduction, reductive amination, and imine reduction”, *Advanced Synthesis & Catalysis* **2010**, *352*, 753–819.
- [9] T. C. Nugent, S. M. Marinova, “Step-efficient access to chiral primary amines”, *Synthesis* **2013**, *45*, 153–166.
- [10] J.-H. Xie, S.-F. Zhu, Q.-L. Zhou, “Recent advances in transition metal-catalyzed enantioselective hydrogenation of unprotected enamines”, *Chemical Society Reviews* **2012**, *41*, 4126.
- [11] X. Zeng, R. Kinjo, B. Donnadieu, G. Bertrand, “Serendipitous discovery of the catalytic hydroammoniumation and methylamination of alkynes”, *Angewandte Chemie International Edition* **2010**, *49*, 942–945.
- [12] T. E. Müller, K. C. Hultsch, M. Yus, F. Foubelo, M. Tada, “Hydroamination: Direct addition of amines to alkenes and alkynes”, *Chemical Reviews* **2008**, *108*, 3795–3892.
- [13] K. W. Fiori, J. Du Bois, “Catalytic intermolecular amination of C–H bonds: Method development and mechanistic insights”, *Journal of the American Chemical Society* **2007**, *129*, 562–568.

- [14] G. K. Friestad, A. K. Mathies, "Recent developments in asymmetric catalytic addition to CN bonds", *Tetrahedron* **2007**, *63*, 2541–2569.
- [15] C. Wang, J. Xiao in *Stereoselective formation of amines: Asymmetric reductive amination*, Vol. 343, (Eds.: W. Li, X. Zhang), Springer Berlin Heidelberg, Berlin, **2013**, pp. 261–282.
- [16] H. Kohls, F. Steffen-Munsberg, M. Höhne, "Recent achievements in developing the biocatalytic toolbox for chiral amine synthesis", *Current Opinion in Chemical Biology* **2014**, *19*, 180–192.
- [17] D. Ghislieri, A. P. Green, M. Pontini, S. C. Willies, I. Rowles, A. Frank, G. Grogan, N. J. Turner, "Engineering an enantioselective amine oxidase for the synthesis of pharmaceutical building blocks and alkaloid natural products", *Journal of the American Chemical Society* **2013**, *135*, 10863–10869.
- [18] M. J. Abrahamson, E. Vázquez-Figueroa, N. B. Woodall, J. C. Moore, A. S. Bommarius, "Development of an amine dehydrogenase for synthesis of chiral amines", *Angewandte Chemie International Edition* **2012**, *51*, 3969–3972.
- [19] T. Knaus, W. Böhmer, F. G. Mutti, "Amine dehydrogenases: efficient biocatalysts for the reductive amination of carbonyl compounds", *Green Chemistry* **2017**, *19*, 453–463.
- [20] O. Mayol, S. David, E. Darii, A. Debard, A. Mariage, V. Pellouin, J.-L. Petit, M. Salanoubat, V. de Berardinis, A. Zaparucha, C. Vergne-Vaxelaire, "Asymmetric reductive amination by a wild-type amine dehydrogenase from the thermophilic bacteria *Petrotoga mobilis*", *Catalysis Science & Technology* **2016**, *6*, 7421–7428.
- [21] M. Fuchs, J. E. Farnberger, W. Kroutil, "The industrial age of biocatalytic transamination", *European Journal of Organic Chemistry* **2015**, *2015*, 6965–6982.
- [22] F. Hollmann, I. W. C. E. Arends, D. Holtmann, "Enzymatic reductions for the chemist", *Green Chemistry* **2011**, *13*, 2285.
- [23] F. F. Noe, W. J. Nickerson, "Metabolism of 2-pyrrolidone and γ -aminobutyric acid by *Pseudomonas aeruginosa*", *Journal of Bacteriology* **1958**, *75*, 674–681.
- [24] K.-h. Kim, "Purification and properties of a mine α -ketoglutarate transaminase from *Escherichia coli*", *Journal of Biological Chemistry* **1964**, *239*, 783–786.
- [25] G. Matcham, M. Bhatia, W. Lang, C. Lewis, R. Nelson, A. Wang, W. Wu, "Enzyme and reaction engineering in biocatalysis: synthesis of (*S*)-methoxyisopropylamine (= (*S*)-1-Methoxypropan-2-amine)", *CHIMIA International Journal for Chemistry* **1999**, *53*, 584–589.
- [26] G. Li, P. Yao, R. Gong, J. Li, P. Liu, R. Lonsdale, Q. Wu, J. Lin, D. Zhu, M. T. Reetz, "Simultaneous engineering of an enzyme's entrance tunnel and active site: the case of monoamine oxidase MAO-N", *Chemical Science* **2017**, *8*, 4093–4099.
- [27] I. Rowles, K. J. Malone, L. L. Etchells, S. C. Willies, N. J. Turner, "Directed evolution of the enzyme monoamine oxidase (MAO-N): Highly efficient chemo-enzymatic deracemisation of the alkaloid (\pm)-Crispine A", *ChemCatChem* **2012**, *4*, 1259–1261.

- [28] K. Mitsukura, M. Suzuki, K. Tada, T. Yoshida, T. Nagasawa, "Asymmetric synthesis of chiral cyclic amine from cyclic imine by bacterial whole-cell catalyst of enantioselective imine reductase", *Organic & Biomolecular Chemistry* **2010**, *8*, 4533–4535.
- [29] J. Mangas-Sanchez, S. P. France, S. L. Montgomery, G. A. Aleku, H. Man, M. Sharma, J. I. Ramsden, G. Grogan, N. J. Turner, "Imine reductases (IREDs)", *Current Opinion in Chemical Biology* **2017**, *37*, 19–25.
- [30] D. Wetzl, M. Gand, A. Ross, H. Müller, P. Matzel, S. P. Hanlon, M. Müller, B. Wirz, M. Höhne, H. Iding, "Asymmetric reductive amination of ketones catalyzed by imine reductases", *ChemCatChem* **2016**, *8*, 2023–2026.
- [31] G. A. Aleku, S. P. France, H. Man, J. Mangas-Sanchez, S. L. Montgomery, M. Sharma, F. Leipold, S. Hussain, G. Grogan, N. J. Turner, "A reductive aminase from *Aspergillus oryzae*", *Nature Chemistry* **2017**, DOI 10.1038/nchem.2782.
- [32] M. Sharma, J. Mangas-Sanchez, N. J. Turner, G. Grogan, "NAD(P)H-dependent dehydrogenases for the asymmetric reductive amination of ketones: Structure, mechanism, evolution and application", *Advanced Synthesis & Catalysis* **2017**, 2011–2025.
- [33] R. Percudani, A. Peracchi, "A genomic overview of pyridoxal-phosphate-dependent enzymes", *EMBO reports* **2003**, *4*, 850–854.
- [34] A. C. Eliot, J. F. Kirsch, "Pyridoxal phosphate enzymes: Mechanistic, structural, and evolutionary considerations", *Annual Review of Biochemistry* **2004**, *73*, 383–415.
- [35] Y.-L. Du, R. Singh, L. M. Alkhalaf, E. Kuatsjah, H.-Y. He, L. D. Eltis, K. S. Ryan, "A pyridoxal phosphate-dependent enzyme that oxidizes an unactivated carbon-carbon bond", *Nature Chemical Biology* **2016**, *12*, 194–199.
- [36] F. W. Alexander, E. Sandmeier, P. K. Mehta, P. Christen, "Evolutionary relationships among pyridoxal-5'-phosphate-dependent enzymes", *The FEBS Journal* **1994**, *219*, 953–960.
- [37] J. N. Jansonius, "Structure, evolution and action of vitamin B6-dependent enzymes", *Current Opinion in Structural Biology* **1998**, *8*, 759–769.
- [38] J. Catazaro, A. Caprez, A. Guru, D. Swanson, R. Powers, "Functional evolution of PLP-dependent enzymes based on active-site structural similarities", *Proteins: Structure Function and Bioinformatics* **2014**, *82*, 2597–2608.
- [39] M. Höhne, U. T. Bornscheuer in *Enzyme Catalysis in Organic Synthesis, Third Edition, Vol. 2*, Wiley-VCH, Weinheim, **2012**, pp. 779–820.
- [40] F. Guo, P. Berglund, "Transaminase biocatalysis: optimization and application", *Green Chemistry* **2017**, *19*, 333–360.
- [41] W. R. Griswold, M. D. Toney, "Role of the pyridine nitrogen in pyridoxal 5'-phosphate catalysis: Activity of three classes of PLP enzymes reconstituted with deazapyridoxal 5'-phosphate", *Journal of the American Chemical Society* **2011**, *133*, 14823–14830.

- [42] M. D. Toney in *Wiley Encyclopedia of Chemical Biology*, John Wiley & Sons, Inc., Hoboken, NJ, USA, **2008**.
- [43] K. E. Cassimjee, B. Manta, F. Himo, "A quantum chemical study of the ω -transaminase reaction mechanism", *Organic & Biomolecular Chemistry* **2015**, *13*, 8453–8464.
- [44] B. Manta, K. E. Cassimjee, F. Himo, "Quantum chemical study of dual-substrate recognition in ω -transaminase", *ACS Omega* **2017**, *2*, 890–898.
- [45] J.-S. Shin, B.-G. Kim, "Asymmetric synthesis of chiral amines with ω -transaminase", *Biotechnology and Bioengineering* **1999**, *65*, 206–211.
- [46] H. Yun, B.-K. Cho, B.-G. Kim, "Kinetic resolution of (*R,S*)-*sec*-butylamine using omega-transaminase from *Vibrio fluvialis* JS17 under reduced pressure", *Biotechnology and Bioengineering* **2004**, *87*, 772–778.
- [47] P. Tufvesson, C. Bach, J. M. Woodley, "A model to assess the feasibility of shifting reaction equilibrium by acetone removal in the transamination of ketones using 2-propylamine", *Biotechnology and Bioengineering* **2014**, *111*, 309–319.
- [48] J.-S. Shin, B.-G. Kim, "Exploring the active site of amine:pyruvate aminotransferase on the basis of the substrate structure–reactivity relationship: How the enzyme controls substrate specificity and stereoselectivity", *The Journal of Organic Chemistry* **2002**, *67*, 2848–2853.
- [49] E.-S. Park, J.-S. Shin, "Free energy analysis of ω -transaminase reactions to dissect how the enzyme controls the substrate selectivity", *Enzyme and Microbial Technology* **2011**, *49*, 380–387.
- [50] J. Jiang, X. Chen, J. Feng, Q. Wu, D. Zhu, "Substrate profile of an ω -transaminase from *Burkholderia vietnamiensis* and its potential for the production of optically pure amines and unnatural amino acids", *Journal of Molecular Catalysis B: Enzymatic* **2014**, *100*, 32–39.
- [51] U. T. Bornscheuer, G. W. Huisman, R. J. Kazlauskas, S. Lutz, J. C. Moore, K. Robins, "Engineering the third wave of biocatalysis", *Nature* **2012**, *485*, 185–194.
- [52] C. K. Savile, J. M. Janey, E. C. Mundorff, J. C. Moore, S. Tam, W. R. Jarvis, J. C. Colbeck, A. Krebber, F. J. Fleitz, J. Brands, P. N. Devine, G. W. Huisman, G. J. Hughes, "Biocatalytic asymmetric synthesis of chiral amines from ketones applied to sitagliptin manufacture", *Science* **2010**, *329*, 305–309.
- [53] A. A. Desai, "Sitagliptin manufacture: A compelling tale of green chemistry, process intensification, and industrial asymmetric catalysis", *Angewandte Chemie International Edition* **2011**, *50*, 1974–1976.
- [54] I. V. Pavlidis, M. S. Weiß, M. Genz, P. Spurr, S. P. Hanlon, B. Wirz, H. Iding, U. T. Bornscheuer, "Identification of (*S*)-selective transaminases for the asymmetric synthesis of bulky chiral amines", *Nature Chemistry* **2016**, *8*, 1076–1082.
- [55] S. Mathew, H. Yun, " ω -Transaminases for the production of optically pure amines and unnatural amino acids", *ACS Catalysis* **2012**, *2*, 993–1001.

- [56] A. Nobili, F. Steffen-Munsberg, H. Kohls, I. Trentin, C. Schulzke, M. Höhne, U. T. Bornscheuer, “Engineering the active site of the amine transaminase from *Vibrio fluvialis* for the asymmetric synthesis of aryl–alkyl amines and amino alcohols”, *ChemCatChem* **2015**, *7*, 757–760.
- [57] M. Genz, C. Vickers, T. van den Bergh, H.-J. Joosten, M. Dörr, M. Höhne, U. Bornscheuer, “Alteration of the donor/acceptor spectrum of the (*S*)-amine transaminase from *Vibrio fluvialis*”, *International Journal of Molecular Sciences* **2015**, *16*, 26953–26963.
- [58] K. S. Midelfort, R. Kumar, S. Han, M. J. Karmilowicz, K. McConnell, D. K. Gehlhaar, A. Mistry, J. S. Chang, M. Anderson, A. Villalobos, J. Minshull, S. Govindarajan, J. W. Wong, “Redesigning and characterizing the substrate specificity and activity of *Vibrio fluvialis* aminotransferase for the synthesis of imagabalin”, *Protein Engineering Design and Selection* **2013**, *26*, 25–33.
- [59] J.-L. Reymond, *Enzyme assays, high-throughput screening, genetic selection and fingerprinting*, Wiley-VCH, Weinheim, **2006**.
- [60] K. L. Tee, T. S. Wong, “Polishing the craft of genetic diversity creation in directed evolution”, *Biotechnology Advances* **2013**, *31*, 1707–1721.
- [61] H. Leemhuis, R. M. Kelly, L. Dijkhuizen, “Directed evolution of enzymes: Library screening strategies”, *IUBMB Life* **2009**, *61*, 222–228.
- [62] M. T. Reetz, D. Kahakeaw, R. Lohmer, “Addressing the numbers problem in directed evolution”, *ChemBioChem* **2008**, *9*, 1797–1804.
- [63] A. R. Martin, R. DiSanto, I. Plotnikov, S. Kamat, D. Shonnard, S. Pannuri, “Improved activity and thermostability of (*S*)-aminotransferase by error-prone polymerase chain reaction for the production of a chiral amine”, *Biochemical Engineering Journal* **2007**, *37*, 246–255.
- [64] M. D. Truppo, N. J. Turner, “Micro-scale process development of transaminase catalysed reactions”, *Organic & Biomolecular Chemistry* **2010**, *8*, 1280–1283.
- [65] B.-Y. Hwang, B.-G. Kim, “High-throughput screening method for the identification of active and enantioselective ω -transaminases”, *Enzyme and Microbial Technology* **2004**, *34*, 429–436.
- [66] J. Hopwood, M. D. Truppo, N. J. Turner, R. C. Lloyd, “A fast and sensitive assay for measuring the activity and enantioselectivity of transaminases”, *Chemical Communications* **2011**, *47*, 773–775.
- [67] L. Pollegioni, P. Motta, G. Molla, “L–Amino acid oxidase as biocatalyst: a dream too far?”, *Applied Microbiology and Biotechnology* **2013**, *97*, 9323–9341.
- [68] I. Dib, D. Stanzer, B. Nidetzky, “*Trigonopsis variabilis* D-amino acid oxidase: Control of protein quality and opportunities for biocatalysis through production in *Escherichia coli*”, *Applied and Environmental Microbiology* **2007**, *73*, 331–333.

- [69] S. Schätzle, M. Höhne, E. Redestad, K. Robins, U. T. Bornscheuer, “Rapid and sensitive kinetic assay for characterization of ω -transaminases”, *Analytical Chemistry* **2009**, *81*, 8244–8248.
- [70] A. P. Green, N. J. Turner, E. O’Reilly, “Chiral amine synthesis using ω -transaminases: An amine donor that displaces equilibria and enables high-throughput screening”, *Angewandte Chemie International Edition* **2014**, *53*, 10714–10717.
- [71] H. Hailes, D. Baud, N. Ladkau, T. Moody, J. M. Ward, “A rapid, sensitive colorimetric assay for the high-throughput screening of transaminases in liquid or solid-phase”, *Chemical Communications* **2015**, 17225–17228.
- [72] T. Scheidt, H. Land, M. Anderson, Y. Chen, P. Berglund, D. Yi, W.-D. Fessner, “Fluorescence-based kinetic assay for high-throughput discovery and engineering of stereoselective ω -transaminases”, *Advanced Synthesis & Catalysis* **2015**, *357*, 1721–1731.
- [73] M. S. Weiß, I. V. Pavlidis, C. Vickers, M. Höhne, U. T. Bornscheuer, “Glycine oxidase based high-throughput solid-phase assay for substrate profiling and directed evolution of (*R*)- and (*S*)-selective amine transaminases”, *Analytical Chemistry* **2014**, *86*, 11847–11853.
- [74] F. Steffen-Munsberg, C. Vickers, A. Thontowi, S. Schätzle, T. Meinhardt, M. Svedendahl Humble, H. Land, P. Berglund, U. T. Bornscheuer, M. Höhne, “Revealing the structural basis of promiscuous amine transaminase activity”, *ChemCatChem* **2013**, *5*, 154–157.
- [75] F. Steffen-Munsberg, C. Vickers, A. Thontowi, S. Schätzle, T. Tumlrirsch, M. Svedendahl Humble, H. Land, P. Berglund, U. T. Bornscheuer, M. Höhne, “Connecting unexplored protein crystal structures to enzymatic function”, *ChemCatChem* **2013**, *5*, 150–153.
- [76] M. Höhne, S. Schätzle, H. Jochens, K. Robins, U. T. Bornscheuer, “Rational assignment of key motifs for function guides in silico enzyme identification”, *Nature Chemical Biology* **2010**, *6*, 807–813.
- [77] S.-W. Han, E.-S. Park, J.-Y. Dong, J.-S. Shin, “Mechanism-guided engineering of ω -transaminase to accelerate reductive amination of ketones”, *Advanced Synthesis & Catalysis* **2015**, *357*, 1732–1740.
- [78] D. Deszcz, P. Affaticati, N. Ladkau, A. Gegel, J. M. Ward, H. C. Hailes, P. A. Dalby, “Single active-site mutants are sufficient to enhance serine:pyruvate α -transaminase activity in an ω -transaminase”, *FEBS Journal* **2015**, *282*, 2512–2526.
- [79] A. Wilke, T. Harrison, J. Wilkening, D. Field, E. M. Glass, N. Kyrpides, K. Mavrommatis, F. Meyer, “The M5nr: a novel non-redundant database containing protein sequences and annotations from multiple sources and associated tools”, *BMC bioinformatics* **2012**, *13*, 141.
- [80] C. Sayer, R. J. Martinez-Torres, N. Richter, M. N. Isupov, H. C. Hailes, J. A. Littlechild, J. M. Ward, “The substrate specificity, enantioselectivity and structure of the (*R*)-selective amine:pyruvate transaminase from *Nectria haematococca*”, *FEBS Journal* **2014**, *281*, 2240–2253.

- [81] M. S. Weiß, I. V. Pavlidis, P. Spurr, S. P. Hanlon, B. Wirz, H. Iding, U. T. Bornscheuer, “Amine transaminase engineering for spatially bulky substrate acceptance”, *ChemBioChem* **2017**, 1022–1026.
- [82] M. Genz, O. Melse, S. Schmidt, C. Vickers, M. Dörr, T. van den Bergh, H.-J. Joosten, U. T. Bornscheuer, “Engineering the amine transaminase from *Vibrio fluvialis* towards branched-chain substrates”, *ChemCatChem* **2016**, 1867–3899.

Author Contributions

Article I Glycine oxidase based high-throughput solid-phase assay for substrate profiling and directed evolution of (*R*)- and (*S*)-selective amine transaminases.

Martin S. Weiß, Ioannis V. Pavlidis, Clare Vickers, Matthias Höhne and Uwe T. Bornscheuer. *Anal. Chem.*, **2014**, 86, 11847–11853.

M.S.W. and M.H. conceived and developed the assay. M.S.W., M.H. and U.T.B. designed the experiments. M.S.W. conducted the majority of the experiments presented in this article, supported by C.V. and I.V.P.. M.S.W. predominantly interpreted the data. M.S.W. prepared the manuscript, which was revised and approved by all authors.

Article II Identification of (*S*)-selective transaminases for the asymmetric synthesis of bulky chiral amines.

Ioannis V. Pavlidis, Martin S. Weiß, Maika Genz, Paul Spurr, Steven P. Hanlon, Beat Wirz, Hans Iding and Uwe T. Bornscheuer. *Nat. Chem.*, **2016**, 8, 1076–1082.

U.T.B., H.I. and B.W. initiated the study and directed the project. P.S. undertook the substrate and product syntheses. I.V.P. performed the bioinformatic analysis. I.V.P., M.S.W. and M.G. prepared and characterized all the variants. I.V.P, S.P.H. and H.I. performed the preparative asymmetric synthesis experiments. I.V.P., H.I. and U.T.B. prepared the manuscript, which was revised and approved by all authors.

Article III Protein-engineering of an amine transaminase for the stereoselective synthesis of a pharmaceutically relevant bicyclic amine.

Martin S. Weiß, Ioannis V. Pavlidis, Paul Spurr, Steven P. Hanlon, Beat Wirz, Hans Iding and Uwe T. Bornscheuer. *Org. Biomol. Chem.*, **2016**, 14, 10249–10254.

U.T.B., H.I. and B.W. initiated the study and directed the project. P.S. performed the substrate and product syntheses and characterization. I.V.P. and M.S.W. performed the bioinformatic analysis. I.V.P. and M.S.W. prepared all the variants. I.V.P. performed the preparative scale asymmetric synthesis and the isolated product was characterized by Roche. All other experiments were conducted by M.S.W.. I.V.P. prepared a first draft of the manuscript that was then extended by M.S.W., which was revised and approved by all authors.

Article IV Amine transaminase engineering for spatially bulky substrate acceptance.

Martin S. Weiß, Ioannis V. Pavlidis, Paul Spurr, Steven P. Hanlon, Beat Wirz, Hans Iding and Uwe T. Bornscheuer. *ChemBioChem*, **2017**, 18, 1022–1026.

U.T.B., H.I. and B.W. initiated the study and directed the project. P.S. performed the substrate and product syntheses and characterization. I.V.P. and M.S.W. performed the bioinformatic analysis. I.V.P. identified the variants with initial activity, which were then subjected to further protein engineering by M.S.W.. The preparative kinetic resolution was performed by I.V.P. and the isolated product was characterized by Roche. M.S.W. conducted all other experiments. U.T.B. determined the publication strategy. I.V.P. prepared a first draft of the manuscript that was then extended by M.S.W., which was revised and approved by all authors.

Book Chapter Solid Phase Agar Plate Assay for Screening Amine Transaminases.

(In press)

Martin S. Weiß, Matthias Höhne and Uwe T. Bornscheuer. *Methods in Molecular Biology*^a

^aAccepted manuscript. The final type-set book chapter will appear in: Protein Engineering: Methods and Protocols, ISBN: 978-1-4939-7364-4, Springer Publishing Company

M.H. and U.T.B. invited M.S.W. to contribute this book chapter and conceived the structure and the intention of the book chapter. M.S.W. did the literature research and wrote the manuscript for the book chapter. M.H. and U.T.B. finalized and revised the manuscript.

Confirmed, Greifswald _____,
(Prof. Dr. Uwe T. Bornscheuer)

Greifswald _____,
(Martin Weiß)

6 Articles I – IV



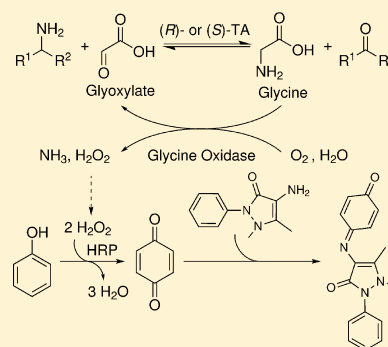
Glycine Oxidase Based High-Throughput Solid-Phase Assay for Substrate Profiling and Directed Evolution of (*R*)- and (*S*)-Selective Amine Transaminases

Martin S. Weiß, Ioannis V. Pavlidis, Clare Vickers, Matthias Höhne,* and Uwe T. Bornscheuer*

Institute of Biochemistry, Department of Biotechnology and Enzyme Catalysis, Greifswald University, Felix Hausdorff-Str. 4, 17487 Greifswald, Germany

S Supporting Information

ABSTRACT: Transaminases represent one of the most important enzymes of the biocatalytic toolbox for chiral amine synthesis as they allow asymmetric synthesis with quantitative yields and high enantioselectivity. In order to enable substrate profiling of transaminases for acceptance of different amines, a glycine oxidase and horseradish peroxidase coupled assay was developed. Transaminase activity is detected upon transfer of an amine group from an amino donor substrate to glyoxylate, generating glycine, which is subsequently oxidized by glycine oxidase, releasing hydrogen peroxide in turn. Horseradish peroxidase uses the hydrogen peroxide to produce benzoquinone, which forms a red quinone imine dye by a subsequent condensation reaction. As glycine does not carry a chiral center, both (*R*)- and (*S*)-selective transaminases accepting glyoxylate as amino acceptor are amenable to screening. The principle has been transferred to establish a high-throughput solid-phase assay which dramatically decreases the screening effort in directed evolution of transaminases, as only active variants are selected for further analysis.



Transaminases belong to the largest group of pyridoxal-5'-phosphate (PLP)-dependent enzymes¹ and catalyze the transfer of an amino group of a donor amine to the carbonyl carbon atom of an α -keto acid, a ketone, or an aldehyde. In the past decade, amine transaminases came into strategic focus to be applied as efficient biocatalysts for the preparation of optically pure amines, which represent highly valuable key intermediates or products in the pharmaceutical, chemical, and agricultural industries.^{2,3} However, for application as efficient biocatalysts, numerous challenges have to be overcome, such as a limited substrate scope, issues of thermostability, or tolerance to high concentrations of organic solvent, achieving high levels of enantioselectivity and unfavorable equilibrium in asymmetric synthesis mode, as well as substrate and product inhibition. Besides rational protein engineering approaches, directed evolution still represents the key to engineer proteins to fit the manufacturing process, inevitably causing huge library sizes predominantly containing inactive or less active variants.⁴ To speed up a directed evolution process, the availability of fast, sensitive, and efficient assays is crucial to avoid time-consuming and technically demanding analysis of each variant by HPLC or GC analysis as successfully applied by Savile et al.⁵ Several assays for amine transaminases have been developed, mostly working in kinetic resolution mode due to the unfavorable equilibrium of asymmetric synthesis, and all of them are based on screening in microtiter plate format only.⁶ Among those, the acetophenone assay represents the most facile screening method for transaminases, as transamination of α -phenylethylamine can be followed directly by spectrophotometric detection

of the corresponding ketone.⁷ However, the assay is restricted to amines carrying a phenyl group in the α position. Hence, Hopwood et al. developed a coupled microtiter plate assay for the detection of alanine by application of an L-amino acid oxidase (L-AAO) for (*S*)-selective transaminases and a D-amino acid oxidase for (*R*)-selective transaminases, respectively.⁸ This way, a range of amine substrates and pyruvate can be applied as substrate pairs for screening, generating hydrogen peroxide which is detected by horseradish peroxidase in turn. However, the drawback of this assay is that L-amino acid oxidases are difficult to access for larger screening projects, as few L-AAOs have been successfully expressed as recombinant proteins in reasonable amounts.^{9,10} Similar assays are also available for amino acid aminotransferases.^{11,12}

Solid-phase assays have been successfully applied for directed evolution of many different proteins to increase the throughput by directly screening colonies expressing variants of the gene of interest.^{13–18} The first solid-phase assay in which the protein of interest is coexpressed together with an additional assay enzyme has been developed for directed evolution of an alanine racemase by Willies and co-workers.¹⁵ While preparing our manuscript, O'Reilly and co-workers published the application of ortho-xylenediamine dihydrochloride as amino donor substrate that forms a colored precipitate via spontaneous polymerization of the aromatic isoindole formed

Received: September 13, 2014

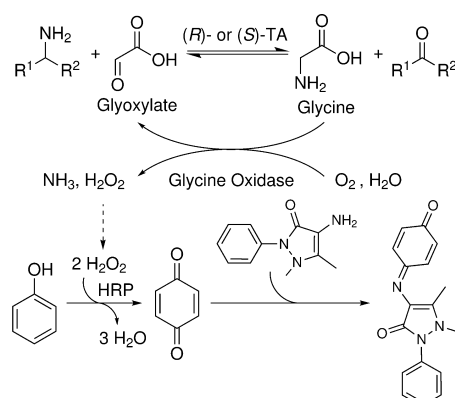
Accepted: October 16, 2014

Published: October 16, 2014

upon transamination.¹⁹ Hence, direct high-throughput screening of transaminase libraries for asymmetric synthesis by application of a range of ketones is feasible owing to a shift of the equilibrium by *in situ* coproduct removal. However, it is yet unclear if this artificial amine donor is a widely accepted substrate for transaminases.

In this study, we report on a solid-phase assay that is amenable to high-throughput screening of both (*R*)- and (*S*)-selective transaminases for activity toward different amine substrates. In order to do so, we took advantage of the fact that many transaminases accept glyoxylate as the amino acceptor at similar rates compared to pyruvate.^{20–22} Glyoxylate is converted into achiral glycine upon transamination of any chiral amine. Formation of glycine is detected by application of a thermostable glycine oxidase from *Geobacillus kaustophilus* that has been characterized by Martínez-Martínez et al.,²³ leading to the formation of hydrogen peroxide. For detection of hydrogen peroxide formation at alkaline pH values up to pH 9.5, the 4-aminoantipyrine assay involving horseradish peroxidase catalyzed oxidation of phenol to benzoquinone and formation of a red quinone imine dye by a subsequent condensation reaction was adapted (Scheme 1).²³ The

Scheme 1. Application of Glyoxylate as Amino Acceptor Substrate Allows Screening for Activity Towards Different Amines by Either (*R*)- or (*S*)-Selective Transaminases (TA)^a



^aProduction of achiral glycine is then followed by oxidation and hydrogen peroxide formation leading to the formation of a red quinone imine dye. Toxic phenol can be substituted by vanillic acid as described by Holt and Palcic (Supporting Information 2.1).^{24,25}

principle of this versatile assay is easily transferable to a microtiter plate assay (liquid-phase assay), by supplementing purified glycine oxidase externally to the reaction mixture.

EXPERIMENTAL PROCEDURES

Materials and Software. The following chemicals and enzymes were ordered from Sigma-Aldrich: Horseradish peroxidase, glyoxylic acid monohydrate, 4-aminoantipyrine, phenol, and agarose. Nitrocellulose membranes (HP44.1, 0.2 μ m pore size, >200 μ g/cm² binding capacity for proteins) were obtained from Carl Roth.

Data analysis and graphs were made using R.²⁶ Where applicable, the ggplot2 package was applied.²⁷

Cloning, Expression, and Purification of *Geobacillus kaustophilus* Glycine Oxidase. Locus tag GK0623 of *Geobacillus kaustophilus* encoding for glycine oxidase was ordered as a codon optimized synthetic gene in the pET28a(+)

vector using *Eco*RI and *Not*I, downstream of the T7 polymerase promoter (GenScript). Subcloning in the compatible pCDF-1b vector was carried out by *Bam*HI and *Not*I restriction and ligation. For addition of the N-terminal His-Tag, a frame shift was carried out using the following oligonucleotides (5'-CGT AGC GAT GCG TCA TTG AAT TCG GAT CC-3' and 5'-GGA TCC GAA TTC AAT GAC GCA TCG CTA CG-3') in a 50 μ L QuikChange-PCR (2 μ L of each oligonucleotide (10 μ M), 13 ng of template vector, 5 μ L of 10 \times PfuPlus buffer, 1 μ L of dNTPs (10 mM), 0.5 μ L of PfuPlus! DNA polymerase (1 U/ μ L)). The reaction was performed using the following thermocycling conditions: (1) 95 $^{\circ}$ C for 2 min, (2) 24 cycles: 95 $^{\circ}$ C for 30 s, 55 $^{\circ}$ C for 30 s, and 72 $^{\circ}$ C for 6 min 30 s, and (3) 72 $^{\circ}$ C for 12 min. Afterward, 10 U of DpnI was added; the reaction mixture was incubated for 2 h at 37 $^{\circ}$ C to digest the parental DNA and finally was used to transform *E. coli* TOP10 cells.

For production of His-tagged glycine oxidase, transformed *E. coli* BL21(DE3) cells were grown at 37 $^{\circ}$ C in LB medium supplemented with 50 μ g/mL spectinomycin. When the OD₆₀₀ reached 0.8, expression was induced by addition of 1 mM IPTG and cells were incubated for 20 h at 30 $^{\circ}$ C at 180 rpm. Harvested cells were resuspended in sodium pyrophosphate buffer (75 mM) pH 8.5 containing 0.5 M NaCl, 0.2 μ M FAD, and 5 mM imidazole and were lysed twice with a French press at 1700 psi. Two mg of DNaseI was added, and the suspension was centrifuged at 8000g for 30 min. The insoluble fraction was washed by resuspending in sodium pyrophosphate buffer (75 mM) pH 8.5 containing 0.5 M NaCl, 0.2 μ M FAD, 5 mM imidazole, and 0.5% Triton X-100 and incubated at 37 $^{\circ}$ C, 180 rpm for 20 min. After another centrifugation, both the supernatant and the lysate were passed through a 0.45 μ m filter and applied for IMAC purification using an ÄKTA-FPLC system at room temperature. A 5 mL His-Trap FF chelating affinity column was equilibrated with the resuspension buffer. After the sample injection, the column was washed with resuspension buffer until the UV-absorption reached baseline level again. Elution was carried out by application of a gradient from 0% to 55% of elution buffer (resuspension buffer supplemented with 0.5 M imidazole) over 24 column volumes. Finally, fractions at around 30% of elution buffer were collected and dialyzed against pyrophosphate buffer (25 mM) pH 8.5 containing 0.2 μ M FAD and 0.1% Triton X-100 overnight at 4 $^{\circ}$ C. For long-term storage, 30% glycerol was added and samples were stored at -80° C.

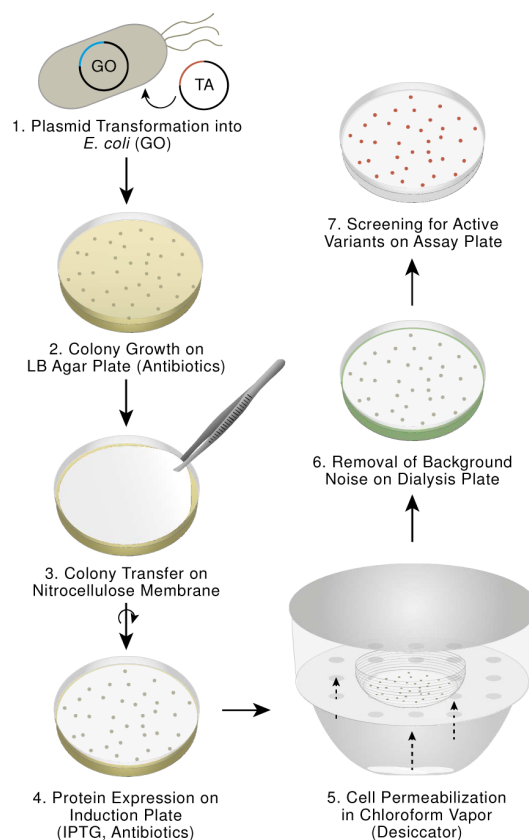
Liquid-Phase Screening. Detailed experimental procedures for expression, preparation of crude lysate of the different transaminases, and screening are given in Supporting Information 2.1. For screening using the GO assay or the acetophenone assay,⁷ 20 μ L of crude lysate dilution was pipetted in a microtiter plate and the reaction was started by adding the corresponding master mix solutions. Final substrate concentrations amounted to 2 mM α -phenylethylamine and 2 mM glyoxylate in CHES buffer (50 mM) pH 9.0 in total reaction volumes of 200 μ L (acetophenone assay) or 150 μ L (GO assay). In the glycine oxidase assay, the following final assay enzyme concentrations and reagents were additionally included: 0.14 mg/mL horseradish peroxidase (52 U/mg lyophilizate), 0.12 mg/mL glycine oxidase, 3 mM 4-aminoantipyrine, and 4.7 mM vanillic acid. In previous experiments, 7 mM phenol was applied instead of vanillic acid (data not shown). An increase of absorbance was followed at 498 nm (GO assay) and at 245 nm in the acetophenone assay at 37 $^{\circ}$ C.

Solid-Phase Assaying. *E. coli* BL21(DE3) cells carrying the pCDF-1b His-tagged glycine oxidase gene construct were made electro-competent and were used for the transformation of different transaminases of interest or for transformation of error-prone PCR (epPCR) libraries of transaminases. These transaminases were available in pET22 vectors subcloned as described previously.²⁸ Transformed libraries were directly plated out on LB agar supplemented with 50 $\mu\text{g/mL}$ of spectinomycin (spec) and 100 $\mu\text{g/mL}$ of ampicillin (amp) and were applied for solid-phase assaying. In the case of wild-type transaminases, transformation was carried out only once and the resulting colonies on LB agar plates (amp, spec) were stored at 4 $^{\circ}\text{C}$. To plate out cells with different wild-type transaminases, a 5 mL LB-medium tube containing 50 $\mu\text{g/mL}$ spec and 100 $\mu\text{g/mL}$ amp was inoculated with the cells carrying both plasmids coding for glycine oxidase and the plasmids for the transaminases of interest. After 75 min of incubation at 37 $^{\circ}\text{C}$ at 180 rpm, the OD_{600} was determined. Finally, 20 μL of a dilution corresponding to an OD_{600} of 3.3×10^{-4} was plated out on LB agar plates containing 100 $\mu\text{g/mL}$ amp and 50 $\mu\text{g/mL}$ spec. After 11 h of incubation of the plates at 37 $^{\circ}\text{C}$, colonies have grown to a reasonable size and a nitrocellulose membrane was placed on top of the agar plate. When the membrane is taken off, colonies stick to it and the membrane can be placed, colonies facing up, on an induction plate containing 50 $\mu\text{g/mL}$ spec, 100 $\mu\text{g/mL}$ amp, and 1 mM IPTG. For coexpression of glycine oxidase and the transaminase of interest, the induction plates with the membranes are incubated for 8 h at 30 $^{\circ}\text{C}$. After expression, the membranes were placed in a desiccator containing chloroform for 45 s at room temperature for cell permeabilization. Afterward, membranes were placed on dialysis plates (0.4% agarose in TRIS buffer (30 mM) pH 8.5, 40 μM PLP, and 5 μM FAD) and incubated overnight at 4 $^{\circ}\text{C}$. Assaying transaminase activity was then carried out by incubation of the membranes on assay plates (1% agarose, 50 mM CHES pH 9.0 or 9.5, 1.2 mM 4-aminoantipyrine, 3.86 mM vanillic acid, 2–10 mM glyoxylate, and variable concentrations of amine donor) at 37 $^{\circ}\text{C}$. Before incubation, 1.3 mg of horseradish peroxidase lyophilizate (52 units/mg solid) dissolved in 150 μL of Milli-Q water was spread on the assay plate applied for screening. In Scheme 2, the solid-phase assay procedure is depicted for screening of an epPCR library of any transaminase of interest.

RESULTS AND DISCUSSION

Expression, Purification, and Cloning of Glycine Oxidase. The gene coding for *Geobacillus kaustophilus* glycine oxidase has been subcloned in a pCDF-1b vector carrying a CloDF13 origin of replication, which is compatible to ColE1 (other pET vectors), P15A, and RSF1030 replicon carrying vectors.²⁹ As reported by Martínez-Martínez et al. and Mortl et al. for *B. subtilis* glycine oxidase, no expression of the *Geobacillus kaustophilus* glycine oxidase was detectable without the N-terminal His-tag.^{30,31} Interestingly, the comparison of the original pET28a construct with the new pCDF-1b_HisTag_GO construct with regard to expression level revealed that the ratio of soluble to insoluble glycine oxidase increased significantly (Supporting Information 2.2). *Geobacillus kaustophilus* glycine oxidase was purified by IMAC purification using an ÄKTA-FPLC system. Desalting was carried out in a convenient one-step dialysis without any detectable protein precipitation. Expression yields of the pCDF-1b glycine oxidase

Scheme 2. General Procedure of the Solid-Phase Assay^a



^a*E. coli* BL21(DE3) cells are transformed with both plasmids coding for glycine oxidase and the transaminase library of interest (1) and colonies are grown on dual selection LB agar plates (2). Afterwards, colonies are transferred to nitrocellulose membranes (3) that are placed, colonies facing up, on induction plates containing IPTG for expression of the proteins (4). Then, cells are permeabilized by chloroform treatment (5). To eliminate false positive background color formation, permeabilized cell colonies are dialyzed overnight by placing the membranes on dialysis plates (6). Finally, screening is conducted by incubation of the membranes on assay plates (7).

construct with the His-tag amounted to 47.5 mg of purified and desalted protein per liter of LB fermentation broth.

Establishment of a Microtiter Plate Assay. In order to establish a liquid-phase assay for transaminases, the standard 4-AAP assay for detection of glycine oxidase activity was adopted for the detection of glycine produced upon the transamination reaction. Apart from horseradish peroxidase, purified glycine oxidase was added and, instead of glycine, the substrates for the transaminase of interest, glyoxylate and a range of amine donors, were added to the assay mixture. Calibration by application of glycine standards and end point measurements of absorbance at 498 nm revealed a linear range up to 0.67 mM (Supporting Information 2.1). In order to investigate the dynamic range of the assay involving continuous glycine formation, sequential dilutions of a purified (*R*)-selective transaminase were applied and screened against racemic α -phenylethylamine by following the increase of absorbance at 498 nm. Thus, an asymptotic relationship between the value of the observed initial rate and the amount of purified transaminase applied in the assay was ascertained (Figure 1).

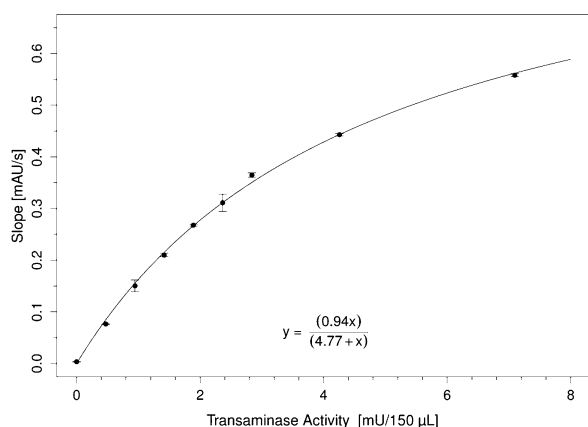


Figure 1. Relation between observed initial rate and transaminase activity. A purified (R)-selective transaminase was sequentially diluted and screened against racemic α -phenylethylamine.

For low transaminase activities up to 2 mU per well, a nearly linear relationship between the observed initial rate and the amount of transaminase activity in the assay has been found. The nonlinear relationship for higher transaminase activities can be explained by the fact that the transamination reaction is no longer the rate-determining step and the amount of assay enzymes has to be increased in turn to guarantee a faster downstream conversion of glycine to form the quinone imine.¹² These results are in accordance with the results of Barber et al., who also needed a >100-fold excess of assay enzymes for a linear relationship.¹² Increasing the amount of glycine oxidase in the assay could potentially lead to a larger dynamic range but would require the use of greater concentrations of purified GO. Controls without transaminase gave a negligible slope of $\sim 3 \times 10^{-3}$ mAU/s which may be explained by autocatalytic quinone imine dye formation. Hence, it was demonstrated that the assay distinguishes different transaminase activities, provided the amount of assay enzymes is adapted.

As a next step, it should be demonstrated that the glycine oxidase assay is suitable to screen different transaminases in crude lysate for acceptance of different amines. In order to do so, 25 different wild-type transaminase genes (Supporting Information 1.1.1) were expressed in *E. coli* BL21(DE3) in duplicates in a 96-deep-well block including a negative control of cells carrying an empty vector. The cells were lysed and two different dilutions of the resulting lysate were applied for a microtiter plate screening in both acetophenone assay and glycine oxidase assay against (R)- and (S)- α -phenylethylamine under identical conditions. On the basis of the data derived from the acetophenone assay, volumetric activities for each transaminase duplicate were calculated and compared with the slopes derived from the glycine oxidase assay.

All transaminases that have been found active against (R)- or (S)- α -phenylethylamine in the photometric assay were also found active in the glycine oxidase assay. As screening in crude lysate causes high deviations, only rough comparisons between the data were made and no quantitative correlation was made (Table 1). In our screening, a slope of more than 2-fold as high as the background signal was detected in the duplicates of the (S)-selective transaminase from *Vibrio fluvialis* in the glycine oxidase assay when screened against the (R)-enantiomer of α -phenylethylamine, while no increase of absorbance could be detected in the acetophenone assay. Particularly, for low

Table 1. Substrate Profiling Results of 15 Different Transaminases (Supporting Information 1.1.1) for Acceptance of (R)- and (S)- α -Phenylethylamine Obtained by the Glycine Oxidase Assay Screening in Crude Lysate Opposed to Results Obtained by Screening with the Acetophenone Assay

	Acetophenone-Assay	GO-Assay	
(R)-Selective	AspFum	+	++
	AspOry	+	++
	AspTer	+	+
	ATA117	+	++
	GamPro	+	+
	JanSp	+++	+++
	LabAle	+	++
	MycVan	+	+++
	NeoFis	+	++
	RhiEtl	+++	++++
(S)-Selective	3IST	0	0
	3FCR	0	0
	Cvi	0	0
	Vfi	0	+
	3HMu	+	+
(R)-Selective	AspFum	0	0
	AspOry	0	0
	AspTer	0	0
	ATA117	0	0
	GamPro	0	0
	JanSp	0	0
	LabAle	0	0
	MycVan	0	0
	NeoFis	0	0
	RhiEtl	0	0
(S)-Selective	3IST	++	++
	3FCR	+	++
	Cvi	+++	+++
	Vfi	++++	++++
	3HMu	++++	++++
	Activity	Activity	

transaminase activities (<0.5 mU per well), the discrimination of actual transaminase activity from background noise is difficult in the glycine oxidase assay and may result in false positives and/or negatives. Prolonged measurements and increased amounts of lysate can help to solve these problems.

For prescreening and substrate profiling, 0.12 mg/mL glycine oxidase (200 mU/well) proved to be sufficient for discrimination of a total transaminase activity of 0.5 mU per well (150 μ L). Hence, one liter of shake flask fermentation broth provides enough glycine oxidase (47.5 mg of glycine oxidase yield) for prescreening of more than 20 microtiter plates (150 μ L for each well).

Establishment of a Solid-Phase Assay. Initially, it was planned to apply purified glycine oxidase together with horseradish peroxidase onto the assay plates to screen colonies having expressed exclusively the transaminase of interest. However, this approach was discarded as only diffuse color formation in the whole assay agar was observed in preliminary experiments (data not shown) as reported by Willies et al. for the alanine racemase solid-phase assay.¹⁵ Additionally, limited expression yields of glycine oxidase would have been a bottleneck for high-throughput screening of large transaminase libraries. Hence, a coexpression approach was followed in which glycine oxidase is expressed together with the transaminase of interest. In this way, high local concentrations of the reactants and the involved enzymes are achieved, which makes accurate staining of the colonies possible. Additionally, no purification of the glycine oxidase is required. Cells carrying the glycine oxidase gene on a pET28a plasmid were made electro-competent and transformed with different transaminases

coded on incompatible pET22 plasmids for proving the assay's principle. As transformation efficiencies amounted to only 20 transformants per 50 ng of incompatible plasmid DNA, later the glycine oxidase gene was subcloned into a compatible pCDF-1b vector to improve transformation efficiencies. Usually, more than 10 000 transformants per 50 ng of plasmid DNA are obtained by application of the compatible glycine oxidase pCDF-1b construct providing the possibility to transform error prone PCR based libraries for directed evolution.

For all published solid-phase assays so far, horseradish peroxidase substrates derived from staining protocols of immunohistochemistry or immunocytochemistry (like 4-chloronaphthol or 3,3-diaminobenzidine) have been applied as chromogenic substrates,^{14–18} as they are initially soluble for good distribution and then precipitate *in situ* upon oxidation by horseradish peroxidase to prevent diffusion and to allow accurate staining.³² However, the pH-working range of these horseradish peroxidase substrates is below pH 8.0,³³ while many transaminases are reported to have a narrow pH optimum above pH 9.0.²⁰ However, in all experiments involving 4-chloronaphthol and α -phenylethylamine, a yellow side product was formed preferably at pH values higher than pH 7.5. Hence, an alternative horseradish peroxidase substrate offering a higher sensitivity and screening at pH values above pH 9.0 was required. In this study, we successfully applied 4-aminoantipyrine and phenol or vanillic acid, respectively, as horseradish peroxidase staining substances for detection of hydrogen peroxide in a solid-phase assay at pH 9.0 and pH 9.5. In this way, we were able to detect low transaminase activities of approximately 50 mU/mg of an ordinarily overexpressed transaminase without problems of diffuse color formation or dye diffusion, despite the fact that the quinone imine dye is soluble. Thus, even transaminase activities corresponding to the activity of 3FCR toward (S)- α -phenylethylamine (0.4 U/mL crude lysate) can be detected in less than 1 h of incubation of the membrane on assay plates. In case of decently active transaminases like the 3HMU transaminase, staining begins already within 5 min of incubation at pH 9.0 or pH 9.5 on assay agar instead of hours of incubation at pH 7.5 by application of 4-chloronaphthol, as screening conditions could be harmonized to the pH optimum of 3HMU. Membranes can be taken off the assay agar after up to approximately 5 h of incubation depending on the amount of dye that has been formed and can be dried before considerable diffusion of the dye is relevant (Supporting Information 2.S.1).

In order to allow discrimination of low initial transaminase activities for acceptance of a desired amine compound, it is required that absolutely no staining of the colonies occurs that is not due to conversion of that amine. Hence, it should be investigated whether background color formation of an active transaminase occurs when no amine is supplemented in the assay agar. To do so, BL21(DE3) *E. coli* cells having coexpressed glycine oxidase and highly active 3HMU transaminase were placed on assay agar without amine donor. However, all colonies placed on assay agar without amine showed considerable color formation most likely due to hydrogen peroxide generated by oxidation of intracellular glycine or transamination of other intracellular amines. In order to solve these problems of high and unspecific background noise, an on-membrane dialysis step at 4 °C was introduced. After cell permeabilization, the nitrocellulose membranes were placed on a 0.45% agarose agar plate overnight to allow low

molecular weight compounds to diffuse into the dialysis agar. Membranes after dialysis did not show any unspecific color formation on assay plates without amine, while controls, that were placed on LB agar plates at 4 °C and treated with chloroform for cell permeabilization afterward, showed unspecific color formation (Figure 2).

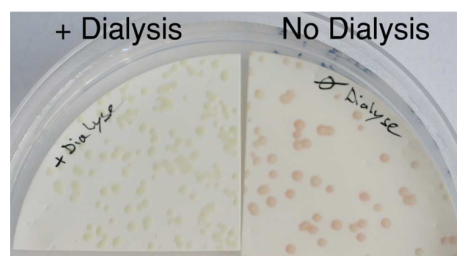


Figure 2. On-membrane dialysis diminishes background color formation. BL21(DE3) *E. coli* cells having coexpressed 3HMU and glycine oxidase after 2 h of incubation at 37 °C on an assay plate without amine donor. The left membrane was treated with chloroform after expression for cell permeabilization and placed on a dialysis plate overnight at 4 °C before screening. The right membrane was placed on an LB agar plate at 4 °C overnight after expression and then treated with chloroform before screening. Overnight dialyzed samples did not show unspecific staining compared to samples that had not been dialyzed.

To investigate the sensitivity of the solid-phase assay, the (S)-selective transaminases 3HMU and 3FCR were applied to the solid-phase assay procedure (Scheme 2) and screened against 10 mM racemic α -phenylethylamine at 37 °C for 30 min (Figure 3). Colonies expressing 3HMU became intensely red

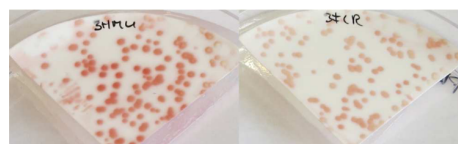


Figure 3. (S)-selective transaminases 3HMU (left) and 3FCR (right) showed different color intensities after 30 min of incubation at 37 °C on assay agar supplemented with 10 mM rac- α -phenylethylamine, owing to the difference in their activity.

colored within minutes of incubation on the assay agar, while the 3FCR sample, which showed a 40-fold lower volumetric activity in crude lysate screened in the acetophenone assay (0.4 U/mL instead of 16 U/mL) was less intensely colored, while samples incubated on assay agar without amine did not develop color at all (Supporting Information 2.S.2). As the detection limit depends also on the expression level of the transaminase of interest, no specific activities shall be compared.

To prove the applicability of the solid-phase assay as a prescreening method for error-prone PCR libraries that usually contain many inactive variants due to stop-codon and/or deleterious mutations incorporation, mixtures of cells carrying plasmids coding for glycine oxidase and different transaminases have been plated out. Mixtures of cells carrying transaminases of variable activity, namely 3HMU (16 U/mL), 3FCR (0.4 U/mL) and 3GJU (inactive), were prepared. These plates were screened against 2 mM (S)-phenylethylamine and 4 mM glyoxylate. Active transaminases 3HMU and 3FCR (Supporting Information 2.S.3) could be discriminated from inactive

transaminase 3GJU carrying colonies. Mixtures of 3HMU and 3FCR transaminases containing colonies showed different staining intensities of colonies on the membrane according to their volumetric activities (Supporting Information 2.5.3).

Currently, the solid-phase assay is applied in our group for screening epPCR libraries. To evaluate the viability of the variants, the libraries are screened against α -phenylethylamine acceptance, a substrate well accepted by the template. The screening results in different pattern of coloring, as expected (Supporting Information 2.5.4). Colored colonies were picked as positive hits, and noncolored colonies were negative (inactive variants). These variants were expressed and were tested for activity in the acetophenone assay against α -phenylethylamine. The results were in line with the solid-phase assay; the positive hits have shown activity, while the negative ones did not have any detectable activity.

Screening of an epPCR library of 3HMU that possesses an average mutation frequency of 10 mutations per gene against the more bulky (S)- α -phenylpropylamine in the solid-phase assay resulted in a small number of colored colonies (Figure 4). These colonies were picked, and their activity toward (S)-phenylpropylamine was confirmed by a photometric assay, similar to the acetophenone assay (data not shown).



Figure 4. Solid-phase assay screening of a 3HMU epPCR library that possesses an average mutation frequency of 10 mutations per gene against (S)- α -phenylpropylamine led to a small number of colored colonies that are currently under investigation.

CONCLUSION

In this study, we demonstrated the proof of principle for a novel assay that allows screening and substrate profiling of transaminases for acceptance of a range of (R)- or (S)-amines. Expression and purification of glycine oxidase is easily manageable in shake flasks using *E. coli* as expression strain leading to high yields of recombinant protein sufficient to screen more than 20 microtiter plates of transaminase variants with GO obtained from one liter of LB fermentation broth. In addition, the assay is amenable for high-throughput prescreening of transaminase libraries on nitrocellulose membranes enabling directed evolution of transaminases for enhanced activity toward any amine substrate. The solid-phase assay provides a sensitivity that allows discrimination of specific activities of 50 mU/mg of an ordinary overexpressed transaminase from inactive variants.

ASSOCIATED CONTENT

Supporting Information

Additional information as noted in text. This material is available free of charge via the Internet at <http://pubs.acs.org>.

AUTHOR INFORMATION

Corresponding Authors

*E-mail: matthias.hoehne@uni-greifswald.de.

*E-mail: uwe.bornscheuer@uni-greifswald.de.

Author Contributions

M.S.W. and M.H. developed the assay. M.S.W., M.H., and U.T.B. designed the experiments. M.W.S. and I.V.P. conducted the experiments. All authors interpreted the data, wrote the manuscript, and have given approval to the final version of the manuscript.

Notes

The authors declare no competing financial interest.

ACKNOWLEDGMENTS

All authors would like to thank Daniel Last for the graphic design of Scheme 2, as well as Enzymicals AG for providing the empty pCDF-1b vector. M.S.W. would like to thank Javier S. Aberturas, Alberto Nobili, and Maika Genz (all from our group) for their general support and Harald Kolmar and Wolf-Dieter Fessner (both Darmstadt University) for making an external master-thesis possible.

REFERENCES

- (1) Percudani, R.; Peracchi, A. *EMBO Rep.* **2003**, *4*, 850.
- (2) Kohls, H.; Steffen-Munsberg, F.; Höhne, M. *Curr. Opin. Chem. Biol.* **2014**, *19*, 180.
- (3) Höhne, M.; Bornscheuer, U. T. *ChemCatChem* **2009**, *1*, 42.
- (4) Bornscheuer, U. T.; Huisman, G. W.; Kazlauskas, R. J.; Lutz, S.; Moore, J. C.; Robins, K. *Nature* **2012**, *485*, 185.
- (5) Savile, C. K.; Janey, J. M.; Mundorff, E. C.; Moore, J. C.; Tam, S.; Jarvis, W. R.; Colbeck, J. C.; Krebber, A.; Fleitz, F. J.; Brands, J.; Devine, P. N.; Huisman, G. W.; Hughes, G. J. *Science* **2010**, *329*, 305.
- (6) Mathew, S.; Shin, G.; Shon, M.; Yun, H. *Biotechnol. Bioprocess Eng.* **2013**, *18*, 1.
- (7) Schätzle, S.; Höhne, M.; Redestad, E.; Robins, K.; Bornscheuer, U. T. *Anal. Chem.* **2009**, *81*, 8244.
- (8) Hopwood, J.; Truppo, M. D.; Turner, N. J.; Lloyd, R. C. *Chem. Commun.* **2011**, *47*, 773.
- (9) Pollegioni, L.; Motta, P.; Molla, G. *Appl. Microbiol. Biotechnol.* **2013**, *97*, 9323.
- (10) Leese, C.; Fotheringham, I.; Escalettes, F.; Speight, R.; Grogan, G. J. *Mol. Catal. B* **2013**, *85–86*, 17–22.
- (11) Donini, S.; Ferrari, M.; Fedeli, C.; Faini, M.; Lamberto, I.; Marletta, A. S.; Mellini, L.; Panini, M.; Percudani, R.; Pollegioni, L.; Cالدinelli, L.; Petrucco, S.; Peracchi, A. *Biochem. J.* **2009**, *422*, 265.
- (12) Barber, J. E. B.; Damry, A. M.; Calderini, G. F.; Walton, C. J. W.; Chica, R. A. *Anal. Biochem.* **2014**, *463*, 23.
- (13) Bornscheuer, U. T.; Altenbuchner, J.; Meyer, H. H. *Biotechnol. Bioeng.* **1998**, *58*, 554.
- (14) Delgrave, S.; Murphy, D. J.; Rittenhouse Pruss, J. L.; Maffia, A. M.; Marrs, B. L.; Bylina, E. J.; Coleman, W. J.; Grek, C. L.; Dilworth, M. R.; Yang, M. M.; Youvan, D. C. *Protein Eng.* **2001**, *14*, 261.
- (15) Willies, S. C.; White, J. L.; Turner, N. J. *Tetrahedron* **2012**, *68*, 7564.
- (16) Gerstenbruch, S.; Wulf, H.; Mußmann, N.; O'Connell, T.; Maurer, K.-H.; Bornscheuer, U. T. *Appl. Microbiol. Biotechnol.* **2012**, *96*, 1243.
- (17) Marina, A.; Enright, A.; Dawson, M. J.; Mahmoudian, M.; Turner, N. J. *Angew. Chem., Int. Ed.* **2002**, *41*, 3177.
- (18) Escalettes, F.; Turner, N. J. *ChemBioChem* **2008**, *9*, 857.

- (19) Green, A. P.; Turner, N. J.; O'Reilly, E. *Angew. Chem., Int. Ed.* **2014**, *53*, 10714.
- (20) Steffen-Munsberg, F.; Vickers, C.; Thontowi, A.; Schätzle, S.; Tumlirsch, T.; Svedendahl Humble, M.; Land, H.; Berglund, P.; Bornscheuer, U. T.; Höhne, M. *ChemCatChem* **2013**, *5*, 150.
- (21) Shin, J.-S.; Kim, B.-G. *Biotechnol. Bioeng.* **2002**, *77*, 832.
- (22) Park, E.-S.; Dong, J.-Y.; Shin, J.-S. *Appl. Microbiol. Biotechnol.* **2014**, *98*, 651.
- (23) Martínez-Martínez, I.; Navarro-Fernández, J.; García-Carmona, F.; Takami, H.; Sánchez-Ferrer, Á. *Proteins* **2007**, *70*, 1429.
- (24) Holt, A.; Sharman, D. F.; Baker, G. B.; Palcic, M. M. *Anal. Biochem.* **1997**, *244*, 384.
- (25) Holt, A.; Palcic, M. M. *Nat. Protocols* **2006**, *1*, 2498.
- (26) R Development Core Team. *R: A language and environment for statistical computing*; R Foundation for Statistical Computing: Vienna, Austria, 2014.
- (27) Wickham, H. *Ggplot2 : Elegant graphics for data analysis*; Springer: New York, 2009.
- (28) Steffen-Munsberg, F.; Vickers, C.; Thontowi, A.; Schätzle, S.; Meinhardt, T.; Svedendahl-Humble, M.; Land, H.; Berglund, P.; Bornscheuer, U. T.; Höhne, M. *ChemCatChem* **2013**, *5*, 154.
- (29) Tolia, N. H.; Joshua-Tor, L. *Nat. Meth.* **2006**, *3*, 55.
- (30) Martínez-Martínez, I.; Navarro-Fernández, J.; Lozada-Ramírez, J. D.; García-Carmona, F.; Sánchez-Ferrer, A. *Biotechnol. Prog.* **2006**, *22*, 647.
- (31) Mortl, M.; Diederichs, K.; Welte, W.; Molla, G.; Motteran, L.; Andriolo, G.; Pilone, M. S.; Pollegioni, L. *J. Biol. Chem.* **2004**, *279*, 29718.
- (32) Lottspeich, F. *Bioanalytik*, 2nd ed.; Spektrum Akademischer Verlag: Heidelberg, 2006.
- (33) Mesulam, M. M.; Rosene, D. L. *J. Histochem. Cytochem.* **1979**, *27*, 763.

Identification of (S)-selective transaminases for the asymmetric synthesis of bulky chiral amines

Ioannis V. Pavlidis^{1,2}, Martin S. Weiß¹, Maika Genz¹, Paul Spurr³, Steven P. Hanlon³, Beat Wirz³, Hans Iding^{3*} and Uwe T. Bornscheuer^{1*}

The use of transaminases to access pharmaceutically relevant chiral amines is an attractive alternative to transition-metal-catalysed asymmetric chemical synthesis. However, one major challenge is their limited substrate scope. Here we report the creation of highly active and stereoselective transaminases starting from fold class I. The transaminases were developed by extensive protein engineering followed by optimization of the identified motif. The resulting enzymes exhibited up to 8,900-fold higher activity than the starting scaffold and are highly stereoselective (up to >99.9% enantiomeric excess) in the asymmetric synthesis of a set of chiral amines bearing bulky substituents. These enzymes should therefore be suitable for use in the synthesis of a wide array of potential intermediates for pharmaceuticals. We also show that the motif can be engineered into other protein scaffolds with sequence identities as low as 70%, and as such should have a broad impact in the field of biocatalytic synthesis and enzyme engineering.

Transaminases (TAs) are emerging as a promising alternative to the use of traditional transition-metal catalysis for the synthesis of chiral amines^{1–3}. TAs are pyridoxal-5'-phosphate (PLP)-dependent enzymes that catalyse the asymmetric synthesis of chiral amines via reductive amination of ketones, with D- or L-alanine or isopropylamine used commonly as amine donors^{4,5}. As a general rule, TAs that belong to fold class IV using D-alanine as amine donor are referred to as (R)-selective TAs, while those belonging to fold class I using L-alanine are referred to as (S)-selective TAs. Asymmetric synthesis is the preferred strategy for the production of chiral amines as the theoretical yield is 100%, in contrast to the thermodynamically favoured kinetic resolution with a maximum of 50% theoretical yield. Although the equilibrium can be shifted to the desired product by means of enzymatic cascades^{3,6,7} or by using amine donors that shift the equilibrium^{2,8}, the major challenge for the application of TAs is their limited substrate scope. All known wild-type TAs form their active site, consisting of a large and a small binding pocket, by dimerization of the monomer. In almost all cases, the small binding pocket is restricted to accommodate only a methyl group⁹. As such, engineering TAs to accept bulkier substituents is of high synthetic relevance.

The synthetic potential of TAs, at least for the fold class IV enzymes, has been highlighted by the biosynthetic large-scale production of the antidiabetic drug sitagliptin, established in a joint effort by researchers from Merck & Co. and Codexis, which replaced the previously applied asymmetric chemical hydrogenation^{2,10}. However, the (R)-selective TA from *Arthrobacter* sp., which was selected as a template, required substantial protein engineering (8% of its entire sequence) to accept the pro-sitagliptin precursor and to tolerate the reaction conditions required for this specific industrial process. The TAs with (S)-stereopreference belong to fold class I and differ substantially in structure from fold class IV (R)-TA. Hence, this precludes a simple transfer of knowledge from (R)-TA to engineer an (S)-TA, especially with respect to the acceptance of bulky substrates.

Although some reports regarding the engineering of (S)-TA have been published, they mostly focus on engineering the small binding

pocket to accept ethyl^{11–13} or propyl^{11,13–15} side chains adjacent to the carbonyl function. In all these publications, similar positions are mentioned, all of which are a reasonable distance from the PLP cofactor and the bound substrate. As each of these studies focused on different enzyme templates and substrates, no general solution has been identified to date. For instance, Han and co-workers suggested that mutation L57A in the *Ochrobactrum anthropic* TA increases 110-fold the acceptance of a propyl residue in the small binding pocket in asymmetric synthesis¹¹, but Nobili *et al.* saturated the respective position (L57) in the *Vibrio fluvialis* TA and screened with the same substrate, and did not find any variant with improved activity¹⁴. Consequently, the transfer of knowledge from one template enzyme for a given substrate to another is not a simple operation.

With this challenge in mind, we targeted the identification of novel TAs that accept sterically highly demanding compounds via a rationalized intelligent design that is easily transferable to other enzyme scaffolds (Fig. 1). To highlight the synthetic potential of the developed biocatalysts, their applicability was exemplified for a set of sterically demanding aromatic compounds that are useful, representatively, for the synthesis of a range of potential pharmaceutical intermediates (Fig. 2, compounds 1–3), in addition to some widely used and less bulky substrates (Fig. 2, compounds 5–7), and acetophenone (4) serving as benchmark substrate.

Results

Initial screening for appropriate enzyme scaffolds. In all protein engineering efforts the most important question is 'Which scaffold is evolvable?'—a question usually answered with hindsight. To identify a suitable scaffold for the present study, all in-house wild type TAs from fold classes I and IV (Supplementary Table 1), as well as some interesting variants discovered previously by our research group^{9,16}, were screened in the thermodynamically favoured kinetic resolution mode, using the racemic amines of interest (1a to 3a) as donors and pyruvate as the amine acceptor. Several of these enzymes had minor activity towards amines 2a and 3a, but no

¹Department of Biotechnology, Institute of Biochemistry, University of Greifswald, Felix-Hausdorff-Str. 4, D-17489 Greifswald, Germany. ²Department of Biochemistry, University of Kassel, Heinrich-Plett-Str. 40, D-34132 Kassel, Germany. ³Process Research and Development, Biocatalysis, F. Hoffmann-La Roche Ltd, Grenzacher Str. 124, 4070 Basel, Switzerland. *e-mail: uwe.bornscheuer@uni-greifswald.de; hans.iding@roche.com

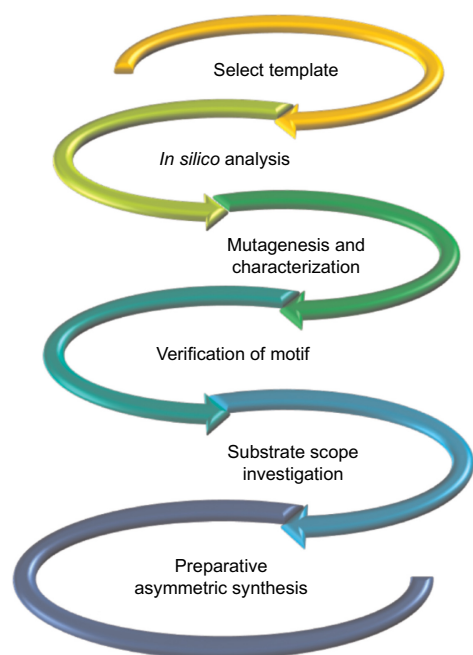


Figure 1 | Schematic representation of the strategy pursued for the identification of novel TAs active towards bulky substrates.

A pre-screening of in-house TAs with the bulky amines of interest (**1a–3a**, Fig. 2) was performed to select the optimal template for engineering. *In silico* analysis of the quinonoid intermediate was then performed to understand the interactions of the substrate with the amino acids in the binding pocket of the selected TA. This analysis identified positions, which were mutated and the corresponding variants were characterized. From this we derived a distinct motif, which was verified by identification of novel TAs with as low as 70% sequence identity. Their substrate scope towards bulky amines was investigated and, finally, the applicability of the identified enzyme variants was exemplified by preparative asymmetric synthesis.

wild-type enzyme was active against **1a**. At this point it needs to be stated that researchers often design their protein engineering efforts around an enzyme that is highly active towards benchmark substrates such as acetophenone (**4b**). In the area of (S)-selective TAs, the enzymes most commonly used for such purposes are the TAs from *Vibrio fluvialis* (VF-TA)^{14,17} or *Chromobacterium violaceum* (CV-TA)^{18,19}. Both enzymes are well studied and their three-dimensional structures are known, so they might appear to be ideal candidates to consider first; they were even among the enzymes that exhibited a minor activity towards amines **2a** and **3a**. However, we decided to proceed with the fold class I TA from *Ruegeria* sp. TM1040 (abbreviated as 3FCR, according to its Protein Data Bank (PDB) code)¹⁶ as the most suitable scaffold, despite it being far from an efficient biocatalyst, even for the benchmark substrate 1-phenylethylamine (**4a**)¹⁶. In previous work by our group, two single mutants of this enzyme (Y59W and T213A) were constructed, based on data derived from an alignment with VF-TA and CV-TA, which exhibit increased catalytic activity towards this benchmark substrate in kinetic resolution²⁰. The specific activity improvement of these single mutants underlined the potential evolvability of this scaffold and thus we selected it for further investigations. Although there was no indication that these mutants would possess any activity towards much bulkier substrates, they did exhibit a minor activity towards all three substrates of interest. The double mutant variant (3FCR Y59W/T213A), which we constructed directly after these positive findings, exhibited surprisingly high activity when challenged with the bulky substrates **2a** and **3a**, and also considerable turnover for amine **1a** (Table 1).

In contrast, while VF-TA and CV-TA have exactly these residues in the respective positions in their sequence, they do not accept amine **1a** at all, which thus supports our engineering strategy and choice of 3FCR as the starting scaffold. As this was the only variant from our collection that exhibited activity towards all bulky ketones, we selected this double mutant of 3FCR for subsequent engineering steps.

Rational design of TAs for the acceptance of bulky amines. To further improve the activity and to identify a motif for the acceptance of the bulky amines selected in this work, we investigated the active site of the selected scaffold (3FCR) via molecular docking and subsequent energy minimization in an aqueous environment (Supplementary Section ‘Bioinformatic analysis’). As formation of the quinonoid intermediate is the most energetically demanding step in the catalytic mechanism of TAs (Supplementary Fig. 1) and at the same time the most spatially demanding due to its planar character²¹, we modelled the respective intermediates for all compounds of interest (**1–3**) in the active centre of the enzyme and subsequently energy-minimized the complex. This analysis served as a first filter to identify possible clashes that could hinder the acceptance of bulky substrates. In a second step, we investigated the interactions of the quinonoids with the neighbouring residues to identify positions of interest, or residues that may result in disfavoured interactions. As shown in Fig. 3 (which shows the quinonoid of amines **1a** and **2a** in the active site of the wild-type 3FCR), we identified three more amino-acid residues as potentially influential: Y87 (located in the small binding pocket), Y152 (which coordinates the PLP) and P423 (which lies above the quinonoid at the entrance of the active site). The rationale for the subsequent protein engineering of each position was based on the following concepts:

First, Y87 interacts with the moiety of the substrate that is accommodated in the small binding pocket. As long as all compounds of interest possess an aromatic ring, which needs to be accommodated there, we anticipated that an aromatic residue could facilitate π – π interactions and lead to favourable interactions. As expected, the mutation to phenylalanine was the best option in this position (Y87F) as it provides more space compared to the tyrosine, while the hydroxyl functionality that introduces polarity to the region is removed (Table 1). To demonstrate that steric hindrance is not in fact the only reason for the inefficiency of TA towards bulky substrates, the valine variant was prepared (Y87V). However, the activity was significantly lower (for instance, 97% decreased activity towards **2a**). This highlights the fact that the aromatic residue is crucial for the acceptance of the substrates of interest. Curiously, wild-type VF-TA and CV-TA already have a phenylalanine residue in this position, but they do not possess significant activity for substrates **1** to **3**.

Second, for residue 152, the aromatic ring of the tyrosine of the wild-type enzyme coordinates the PLP and thus it appears prudent to keep an aromatic amino acid in this position. Consequently, a phenylalanine substitution was chosen in order to remove any negative effect of the hydroxyl functionality of tyrosine, which points towards the PLP phosphate group. Indeed, mutation Y152F provided a positive impact on the catalytic behaviour of 3FCR by having a pronounced effect on the stability of the enzyme (Supplementary Fig. 2), probably due to the stabilization of the PLP in the active site. More than that, the activity towards bulky substrates **1a** and **3a** was significantly increased (Table 1), possibly due to the decreased polarity around the PLP molecule. As this specific residue does not directly interact with the substrate, a saturation mutagenesis was performed using the NNK codon, yet no additional useful variants were found for amines **1a** to **3a**.

Third, prolines are known to provide rigidity due to restrictions on the protein’s secondary structure²². P423 lies at a loop at the entrance of the active site, directly above the quinonoid (Fig. 3)

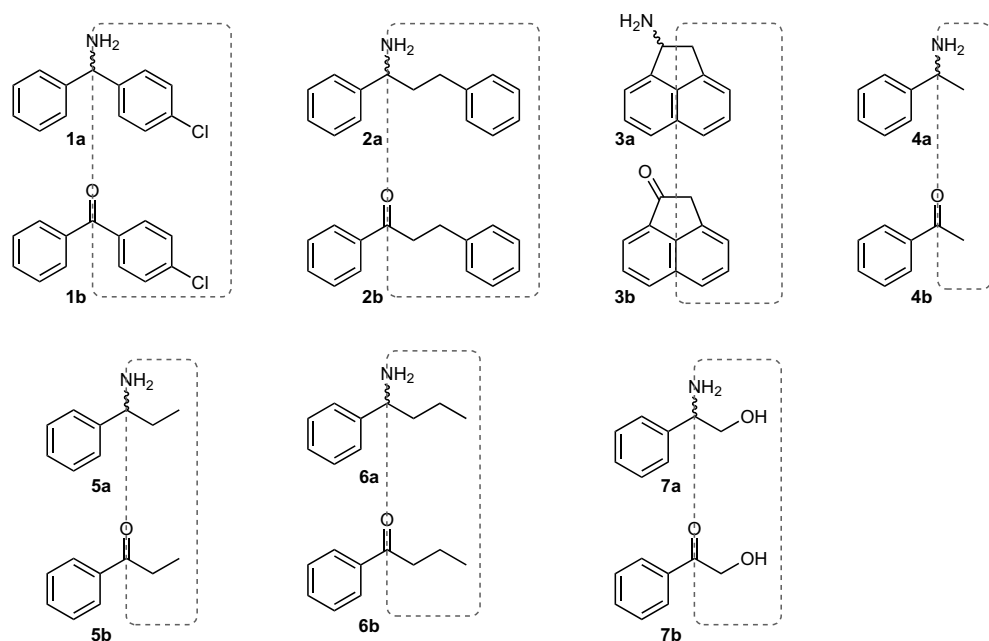


Figure 2 | Selected compounds of interest for the present study. Amines **1a–3a** were selected as primary targets for the identification of novel TAs. 1-Phenylethylamine (**4a**) was selected as the benchmark compound, because it is widely accepted by most TAs, as is well documented in the literature. To further highlight the applicability of the novel biocatalysts identified, they were further used for amines **5a–7a**, all still bulkier than the benchmark amine **4a**. The objective was the preparation of optically pure amines starting from the respective ketones **1b–7b**. The region delineated by a box for each molecule is accommodated within the small binding pocket of the TAs according to the experimental results. As observed, it is not always the smaller substituent that is directed to the small binding pockets (as exemplified by compounds **1** and **2**).

and thus a more flexible loop was potentially expected to be beneficial for the diffusion of the bulky substrates to the active sites and facilitate their acceptance. Interestingly, the respective loop in the case of CV-TA is shorter by two residues, leaving the active site more accessible, while VF-TA has a glycine, which should provide enough flexibility. Histidine was selected as replacement for our template, as it could coordinate the aromatic compounds into and out of the active site. Variant P423H indeed increased the activity significantly (Table 1), but at the expense of stability (Supplementary Fig. 2). Therefore, although this histidine variant is useful for early supply of chiral intermediates via the thermodynamically favoured kinetic resolution, the targeted asymmetric synthesis requires TAs with high process stability (for example, elevated temperature, increased organic solvent content, substrate and amine donor concentration) to shift the reaction equilibrium and to achieve complete conversion. As the mutation P423H variant lacked sufficient stability, it was discarded from the motif identified by us.

Intriguingly, the rational mutations introduced one after another to effect increasing acceptance of bulky amines continuously raised the apparent activity except for the benchmark substrate **4a** (Table 1), indicating that steric hindrance is not the only reason for non-acceptance of the substrates; indeed, specific interactions for the binding of the reactants are a crucial factor to achieve catalytic efficiency. Compared to the initial activities of the starting scaffolds (3FCR wild-type or 3FCR Y59W), the specific activities of the mutants could be increased up to 8,900-fold, as shown for compound *rac*-**2a** using the variant bearing all five mutations (Table 1).

The individual positions identified for the functional motif have been mentioned in previous publications in which the interactions of the PLP or the quinonoid of (S)-selective TAs were systematically analysed. For instance, Han and co-workers identified several positions as beneficial during their bioinformatics analysis of the TA from *Ochrobactrum anthropi*, including the positions corresponding to 59, 87 and 152 (ref. 11). Nonetheless, even though they

were working with bulky aryl-alkylamines, their screening led them to discard alterations to all these positions and to focus on a different one (corresponding to L58 in 3FCR). Midelfort *et al.* focused on 55 positions in VF-TA (12% of the entire sequence) including the positions corresponding to 59 and 87 in 3FCR (ref. 17). In their work an improved variant with eight mutations was identified, which in this case included the respective mutants W59F and F87A (two of the four positions of the motif proposed herein). Similarly, Deszcz and co-workers engineered the CV-TA to transform it from an ω -TA to an α -TA and they identified 11 interesting positions, including all four positions we have suggested²³. However, after an NNK saturation of all positions, they diverged from the motif we identified. Wild-type CV-TA already contains the W59, F87 and A231 amino-acid residues, but in respective position 152, they identified methionine as the best variant. This result is interesting, as Nobili *et al.*, who worked with VF-TA and identified positions corresponding to 87 and 152 as favourable for the acceptance of phenylbutylamine (**6a**) and phenylglycinol (**7a**), also identified a methionine substitution as the best choice for position 152 in kinetic resolutions¹⁴. When we investigated the best variants of VF-TA in this work (namely Y150M/V152A, F85L/Y150M/V153A and F85L/V153) in the kinetic resolution of our amines of interest, we noticed significantly lower activities (for instance, 0.3 U mg^{−1} for **2a**, while our best variant had 8.9 U mg^{−1}).

All the aforementioned examples highlight that, although certain positions have been mentioned in the literature (numerous further positions have been targeted), an effective combination for the acceptance of bulky substrates has not been determined. Strikingly, although the wild-type VF-TA and CV-TA already contain the suggested amino-acid residues at three positions (W59, F87 and A231) they are not efficient catalysts for the desired bulky substrates **1** to **3** addressed here. Incorporating all four amino acids identified as crucial motifs (Y59W, Y87F, Y152F and T213A) and choosing the much more appropriate scaffold 3FCR enabled us to create a TA with significant activity for all

Table 1 | Specific activity (U mg⁻¹) of purified 3FCR and 3GJU mutants as determined in kinetic resolution mode using pyruvate as amine acceptor.

	<i>rac</i> -(1a)	<i>rac</i> -(2a)	<i>rac</i> -(3a)	<i>rac</i> -(4a)
3FCR wild-type	NA	0.001 ± 0.000	0.014 ± 0.000	0.017 ± 0.000
3FCR Y59W	0.002 ± 0.000	0.50 ± 0.02	0.27 ± 0.01	0.502 ± 0.004
3FCR T231A	NA	0.019 ± 0.001	0.065 ± 0.001	0.16 ± 0.01
3FCR Y59W/T231A	0.005 ± 0.000	0.92 ± 0.03	0.075 ± 0.005	0.83 ± 0.01
3FCR Y59W/Y87F/T231A	0.32 ± 0.01	3.3 ± 0.4	0.51 ± 0.01	2.3 ± 0.1
3FCR Y59W/Y87F/Y152F/T231A	0.54 ± 0.01	2.9 ± 0.1	0.66 ± 0.08	1.0 ± 0.4
3FCR Y59W/Y87F/Y152F/T231A/P423H	0.62 ± 0.04	8.9 ± 1.1	1.38 ± 0.01	1.4 ± 0.1
3GJU wild-type	NA	0.003 ± 0.000	ND	0.003 ± 0.000
3GJU Y60W/T232A	0.003 ± 0.000	0.66 ± 0.02	0.11 ± 0.01	0.34 ± 0.01
3GJU Y60W/Y88F/Y153F/T232A/P423H	0.22 ± 0.02	0.92 ± 0.07	0.90 ± 0.08	0.45 ± 0.01

NA, not active or below the detection limit. ND, not determined. Assay conditions: 50 mM CHES buffer pH 9.0, 0.1 mM PLP, 1 mM *rac*-amine, 2 mM pyruvate, 5% (vol/vol) DMSO, 0.002–0.8 mg ml⁻¹ purified enzyme, 30 °C.

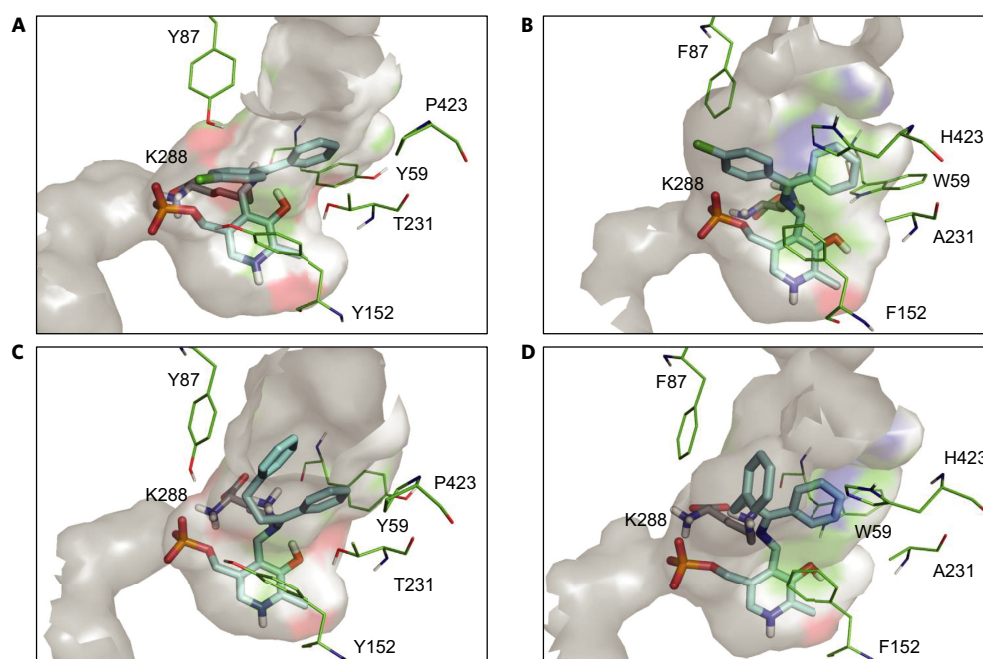


Figure 3 | Quinonoid of compounds 1a and 2a accommodated in the active site of 3FCR. A–D, The quinonoid (cyan sticks) of 1a (**A,B**) and 2a (**C,D**) was modelled and energy-minimized *in silico* into the active site of wild-type 3FCR (**A,C**) and the variant exhibiting the highest activity (3FCR Y59W/Y87F/Y152F/T231A/P423H) (**B,D**). The bulky substrates cannot be accommodated in the binding pockets of wild-type 3FCR and thus the quinonoid cannot be planar (**A,C**). When the motif of the five mutations is implemented in the scaffold, the quinonoid is accommodated much better within the engineered active site. The catalytic lysine K288 (grey stick) is located behind PLP, the residues of interest are shown as green lines, and the surface of the residues 5 Å around the quinonoid is represented in grey (40% transparency). Non-polar electrons are hidden for clarity.

substrates of interest, suggesting that both are important: the right motif and a concomitantly suitable enzyme scaffold. To support this hypothesis further, we incorporated this motif in other proteins with only moderate sequence identity to 3FCR.

Validation of the identified motif in other proteins. As our goal is a universal solution to provide researchers with a toolbox of novel TAs that can accept bulky amines, we wished to demonstrate the general applicability of the identified motif (Y59W, Y87F, Y152F, T231A and P423H). To do so, the aforementioned mutations were transferred to the fold class I TA from *Mesorhizobium loti* maff303099 (abbreviated as 3GJU from its PDB code), which has 71.5% amino-acid sequence identity to 3FCR. As in the case of the 3FCR scaffold, the wild-type 3GJU has negligible activity for the selected bulky substrates 1 to 3 (Table 1). Satisfyingly, incorporation of these five mutations into the corresponding

positions of 3GJU also enabled the acceptance of amine 1a and increased significantly the basal activity exhibited for the other two bulky amines (Table 1). These results confirm that the identified motif can be transferred to putative TAs sharing sufficient homology to the original scaffold, 3FCR, yielding variants with significant activity towards bulky substrates. To identify more TAs active towards bulky substrates we searched our in-house M5nr database²⁴ using 3FCR Y59W/Y87F/Y152F/T231A as the template. This *in silico* screening identified 100 optimal matches and, despite the fact that the sequence identity was as low as 69.2% (Supplementary Table 2), the residues in the four selected positions were conserved with respect to the 3FCR wild-type. To experimentally verify them, seven sequences of variable sequence identity towards 3FCR (see Supplementary Table 2 for identity and Supplementary Table 3 for sequences) were chosen and ordered as synthetic genes already having the four suggested

Table 2 | Specific activity and enantiomeric excess of purified TAs identified from the database analysis determined in kinetic resolution mode using pyruvate as amine acceptor.

	Specific activity (U mg ⁻¹) (enantiomeric excess)			
	<i>rac</i> -(1a)	<i>rac</i> -(2a)	<i>rac</i> -(3a)	<i>rac</i> -(4a)
TA-3	0.071 ± 0.001 (>99% (R))	1.0 ± 0.1 (>99% (S))	0.16 ± 0.03 (79% (S))	0.079 ± 0.002
TA-5	0.16 ± 0.01 (>99% (R))	0.4 ± 0.1 (>99% (S))	0.18 ± 0.02 (56% (S))	0.38 ± 0.05
TA-6	0.117 ± 0.003 (>99% (R))	0.6 ± 0.1 (>99% (S))	0.058 ± 0.005 (58% (S))	0.32 ± 0.03
TA-7	0.17 ± 0.03 (>99% (R))	0.9 ± 0.2 (>99% (S))	0.40 ± 0.03 (76% (S))	0.90 ± 0.08
TA-8	0.40 ± 0.05 (>97% (R))	1.9 ± 0.1 (>99% (S))	0.54 ± 0.02 (63% (S))	1.2 ± 0.1
TA-9	0.35 ± 0.03 (>99% (R))	4.3 ± 0.2 (>99% (S))	0.50 ± 0.02 (82% (S))	0.9 ± 0.1

Assay conditions for kinetic resolution: 50 mM CHES buffer pH 9.0, 0.1 mM PLP, 1 mM *rac*-amine, 2 mM pyruvate, 5% (vol/vol) DMSO, 0.002–0.8 mg ml⁻¹ purified enzyme, 30 °C. Assay conditions for asymmetric synthesis: 50 mM HEPES–NaOH buffer pH 8.0, 1 mM PLP, 8 mM ketone, 200 mM D,L-alanine, NAD⁺ (2–3 mM), GDH (15 U ml⁻¹), D-glucose (220 mM) and LDH (50 U ml⁻¹), 20% DMSO, 0.3–1.4 mg ml⁻¹ purified enzyme, 30 °C and 600 r.p.m. Enantiomeric excess was determined via analytical asymmetric synthesis using racemic alanine as amine donor. Note that the absolute configuration given refers to the preferentially converted enantiomer, but not the remaining enantiomer.

mutations incorporated (P423H was excluded as this mutation exhibited reduced stability and had little effect on activity). Of note, none of these seven proteins had ever been biochemically characterized, and some were not even annotated as putative TAs. Of these seven synthetic genes, six proteins could be expressed in *Escherichia coli* BL21 (DE3) using a standard protocol, and every one exhibited significant transamination activity for all bulky substrates (Table 2). These findings confirm that the motif defined herein with the selected template 3FCR has enabled us to identify novel fold type I TAs in protein sequence databases. More importantly, some of the identified enzymes exhibited higher specific activity than the 3FCR variant serving as template for their identification (for instance, TA-9 towards *rac*-2a), while several exhibited higher enantioselectivity (94% enantiomeric excess (e.e.) for 1a using the 3FCR variant, while all identified TAs exhibit higher enantioselectivity).

Nevertheless, the motif by itself is not enough to evolve significant catalytic activity towards bulky substrates in any scaffold. For instance, the well-studied VF-TA and CV-TA, with a homology identity less than 40% to 3FCR (Supplementary Table 2), already have three of the suggested amino acids (59W, 87F and 231A) incorporated into the respective required positions. For position 423, which requires flexibility at the loop, VF-TA already has a residue to provide this (glycine), while CV-TA has a shorter loop (missing two amino acids), which should provide sufficient space for the accommodation of bulky substrates. However, these enzymes still do not possess useful activity. Only phenylalanine in position 152 seems to have a universal effect, as this mutation in VF-TA confers acceptance of phenyl-propylamine¹⁴. It appears that the efficiency of this variant emerges from an improvement to the stability and to a lesser extent from an improved geometry of the active site, as discussed earlier. Hence, a certain motif is not sufficient in itself, but needs to be presented within an appropriate scaffold, which our work has identified as 3FCR.

These results are in line with protein evolutionary theory, which proposes that generalist proteins evolved to become specialists of high efficiency in a specific reaction, but with almost no promiscuous activity. This suggests that it would potentially be more successful to start from an inferior indiscriminate enzyme and evolve it, rather than attempt to evolve or reverse engineer a highly specific enzyme^{25,26}. 3FCR may have seemed at first glance unappealing, but after only four (respectively five) mutations (~1% of the entire sequence) could be tuned into a very efficient biocatalyst for the conversion of bulky ketones. At the same time, enzymes that already possess some activity towards the benchmark substrates did not leave much room for improvement, at least with the motif identified in the present study.

Substrate scope investigation. To further investigate the potential of the novel TAs for the acceptance of bulky substrates, three more compounds were selected from the literature for evaluation

Table 3 | Specific activity of purified TAs identified from the database analysis determined in kinetic resolution mode using pyruvate as amine acceptor.

	Specific activity (U mg ⁻¹)		
	<i>rac</i> -(5a)	<i>rac</i> -(6a)	<i>rac</i> -(7a)
3FCR wild-type	NA	NA	NA
3FCR Y59W/Y87F/Y152F/T231A	1.9 ± 0.2	2.06 ± 0.08	0.10 ± 0.01
TA-3	0.27 ± 0.17	0.27 ± 0.01	NA
TA-5	0.33 ± 0.03	0.328 ± 0.003	0.125 ± 0.015
TA-6	0.55 ± 0.16	0.33 ± 0.02	0.044 ± 0.001
TA-7	1.70 ± 0.03	1.81 ± 0.03	0.26 ± 0.02
TA-8	1.53 ± 0.06	1.59 ± 0.14	0.13 ± 0.03
TA-9	0.98 ± 0.03	1.39 ± 0.03	0.108 ± 0.002

All enzymes exhibited perfect enantioselectivity (>99% enantiomeric excess) towards (S)-5a, (S)-6a and (R)-7a. NA, not active or below the detection limit. Assay conditions for kinetic resolution: 50 mM CHES buffer pH 9.0, 0.1 mM PLP, 1 mM *rac*-amine, 2 mM pyruvate, 0.1% (vol/vol) DMSO, 0.02 mg ml⁻¹ purified enzyme, 30 °C. Assay conditions for asymmetric synthesis: 50 mM HEPES buffer pH 8.0, 1 mM PLP, 8 mM ketone, 200 mM D,L-alanine, NAD⁺ (2–3 mM), GDH (15 U ml⁻¹), D-glucose (220 mM) and LDH (50 U ml⁻¹), 20% DMSO, 0.3–1.4 mg ml⁻¹ purified enzyme, 30 °C and 600 r.p.m. Enantiomeric excess was determined via analytical asymmetric synthesis using racemic alanine as amine donor. Note that the absolute configuration given refers to the preferentially converted enantiomer, but not the remaining enantiomer.

(substrates 5–7). Although these substrates do not have much apparent synthetic significance for pharmaceutical applications, they have been widely investigated for the protein engineering of TAs^{11–15}. The enzymes of interest should either accommodate an aliphatic group (compounds 5 and 6) or an alcohol (compound 7) in their small binding pocket (Fig. 2). Although the wild-type 3FCR does not accept these substrates (as observed for the much bulkier substrates 1 to 3), mutations Y59W/Y87F/Y152F/T231A enabled the acceptance of these bulky substrates with very high activity (2 U mg⁻¹, Table 3). Even the amino alcohol 7a, a polar bulky substrate, was moderately well accepted. The novel TAs follow a similar pattern in their activity, yet some differentiate and even exhibit higher activity than the 3FCR variant, as in the case of TA-7 for *rac*-7a. Notably, all the enzymes exhibit perfect enantioselectivity towards amines 5 to 7, possibly due to the high asymmetry of the substituents at the chiral centre (Fig. 2). The enzymes are selective towards the (S)-aryl-alkylamines (S)-5a and (S)-6a, in line with their fold class, and towards the (R)-amino alcohol 7a, and the switch in enantiopreference is only due to the inverted priority based on the Cahn–Ingold–Prelog rules.

These results suggest that the variants we have identified are not only useful for aromatic substrates; indeed, all the newly created TAs possess a substantially expanded substrate spectrum.

Preparative synthesis of chiral amines. As already described, motif incorporation facilitates the acceptance of bulky amines in the kinetic resolution mode, but the ultimate goal of this work is

Table 4 | Asymmetric synthesis of chiral amines with the purified variant 3FCR Y59W/Y87F/Y152F/T231A using L-alanine as amine donor.

Product	Reaction time (h)	Ratio of substrate to enzyme (wt/wt)	Conversion (%)	Isolated yield (%)	Enantiomeric excess (%)
(R)-1a	24	2	>98	82 (HCl salt)	94.2
(S)-2a	24	5	>99	71 (HCl salt)	>99.9
(S)-3a	46	2.5	>97	69 (HCl salt)	63.0
(S)-5a	24	1.5	>97	39*	99.4
(S)-6a	24	1.5	>97	76*	96.6
(R)-7a	24	1.5	95	62*	99.8

Assay conditions for asymmetric synthesis: 100 ml: final volume, 50–70 mM HEPES buffer pH 8.0, 1 mM PLP, 100 mg ketone, 200–275 mM D,L-alanine, NAD⁺ (2–3 mM), GDH (3 U ml⁻¹), D-glucose (220 mM) and LDH (6 U ml⁻¹), DMSO 20% (1–3) or 2% (5–7), 20–66 mg purified enzyme, 30 °C under stirring. *The isolation protocol was not optimized.

the asymmetric synthesis of optically pure bulky amines using the engineered variants, as only then is a 100% theoretical yield possible and the synthesis rendered economical. Thus, the best variant of 3FCR (3FCR Y59W/Y87F/Y152F/T231A) was used for the asymmetric synthesis of bulky chiral amines on a preparative scale (100 mg ketone as substrate, compounds **1–3** and **5–7**). To favourably shift the equilibrium, a pyruvate removal system comprising lactate dehydrogenase (LDH) and glucose dehydrogenase (GDH)⁷ was employed, and the amine donor (alanine) was used in excess. In the kinetic resolution mode, the optimum activity was observed at pH 9.0–9.5; however, the catalytic efficiency of auxiliary enzymes and especially that of LDH dropped significantly at pH 8.5 or higher. Consequently, all reactions were performed at pH 8.0. As indicated in Table 4, for all six demanding substrates, every reaction reached high conversion within reasonable reaction times, highlighting the synthetic potential of the identified variants in industrial processes. The enantioselectivity is perfect (>99% e.e., (S)) for ketones **2b** and **5b**, which possess two very diverse residues, excellent (94% e.e., (R)) for the highly symmetrical ketone **1b**, and still moderate (63% e.e., (S)) for cyclic ketone **3b**. Clearly, the smaller the differences between the two moieties, the lower the enantioselectivity.

Furthermore, a correlation between the enzymatic activity and flexibility of the substrates can be drawn from the data generated (Tables 1 and 4). A higher catalytic efficiency was observed towards ketone **2b**, which, owing to its alkane chain linkage, is the most flexible of the three substrates studied, as well for the aryl-alkyl-amines (the alkyl groups have a significant degree of freedom). In contrast, the reaction was slower for ketones **1b** and **3b**, which are both more rigid in comparison. Keto-alcohol **7b** cannot be directly compared with the other substrates because the polarity of the hydroxyl group in the small binding pocket apparently triggers additional interactions.

Notably, although in most cases the variant delivered the (S)-amine, as suggested from the fold class I enzymes, in the case of ketones **1b** and **7b** the results are different. The (R)- rather than (S)-configuration of **1a** is the result of the associated correlating energy minimized quinonoid model (Fig. 3A,B). The chloro-substituted aromatic ring orients selectively towards the enlarged binding pocket in the same manner as the bulky moieties in the cases of (S)-amines **2a** and **3a**. The absolute configuration is therefore altered due to the Cahn–Ingold–Prelog rules, as clearly indicated for (R)-**7a**, albeit all amines and their respective ketones bind in the same fashion with respect to the steric demands of their contrasting substituents.

Discussion

The aim of our research was to evolve a toolbox of TAs that are active towards bulky chiral amines and their respective prochiral ketones (differing substantially in size and rigidity). We have identified an (S)-selective TA (3FCR, belonging to fold class I) and evolved it by rational design, leading to a synthetically highly useful variant bearing only four mutations. This proved sufficient

for acceptance of the desired ketones and to enable asymmetric synthesis of a wide set of bulky chiral amines on a preparative scale. The identified motif, in combination with the selected template, led to the discovery of six new TAs active towards bulky substrates, demonstrating the potential of this design to deliver a set of novel biocatalysts. All enzymes identified herein were active towards a diverse set of bulky substrates, accommodating in the small binding pocket alkyl chains, an alcohol moiety and especially voluminous aryl groups. A direct comparison to the benchmark TA from Codexis, used for the production of Sitagliptin, is not feasible, as this is an (R)-selective TA belonging to a different fold class^{2,27}. Furthermore, Savile *et al.* needed to introduce 27 mutations (~8% of the total sequence) to evolve the TA from *Arthrobacter* sp. for the production of the sterically demanding Sitagliptin². In this current work, only four mutations (~1% of the entire sequence) were sufficient to enable the synthesis of six bulky amines, all accomplished on a preparative scale. More significantly, understanding their specific function enabled these key mutations to be transferred successfully to other fold class I TA scaffolds that share only a modest sequence identity to the 3FCR scaffold. The identified TAs not only accepted the three aromatic bulky test substrates, yielding chiral amines of pertinent pharmaceutical relevance, but they could be used effectively for the production of aryl-alkylamines or an aryl amino alcohol. This rationale will greatly facilitate the discovery from sequence databases of novel TAs that are capable of accepting challenging ketones. Furthermore, the concept used here to analyse a wide variety of enzymes based on their protein sequences, with special emphasis on the discovery of distinct motifs, may also guide protein engineering efforts for enzymes other than TAs to facilitate efficient enzymatic syntheses of salient compounds.

Methods

Only the most relevant methods are provided here. Materials and details of the experiments are described in the Supplementary Information.

Preparation of enzymes. In a 2 l shake flask, 400 ml of Terrific Broth containing 100 µg ml⁻¹ ampicillin was inoculated with 1% (vol/vol) of an overnight culture of a microbial colony of *E. coli* BL21 (DE3) transformed with the plasmid containing the gene of interest. The *E. coli* strain was incubated at 37 °C with shaking at 180 r.p.m. to grow to an optical density at 600 nm (OD₆₀₀) of 0.5–0.7. The culture was cooled to 20 °C and isopropyl-β-D-thiogalactoside (IPTG) was added to a final concentration of 0.2 mM to induce expression of the transaminase. Incubation was continued overnight (~16 h) at 20 °C with shaking. Cells were collected by centrifugation (6,000g, 10 min, 4 °C) and the supernatant was discarded. The cell pellet was resuspended in 30 ml pre-cooled (4 °C) HEPES buffer (50 mM, pH 7.5) containing 0.1 mM pyridoxal-5'-phosphate (PLP), 0.3 M NaCl, 5 mM imidazole and 50 µg ml⁻¹ DNase. The cells were disrupted with a French Press (1,600 psi) and the cell debris was removed by centrifugation (9,000g, 30 min, 4 °C). Protein purification was performed using metal affinity chromatography. The crude lysate was filtered with 0.2 µm filters (Millipore) and was loaded onto a HisTrap FastFlow 5 ml column using the ÄKTA protein chromatography system after equilibration with the lysis buffer. Non-specifically bound proteins were removed by application of two column volumes of 10 mM imidazole. The TA was eluted from the column by the application of two column volumes of 300 mM imidazole. The purified TA fractions were pooled and subsequently desalted on the ÄKTA system using a Sephadex G60 column equilibrated with a HEPES buffer (50 mM, pH 7.5).

containing 0.1 mM PLP. The purified enzyme solutions were stored at +4 °C, or at –20 °C in 30% glycerol.

Determination of activity in kinetic resolution mode. The activity measurements were performed in a TECAN Infinite 200 PRO reader, and all measurements were performed at least in triplicate. A direct photometric assay was used²⁸, in which the enzymatic reaction took place in CHES buffer (50 mM, pH 9.0) at 30 °C in a total volume of 200 µl. 1 mM racemic amine (**1a–4a**) and 2 mM pyruvate were added to the buffer (final concentrations) containing the TA of interest. Due to the preparation of the amine stock solution in organic solvent, 5% (vol/vol) 2-propanol or dimethylsulfoxide (DMSO, 0.1% for compounds **5–7**) was present in the final reaction medium. The kinetic resolution was initiated by the addition of the amine acceptor (pyruvate). The final concentration of the enzyme varied between 2 and 800 µg ml^{–1}, depending on the specific activity towards the substrates under examination. The production of the corresponding ketones (**1b–7b**) was monitored at the optimum wavelength for each compound (**1b**, 16,562 M^{–1} cm^{–1} at 264 nm; **2b**, 9,646 M^{–1} cm^{–1} at 245 nm; **3b**, 5,714 M^{–1} cm^{–1} at 340 nm; **4b**, 6,115 M^{–1} cm^{–1} at 245 nm (ref. 27); **5b** and **6b**, 6,530 M^{–1} cm^{–1} at 242 nm (ref. 15); and **7b**, 7,098 M^{–1} cm^{–1} at 252 nm (ref. 14)).

Preparative asymmetric synthesis. The starting volume of all reactions was 100 ml and the substrate amount 100 mg ketone. The reaction mixture also contained HEPES buffer (50–70 mM) including 1 mM PLP, DMSO (20% (vol/vol) for **1b–3b** or 2% (vol/vol) for **5b–7b**), D,L-alanine (200–275 mM), oxidized nicotinamide adenine dinucleotide (NAD⁺, 2–3 mM), GDH (3 U ml^{–1}), D-glucose (220 mM) and LDH (6 U ml^{–1}). The slight variations in the reagent concentrations depended on the applied amount of purified enzyme solution (protein applied: 57 mg for synthesis of (*R*)-**1a**, 20 mg for (*S*)-**2a** and 39 mg for (*S*)-**3a**) or 100 mg enzyme lyophilisate (66 mg protein for the synthesis of (*S*)-**5a**, (*S*)-**6a** and (*R*)-**7a**). The addition of the respective ketone as DMSO solution started the reaction at pH 8.0 and 30 °C. The pH of the stirred reaction was kept constant by the addition of 0.1 N NaOH until full conversion was indicated by HPLC (Table 3). Afterwards, the reaction was quenched with HCl to pH 2.0 and the precipitated proteins could be removed by dialysis treatment and filtration. The products were extracted with *tert*-butyl methyl ether (TBME) at pH 10 (NaOH addition), delivering (after drying and evaporation) the crude amines as oils. These were characterized (NMR, MS, chiral and achiral HPLC) either as their HCl salts (**1–3a**) or as free amines (**5–7a**).

For amine **3a**, salt formation was essential due to the instability of the free base, which degraded, with discoloration, fairly rapidly, most probably due to oxidative aromatization. Secondary product formation was suppressed further by applying a nitrogen atmosphere, minimizing the risk of oxidation by air. For amine **7a**, the aqueous solution needed to be saturated with NaCl before its extraction with TBME.

Received 4 February 2016; accepted 16 June 2016;
published online 18 July 2016

References

- Truppo, M. D., Rozzell, J. D. & Turner, N. J. Efficient production of enantiomerically pure chiral amines at concentrations of 50 g/L using transaminases. *Org. Process Res. Dev.* **14**, 234–237 (2010).
- Savile, C. K. *et al.* Biocatalytic asymmetric synthesis of chiral amines from ketones applied to sitagliptin manufacture. *Science* **329**, 305–309 (2010).
- Fuchs, M., Farnberger, J. E. & Kroutil, W. The industrial age of biocatalytic transamination. *Eur. J. Org. Chem.* **2015**, 6965–6982 (2015).
- Steffen-Munsberg, F. *et al.* Bioinformatic analysis of a PLP-dependent enzyme superfamily suitable for biocatalytic applications. *Biotechnol. Adv.* **33**, 566–604 (2015).
- Koszelewski, D., Tauber, K., Faber, K. & Kroutil, W. ω -Transaminases for the synthesis of non-racemic α -chiral primary amines. *Trends Biotechnol.* **28**, 324–332 (2010).
- Cassimjee, K. E., Branneby, C., Vahak, A., Wells, A. & Berglund, P. Transaminations with isopropyl amine: equilibrium displacement with yeast alcohol dehydrogenase coupled to *in situ* cofactor regeneration. *Chem. Commun.* **46**, 5569–5571 (2010).
- Koszelewski, D., Lavandera, I., Clay, D., Rozzell, D. & Kroutil, W. Asymmetric synthesis of optically pure pharmacologically relevant amines employing ω -transaminases. *Adv. Synth. Catal.* **350**, 2761–2766 (2008).
- Green, A. P., Turner, N. J. & O'Reilly, E. Chiral amine synthesis using ω -transaminases: an amine donor that displaces equilibria and enables high-throughput screening. *Angew. Chem. Int. Ed.* **53**, 10714–10717 (2014).
- Höhne, M., Schätzle, S., Jochens, H., Robins, K. & Bornscheuer, U. T. Rational assignment of key motifs for function guides *in silico* enzyme identification. *Nature Chem. Biol.* **6**, 807–813 (2010).
- Desai, A. A. Sitagliptin manufacture: a compelling tale of green chemistry, process intensification, and industrial asymmetric catalysis. *Angew. Chem. Int. Ed.* **50**, 1974–1976 (2011).
- Han, S.-W., Park, E.-S., Dong, J.-Y. & Shin, J.-S. Mechanism-guided engineering of ω -transaminase to accelerate reductive amination of ketones. *Adv. Synth. Catal.* **357**, 1732–1740 (2015).
- Sayer, C. *et al.* The substrate specificity, enantioselectivity and structure of the (*R*)-selective amine: pyruvate transaminase from *Nectria haematococca*. *FEBS J.* **281**, 2240–2253 (2014).
- Jiang, J., Chen, X., Feng, J., Wu, Q. & Zhu, D. Substrate profile of an ω -transaminase from *Burkholderia vietnamiensis* and its potential for the production of optically pure amines and unnatural amino acids. *J. Mol. Catal. B* **100**, 32–39 (2014).
- Nobili, A. *et al.* Engineering the active site of the amine transaminase from *Vibrio fluvialis* for the asymmetric synthesis of aryl-alkyl amines and amino alcohols. *ChemCatChem* **7**, 757–760 (2015).
- Genz, M. *et al.* Alteration of the donor/acceptor spectrum of the (*S*)-amine transaminase from *Vibrio fluvialis*. *Int. J. Mol. Sci.* **16**, 26953–26963 (2015).
- Steffen-Munsberg, F. *et al.* Connecting unexplored protein crystal structures to enzymatic function. *ChemCatChem* **5**, 150–153 (2013).
- Middelfort, K. S. *et al.* Redesigning and characterizing the substrate specificity and activity of *Vibrio fluvialis* aminotransferase for the synthesis of imigabalin. *Protein Eng. Des. Sel.* **26**, 25–33 (2013).
- Kaulmann, U., Smithies, K., Smith, M. E. B., Hailes, H. C. & Ward, J. M. Substrate spectrum of ω -transaminase from *Chromobacterium violaceum* DSM30191 and its potential for biocatalysis. *Enzyme Microb. Technol.* **41**, 628–637 (2007).
- Cassimjee, K. E., Humble, M. S., Land, H., Abedi, V. & Berglund, P. *Chromobacterium violaceum* ω -transaminase variant Trp60Cys shows increased specificity for (*S*)-1-phenylethylamine and 4'-substituted acetophenones, and follows Swain–Lupton parameterisation. *Org. Biomol. Chem.* **10**, 5466–5470 (2012).
- Steffen-Munsberg, F. *et al.* Revealing the structural basis of promiscuous amine transaminase activity. *ChemCatChem* **5**, 154–157 (2013).
- Cassimjee, K. E., Manta, B. & Him, F. A quantum chemical study of the ω -transaminase reaction mechanism. *Org. Biomol. Chem.* **13**, 8453–8464 (2015).
- Yu, H., Zhao, Y., Guo, C., Gan, Y. & Huang, H. The role of proline substitutions within flexible regions on thermostability of luciferase. *Biochim. Biophys. Acta Prot. Proteomics* **1854**, 65–72 (2015).
- Deszcz, D. *et al.* Single active-site mutants are sufficient to enhance serine:pyruvate α -transaminase activity in an ω -transaminase. *FEBS J.* **282**, 2512–2526 (2015).
- Wilke, A. *et al.* The M5nr: a novel non-redundant database containing protein sequences and annotations from multiple sources and associated tools. *BMC Bioinformatics* **13**, 141 (2012).
- Levin, K. B. *et al.* Following evolutionary paths to protein–protein interactions with high affinity and selectivity. *Nature Struct. Mol. Biol.* **16**, 1049–1055 (2009).
- Shafee, T., Gatti-Lafronconi, P., Minter, R. & Hollfelder, F. Handicap-recover evolution leads to a chemically versatile, nucleophile-permissive protease. *ChemBioChem* **16**, 1866–1869 (2015).
- Grishin, N. V., Phillips, M. A. & Goldsmith, E. J. Modeling of the spatial structure of eukaryotic ornithine decarboxylases. *Protein Sci.* **4**, 1291–1304 (1995).
- Schätzle, S., Höhne, M., Redestad, E., Robins, K. & Bornscheuer, U. T. Rapid and sensitive kinetic assay for characterization of ω -transaminases. *Anal. Chem.* **81**, 8244–8248 (2009).

Acknowledgements

The authors thank J.F. Kabisch for preparing the M5nr database, M. Althaus and I. Duffour for developing the chiral and achiral analysis methods, J. Joergers and M. Rothe for the preparative separation of the chiral amines, C. Wyss-Gramberg for the NMR analysis of the Mosher amides, I. Menyes for support with HPLC and gas chromatography analyses and P. Meier for performing the preparative asymmetric synthesis experiments.

Author contributions

U.T.B., H.I. and B.W. initiated the study and directed the project. P.S. undertook the substrate and product syntheses. I.V.P. performed the bioinformatics analysis. I.V.P., M.S.W. and M.G. prepared and characterized all the variants. I.V.P., S.P.H. and H.I. performed the preparative asymmetric synthesis experiments. I.V.P., H.I. and U.T.B. prepared the manuscript, which was revised and approved by all authors.

Additional information

Supplementary information is available in the [online version of the paper](#). Reprints and permissions information is available online at www.nature.com/reprints. Correspondence and requests for materials should be addressed to H.I. and U.T.B.

Competing financial interests

The biocatalysis group of Roche has a committed interest over the long term in establishing a set of technically applicable TAs with broad substrate acceptance to assist devising more attractive, shorter, economical and greener synthetic routes to investigational drugs and beyond.



Cite this: *Org. Biomol. Chem.*, 2016, **14**, 10249

Protein-engineering of an amine transaminase for the stereoselective synthesis of a pharmaceutically relevant bicyclic amine†

Martin S. Weiß,^a Ioannis V. Pavlidis,^{a,b} Paul Spurr,^c Steven P. Hanlon,^c Beat Wirz,^c Hans Iding^{*c} and Uwe T. Bornscheuer^{*a}

Application of amine transaminases (ATAs) for stereoselective amination of prochiral ketones represents an environmentally benign and economically attractive alternative to transition metal catalyzed asymmetric synthesis. However, the restrictive substrate scope has limited the conversion typically to non-sterically demanding scaffolds. Recently, we reported on the identification and design of fold class I ATAs that effect a highly selective asymmetric synthesis of a set of chiral aromatic bulky amines from the corresponding ketone precursors in high yield. However, for the specific amine synthetic approach extension targeted here, the selective formation of an *exo*- vs. *endo*-isomer, these biocatalysts required additional refinement. The chosen substrate (*exo*-3-amino-8-aza-bicyclo[3.2.1]oct-8-yl-phenyl-methanone), apart from its pharmacological relevance, is a demanding target for ATAs as the bridged bicyclic ring provides substantial steric challenges. Protein engineering combining rational design and directed evolution enabled the identification of an ATA variant which catalyzes the specific synthesis of the target *exo*-amine with >99.5% selectivity.

Received 23rd August 2016,
Accepted 7th October 2016

DOI: 10.1039/c6ob02139e

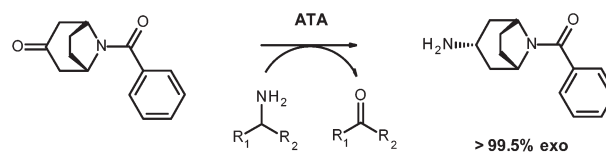
www.rsc.org/obc

Introduction

Transaminases are pyridoxal-5'-phosphate (PLP) dependent enzymes that catalyse the transfer of an amino group of a donor amine to the carbonyl carbon atom of an α -keto acid, ketones, or an aldehyde.¹ In the past decade, amine transaminases (ATAs) came into focus as efficient biocatalysts for the preparation of optically pure amines which represent highly valuable key intermediates or products in the pharmaceutical, chemical, and agricultural sectors.² However, for application as suitable biocatalysts for stereoselective amination, extensive protein engineering of ATAs is required in many cases, primarily due to their generally limited substrate scope. The most prominent example of such a successful ATA engineering resulted from a collaboration between Merck & Co. and Codexis which led to the realisation of an industrial process for the enzymatic asymmetric synthesis of the anti-

diabetic drug (*R*)-sitagliptin with >99.95% optical purity.³ Prior to this, access to (*R*)-sitagliptin was *via* enamine formation followed by asymmetric hydrogenation at high pressure (*ca.* 20 atm) using a rhodium-based chiral catalyst which rendered lower stereoselectivity and a rhodium contaminated product stream.³ The biocatalytic approach using the engineered variant ATA-117 represents therefore a prime example of green chemistry in terms of overall waste reduction, lower energy consumption and avoidance of hazardous heavy metal catalyst waste treatment.

3-Amino-8-aza-bicyclo[3.2.1]oct-8-yl-phenyl-methanone (**2**) (Scheme 1) represents a model building block for pharmaceutically active ingredients and thus an attractive target for biocatalytic selective synthesis mediated by transaminases. The 8-azabicyclo[3.2.1]octane motif constitutes a structural



Scheme 1 Selective synthesis of *exo*-3-amino-8-aza-bicyclo[3.2.1]oct-8-yl-phenyl-methanone **2** *via* reductive amination of ketone **1** catalysed by the ATA 3FCR and its variants. Isopropylamine or alanine can be applied as amine donors.

^aDept of Biotechnology and Enzyme Catalysis, Institute of Biochemistry, University of Greifswald, Felix-Hausdorff-Str. 4, D-17489 Greifswald, Germany.

E-mail: uwe.bornscheuer@uni-greifswald.de

^bGroup of Biotechnology, Dept of Biochemistry, University of Kassel, Heinrich-Plett-Str. 40, D-34132 Kassel, Germany

^cProcess Research and Development, Biocatalysis, F. Hoffmann-La Roche Ltd., Grenzacher Str.124, 4070 Basel, Switzerland. E-mail: hans.iding@roche.com

†Electronic supplementary information (ESI) available. See DOI: 10.1039/c6ob02139e



element within many neuroactive compounds, among which cocaine and atropine⁴ and various derivatives thereof have been patented *e.g.* as modulators of chemokine receptor activity,⁵ an important target in the treatment of a number of diseases. Besides its pharmacological relevance, amine **2** is also a challenging compound for protein engineering of transaminases due to its bicyclic and bridged ring system.

Recently, we succeeded in identifying and evolving ATAs of the fold class I ((*S*)-selective ATAs) that accept a broad spectrum of sterically demanding, but planar substrates.⁶ The best ATA variant enabled asymmetric synthesis of the target amines on a preparative scale with essentially perfect optical purities. Enzymatic routes to access the target amine **2** (Scheme 1) have not been described before and the bicyclic bridged ring system poses an unaddressed challenge. Thus, we herein describe the protein engineering of the (*S*)-selective amine transaminase from *Ruegeria* sp. TM1040 (3FCR)^{6,7} to transform the ketone **1** selectively to the desired *exo*-amine **2**.

Results and discussion

Protein engineering of 3FCR

In order to identify the optimal starting scaffold for engineering we first screened our in-house transaminases. Among them, the wild-type transaminase from *Ruegeria* sp. TM1040 (pdb-code: 3FCR⁷) and its mutants 3FCR_DM and 3FCR_QM from our recent study⁶ were found to possess low activity (Table 1). Interestingly, the single mutation Y59W reduced the wild-type's activity, while mutation T231A exhibited doubled activity. These results prompted us to apply saturation mutagenesis at the four positions already identified within 3FCR_QM. The variant 3FCR_QM exhibited perfect stereoselectivity towards the *exo*-isomer in the reductive transamination while the variants without the Y152F mutation had only moderate selectivity (<40% *exo* to *endo* preference). This revealed that at three of the four positions (87, 152, 231), the optimal amino acids were already incorporated into the starting scaffold. However, we had to replace tryptophan in position 59. Saturation of this position resulted in a leucine substitution which provided a 3-fold increase of activity (145 mU

mg⁻¹) compared to the 3FCR_QM scaffold (45 mU mg⁻¹) (Table 1).

Having achieved this increase in activity, further rationally guided protein engineering was hampered by the fact that the substrate of interest does not allow following the typical transaminase design concepts. As the active site of ATAs is composed of a small and a large binding pocket, the common aim of most studies is to widen the small binding pocket. For the bicyclic and bridged ketone **1**, its orientation in the active site is difficult to model due to its "three-dimensional bulkiness". For this reason, parallel to the optimization of the four aforementioned positions, we performed directed evolution of the 3FCR scaffold using error-prone PCR in combination with our recently developed high-throughput glycine oxidase assay.⁸ Accordingly, the assay was adapted for liquid phase analysis in microtiter plates using the racemic amine **2** as an amine donor and glyoxylate as the acceptor. Our direct photometric assay⁹ could not be used in this case as ketone **1** and amine **2** possess virtually identical spectrophotometric properties.

Screening of *ca.* 4600 variants from two different error-prone PCR libraries based on the 3FCR_DM scaffold with the glycine oxidase agar plate assay provided a variant with increased activity and three amino acid exchanges. Characterization of the respective single mutants identified mutation I234F to be responsible for a 3.5-fold increased activity in the 3FCR_DM (data not shown). Further investigations by saturation of this position revealed that both phenylalanine and methionine are the most promising residues at this position in the kinetic resolution of amine **2**. The beneficial effect of these two mutations was confirmed both in 3FCR_DM and 3FCR_QM. When the specific activity of the 3FCR_QM was only 45 mU mg⁻¹, the 3FCR_QM/I234F exhibited 80 mU mg⁻¹ and the 3FCR_QM/I234M 116 mU mg⁻¹ while maintaining absolute stereoselectivity (Table 1).

These two new variants were applied in the selective synthesis (Scheme 1) using either alanine or isopropylamine (IPA) as an amine donor (Table 2), and they both proved to be beneficial. 3FCR_QM/I234M provided the best conversions, independently of the amine donor. However, in terms of catalytic

Table 1 Specific activity of 3FCR variants in the kinetic resolution of **2** using glyoxylate as an amine acceptor

Variant	Specific activity (mU mg ⁻¹)
3FCR (wild-type)	70
3FCR_Y59W	35
3FCR_T231A	130
3FCR_Y59W/T231A (3FCR_DM)	45
3FCR_Y59W/Y87F/Y152F/T231A (3FCR_QM)	45
3FCR_Y59L/Y87F/Y152F/T231A	145
3FCR_Y59W/Y87F/Y152F/T231A/I234F (3FCR_QM/I234F)	80
3FCR_Y59 W/Y87F/Y152F/T231A/I234M (3FCR_QM/I234M)	116

Table 2 Asymmetric synthesis of *exo*-amine **2** using alanine or IPA as amine donors^a

Variant	Conversion [%] (% <i>exo/endo</i> excess)	
	With IPA	With alanine
3FCR_DM	0 (n.d. ^b)	4 (n.d. ^b)
3FCR_QM	10 (>99)	35 (>99)
3FCR_QM/I234M	19 (>99)	66 (>99)
3FCR_QM/I234F ^c	8 (>99)	40 (>99)

^a Conditions for isopropylamine experiments: 2 mM **1**, 0.2 M IPA, HEPES buffer (pH 8.0, 50 mM), 1 mM PLP, 5% DMSO, 30 °C, 600 rpm, 20 h. Conditions for alanine experiments: 8 mM **1**, 0.2 M L-alanine, HEPES buffer (pH 8.0, 50 mM), 1 mM PLP, 20% DMSO, 5 mM NADH, 25 mM glucose, 0.05 mg mL⁻¹ GDH, 5 μL mL⁻¹ LDH, 30 °C, 600 rpm, 20 h. ^b n.d. = not determined. ^c Lower conversions as only small amounts of enzyme could be applied due to expression issues, see text.



efficiency 3FCR_QM/I234F appeared to be more appropriate, as it led to conversions comparable to 3FCR_QM/I234M despite the fact that 8-fold less enzyme was applied. For unclear reasons, introduction of mutation I234F resulted to significantly lower expression yield and hence this variant was not considered further. 3FCR_QM/I234M was subjected to a second round of error-prone PCR (~8000 variants screened) revealing position 382 as a new hot spot. Its subsequent NNK saturation-mutagenesis identified L382M as the most promising variant (Table 3). In parallel, *via* rational design (see *in silico* analysis paragraph) we decided to mutate S86 to alanine to provide a little more flexibility in the loop where F87 is located. However, this mutation did not have the desired outcome and even decreased the activity when incorporated into 3FCR_QM/I234M/L382M.

When we investigated the catalytic efficiency of all interesting variants for selective synthesis, the results were quite different from those observed in the kinetic resolution mode.

Table 3 Characterization of most interesting variants in the kinetic resolution of **2** (specific activity, %) and asymmetric synthesis of **1** (conversion, %)^a

Variant	Specific activity [mU mg ⁻¹]	Conversion [% <i>exo</i>]
3FCR_QM	45	23 (>99)
3FCR_QM/Y59L	173	96 (>99)
3FCR_QM/I234M	137	55 (>99)
3FCR_QM/I234M/L382M	198	60 (>99)
3FCR_QM/S86A/I234M/L382M	185	51 (>99)
3FCR_QM/Y59L/S86A/I234M/L382M	295	94 (>99)

^a Conditions for kinetic resolution: 1 mM *rac*-amine **2**, 2 mM glyoxylate, CHES buffer (50 mM, pH 9.5), 37 °C, measurement for 40 min; conditions for asymmetric synthesis experiments: 2 mM prochiral ketone **1**, 0.2 M IPA, HEPES buffer (pH 8.0, 50 mM), 1 mM PLP, 0.5 mg mL⁻¹ of the respective variant, 5% DMSO, 30 °C, 600 rpm, 45 h.

Although all three mutations (namely Y59L, I234M and L382M) were beneficial for kinetic resolution, it seems that the key mutation for efficiency is Y59L. The other two mutations did lead to an improvement compared to the scaffold (3FCR_QM) but not to the same extent. Nevertheless, all variants presented in Table 3 maintained perfect *exo/endo*-selectivity (>99%) in the formation of the *exo*-amine **2**.

Finally, a non-optimized small scale preparative synthesis with 3FCR_QM/I234M was performed using isopropylamine as an amine donor, which provided 75% conversion (60% isolated yield) and >99.5% selectivity for the *exo*-amine as determined by HPLC analysis.

In silico analysis

In order to discern the underlying reasons for the improved activity of the best variants towards **1**, we performed an *in silico* analysis to identify possible interactions with the sterically demanding target compound. As seen in Fig. 1, position 59 can directly interact with the quinonoid of **2**. Here, mutation to leucine provides significantly more space than tryptophan or tyrosine and it increases the hydrophobicity of the binding pocket. Position 87 seems to interact with the keto group of the substrate and thus the removal of the hydroxyl group of the tyrosine is beneficial. In order to provide more space, we aimed at introducing additional flexibility for residue 87 by mutating the neighboring positions. By sequence alignment, we observe that in several other ATAs, such as the one from *Vibrio fluvialis*, the adjacent position 86 is an alanine, while in 3FCR it is a serine. This mutation was investigated but as shown in Table 3, the mutants did not exhibit improved activity. Another significant mutation is Y152F. As described earlier,⁶ this mutation significantly stabilizes the 3FCR scaffold and thus facilitates the asymmetric synthesis performance which requires transaminases being stable for

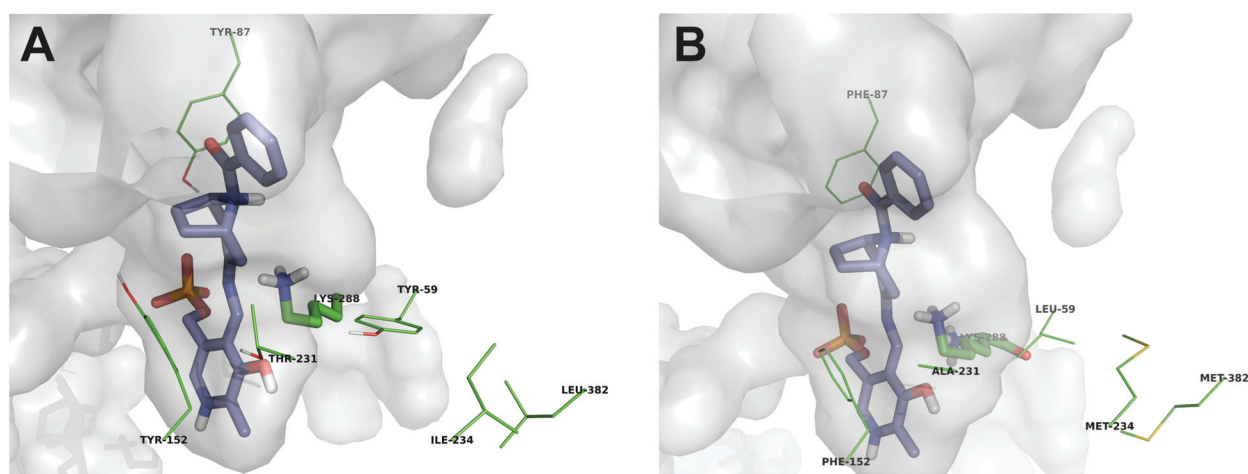


Fig. 1 *In silico* analysis of the quinonoid of *exo*-3-amino-8-aza-bicyclo[3.2.1]oct-8-yl-phenyl-methanone **1** (blue sticks) in the active site of (A) 3FCR wild-type and (B) 3FCR_QM/Y59L/I234M/L382M. The side chains of the interesting positions are presented with green lines. The catalytic lysine (K288) is also shown (green sticks). It is obvious that in the variant (B) the binding pocket is significantly enlarged, mainly due to the Y59L and the Y152F mutations. It can also be seen that residues in positions 234 and 382 do not directly interact with the quinonoid, but they appear to have a secondary interaction with residue 59.



several hours, or even days. In this case another benefit arose: the removal of the hydroxyl group generated more volume for the bicyclic substrate, with its five-membered ring facing residue 152 and hence favoring formation of the *exo*-amine **2** (Fig. 1). All variants bearing mutation Y152F exhibited perfect selectivity producing as such the *exo*-amine exclusively. The variants without mutation Y152F displayed only moderate selectivity (<40% *exo/endo* excess). A reason might be the interaction between the hydroxyl group of the tyrosine and the nitrogen atom in the bicyclic ring structure, which enables the binding of the *endo*-isomer.

As expected, the mutations identified within the error-prone PCR-derived libraries are not present in the first sphere of the interactions of the quinonoid with the enzyme and thus it is also more difficult to understand their effects. Both residues 234 and 382 are located behind residue 59 (Fig. 1). These mutations might stabilize residue 59 in a catalytically favored orientation, while residue 234 could affect *via* the backbone the orientation of the neighboring residue 231, which also has a significant impact on the catalytic activity.

Experimental

Materials

Ketone **1** and amine **2** as a mixture of *exo*- and *endo*-isomers as well as the individual isomers were made available by F. Hoffmann-La Roche (Scheme S1†). All other reagents were of analytical grade. Recombinant expression of the (*S*)-selective ATA from *Ruegeria* sp. TM1040 and all variants were performed as described previously, see also below for details.⁶ The glycine oxidase was produced also as described previously.⁸

Directed evolution libraries

For the preparation of error-prone PCR libraries, the genes encoding the respective variants of the ATA from *Ruegeria* sp. TM1040 were amplified using the GeneMorph II Random Mutagenesis Kit from Agilent Technologies according to the manual instructions and using the following flanking primers: ePCR_Left_pET22b (GTTTAACTTTAAGAAGGAGATATACATATGC); ePCR_Right_3FCR (GTGGTGGTGATGGTGATGTGAACC). In order to adjust the mutation frequency, the amount of the parental plasmid template was varied between 25–50 ng of the pET22b plasmid template in a 50 μ L reaction volume and 30 cycles of mutagenesis amplification were performed. Usually a set of libraries with different amounts of the parental plasmid template were prepared to cover variants with higher and lower mutation frequencies. For the preparation of the error-prone PCR libraries based on the 3FCR_DM, 25 ng or 50 ng template and for the library based on the 3FCR_QM/I234M 35 ng or 45 ng template were applied. For the latter libraries a random sample of 3 variants was sent for sequencing and revealed an average mutation frequency of 5 (35 ng template) and 2–5 (45 ng template) nucleotide exchanges per gene. The resulting PCR products were purified using the NucleoSpin® Gel and PCR Clean-up Kit from Macherey & Nagel according to the

manual instructions, but with 50% diluted NTI buffer. The sample was eluted in 25 μ L for application as megaprimers in a MEGAWHOP (mega primers and whole plasmid PCR). The MEGAWHOP reaction mixture (50 μ L reaction volume) was prepared as follows: Pfu buffer, 0.3 mM dNTPs, 1–1.5 ng μ L⁻¹ parental plasmid, 5 μ L purified megaprimers from the ep-PCR and 0.3 μ L of Pfu Plus! DNA polymerase. The amplification was performed as follows: (a) 94 °C, 2 min; (b) 28 cycles: 94 °C, 30 s; 55 °C or 60 °C, 30 s; 72 °C, 7:05 min; (c) 72 °C, 14 min. The PCR product was digested with DpnI (20 μ L mL⁻¹) for 2 h at 37 °C and the restriction enzyme was inactivated by incubation at 80 °C for 20 min. 6 μ L of the DpnI digested sample was transformed in 50 μ L of electro-competent TOP10 cells (1.5 kV, 5 ms). After transformation, 1 mL LB-SOC was added and after 1 h incubation at 37 °C and 800 rpm a sample of 40 μ L was plated out on an LB-amp (100 μ g mL⁻¹ ampicillin) and the remaining sample was used for inoculation of a 50 mL LB-amp (100 μ g mL⁻¹ ampicillin) overnight culture. After overnight incubation the colonies were counted on the agar plate to calculate the number of variants in the library (5 000–20 000 transformants were usually obtained). The overnight culture was then applied for plasmid isolation. Electro-competent *E. coli* BL21(DE3) cells containing the compatible pCDF-1 glycine oxidase coding plasmid were transformed with 30 ng of the library plasmid DNA as described above. After incubation at 37 °C different amounts (30–60 μ L) were plated out on amp/spec plates (100 μ g mL⁻¹ ampicillin, 50 μ g mL⁻¹ spectinomycin) for screening on nitrocellulose membranes as described further below.

Point and site-saturation mutagenesis

All variants were prepared using a modified version of the QuikChange PCR method. Primers were designed with the desired mismatches to provide the desired mutations. For site-saturation mutagenesis primers with NNK in the desired region were applied. For each reaction Pfu buffer, 0.2 mM dNTPs, 0.2 ng μ L⁻¹ parental plasmid, 0.2 μ M of each primer and 0.2 μ L of Pfu Plus! DNA polymerase were applied. 3% (v/v) DMSO was applied only for reactions using primers without NNK-codons. The amplification was performed as follows: (a) 94 °C, 2 min; (b) 25 cycles (QuikChange)/30 cycles (site-saturation): 94 °C, 30 s; 55 °C or 60 °C, 30 s; 72 °C, 7:05 min (c) 72 °C, 14 min. The PCR product was digested with DpnI (20 μ L mL⁻¹) for 2 h at 37 °C and the restriction enzyme was inactivated by incubation at 80 °C for 20 min. Chemo-competent Top10 *E. coli* cells were transformed with the PCR product. After confirmation of codon distribution in the case of a site-saturation mutagenesis or after confirmation of the correct sequence for QuikChange variants, the PCR products were transformed in chemo-competent BL21(DE3) *E. coli* cells for expression.

Protein expression and purification

The glycine oxidase was expressed and purified as described previously.⁸ As the expression medium, TB-medium (Terrific Broth) instead of LB-medium was applied.



The expression of the transaminase variants was carried out in baffled 250 mL flasks using 50 mL TB-medium containing 100 $\mu\text{g mL}^{-1}$ ampicillin. Inoculation was carried out using 1 mL of an overnight culture of a microbial colony of *E. coli* BL21 (DE3) transformed with the plasmid containing the gene of interest. The *E. coli* strain was incubated at 37 °C with shaking at 180 rpm to grow to an optical density at 600 nm (OD₆₀₀) of 0.6 to 0.8. The flasks were moved to a 20 °C shaker and after 10 min of incubation with shaking at 180 rpm isopropyl- β -D-thiogalactoside (IPTG) was added to a final concentration of 0.5 mM to induce the expression of the transaminase. Incubation was continued overnight (*ca.* 16 h) at 20 °C with shaking. Cells were harvested by centrifugation (4500g, 15 min, 4 °C) and the supernatant was discarded. The cell pellets were stored at -20 °C or were directly used for cell disruption and purification. For purification the cell pellets were resuspended in 6 mL pre-cooled (4 °C) lysis buffer (HEPES buffer 50 mM, pH 7.5 containing 0.1 mM PLP, 0.5 M NaCl, 10 mM imidazole and 50 $\mu\text{g mL}^{-1}$ DNase). The cells were disrupted *via* ultrasonication (Bandelin Sonopuls HD2070, Bandelin UW2070, MS 73 sonotrode) at 50% cycle and 55% power 5 minutes on ice, twice handled. The suspension was transferred to 2 mL tubes. To remove the cell debris, the tubes were centrifuged for 20 min at 16 000g and 4 °C. The supernatant was applied for protein purification *via* metal affinity chromatography using Roti@garose-His/Co Beads self-packed columns (~1.5 mL bed volume). The clear lysate was loaded onto the columns and after 5 min of incubation the cap was opened and the flow-through was discarded. The column was washed 3 times with application buffer (HEPES buffer 50 mM, pH 7.5 containing 0.1 mM PLP, 0.5 M NaCl, 10 mM imidazole) and the flow-through was discarded. The cap was closed and 2.5 mL of elution buffer (HEPES buffer 50 mM, pH 7.5 containing 0.1 mM PLP, 0.5 M NaCl, 350 mM imidazole) was applied onto the columns. After 5 min of incubation the cap was opened and the protein solution was gathered for desalting using GE Healthcare PD10 desalting columns and desalting buffer (HEPES buffer 50 mM, pH 7.5 containing 0.1 mM PLP) according to the manual of instructions. Fig. S2† shows an SDS-PAGE of the purified variants. Protein concentrations were determined *via* the Pierce BCA Protein Assay Kit. The purified enzyme solutions were stored at +4 °C, or at -20 °C in 30% glycerol. For asymmetric synthesis experiments the desalting buffer was adjusted to pH 8.0 instead of pH 7.5. For preparative scale asymmetric synthesis experiments the transaminase variants were prepared as described previously.⁶

Quantification of activity in liquid phase assay

To investigate our variants for activity in kinetic resolution, the glycine oxidase coupled assay⁸ was adapted for the application in microtiter plates. The assay was optimized for a reaction volume of 150 μL and to have a linear range under the further below specified conditions on the condition that the detected slope is below 0.8 OD h⁻¹. For any samples providing higher slopes the assay was repeated with diluted samples in order to have a linear relationship between the activity and detected

slope. Thus, we standardized protein concentrations to 0.25–1.0 mg mL⁻¹ depending on the respective activity using desalting buffer (HEPES buffer 50 mM, pH 7.5, containing 0.1 mM PLP). To certify that the assay was working accordingly, an additional 1 : 5 dilution of each sample was prepared. To run the assay, 20 μL of each sample and each dilution were added in triplicates in a microtiter plate. The reaction was started by adding 130 μL of the mastermix solution and the increase of absorbance was followed at 498 nm for at least 40 min at 37 °C. The final assay concentrations were as follows: CHES buffer (pH 9.5, 50 mM), 1 mM *rac*-amine 2 (3-amino-8-aza-bicyclo[3.2.1]oct-8-yl-phenyl-methanone), 2 mM glyoxylate, 0.17 mg mL⁻¹ glycine oxidase from *Geobacillus kaustophilus*, 5 U mL⁻¹ horseradish peroxidase, 3.9 mM vanillic acid, 0.5% (v/v) methanol, 1.2 mM 4-aminoantipyrine and 0.08% ethanol (v/v). To guarantee the best comparability as possible, we always compared the activity with the parental mutant which was purified in parallel and treated identically with the variants of interest.

To quantify the specific enzymatic activity, a calibration curve was recorded by using sequential dilutions of an aqueous 1 M glycine stock solution. 20 μL were applied in triplicates to the microtiter plate and 130 μL of the mastermix solution described above, were added. After incubation at 37 °C, an endpoint measurement at 498 nm was made. Linear regression provided a slope of 12.44 AU μmol^{-1} of glycine in 150 μL that allowed quantifying the reaction velocities from the slopes obtained in the kinetic assays (Fig. S1†).

Solid-phase assay screening of error-prone PCR libraries

The screening procedure of the error-prone PCR libraries was performed as described previously.⁸ The pH of the assay plates was pH 9.25 (first screening round) and pH 9.5 (second screening round) and the assay plates had the following final composition: CHES buffer (pH 9.5/9.25, 50 mM), 100 mM isopropylamine, 10 mM glyoxylate, in 3.9 mM vanillic acid, 0.5% (v/v) methanol, 1.2 mM 4-aminoantipyrine and 0.08% ethanol (v/v), and 1% (w/w) agarose. 100 U of horseradish peroxidase dissolved in 100 μL MilliQ water were spread on the surface of each plate directly before placing the membranes on top of the plates for screening. After incubation of the assay plates at 37 °C the most colored colonies were picked from each plate for expression in 96-well deep-well blocks and screening in microtiter plates as described previously.⁸

Analytical reductive amination experiments

Reductive amination reactions in the analytical scale were performed in a total volume of 400 μL in glass vials using a glass vial shaker from Eppendorf. Detailed final concentrations and conditions are given in the main text. For HPLC analysis 50 μL of the sample were mixed with 50 μL of acetonitrile including 0.1% diethylamine that was passed through a tip filter before injection into HPLC.

Preparative reductive amination

Into 82 mL reaction buffer (HEPES 50 mM; 2 mM PLP; 0.2 M 2-propylamine hydrochloride; pH 7.5) the purified mutant



transaminase 3FCR Y59W/Y87F/Y152F/T231A/I234M solution (in total 78 mL, protein 1.1 mg mL⁻¹) and 100 mg 8-benzoyl-8-aza-bicyclo[3.2.1]octan-3-one (**1**) dissolved in 20 mL DMSO were added under stirring at 30 °C. The reaction was allowed to proceed for 9 d (non-optimized) enabling a conversion of 75 area% (IPC-HPLC). The reaction mixture was acidified to pH 2.0 to precipitate the enzyme and stirring was continued for 15 min. Subsequently, the reaction mixture was filtered through a 25 g filter aid (Dicalite) bed and extracted twice with 50 mL dichloromethane to remove the remaining ketone **1**. The combined organic phases were dried over anhydrous MgSO₄, filtered and evaporated under vacuum at 40 °C yielding 37 mg of (HPLC: 97 area%) ketone **1** as a slightly yellow oil. The pH of the aqueous phase was adjusted to 12 using 2 N NaOH and extracted four times with 50 mL dichloromethane. The combined organic phases were dried over anhydrous MgSO₄, filtered, evaporated under vacuum at 40 °C and dried 36 h under high vacuum at 60 °C yielding 60 mg of target amine **2** (60%) as a yellow oil. Optimization and scale-up of this proof-of-concept small scale preparative reaction to reduce reaction times and replace dichloromethane for work-up is the subject of future studies.

HPLC methods for analytical scale reactions

HPLC-analysis of analytical scale reactions was performed *via* direct injection of the 20 µL sample on a 150 × 4.6 analytical OD-RH column from Chiralcel running 27% acetonitrile and 73% water, 0.1% diethylamine at 30 °C and 0.55 mL min⁻¹ flow. Detection of the analytes took place at 230 nm.

Analysis of preparative scale reaction product **2**

Chemical purity HPLC (see also Fig. S3†): 98.9 area% [210 nm; X-Bridge C8; 50 × 2.1 mm, 2.5 µm, flow 1 mL min⁻¹, 40 °C, A: 90% 10 mmol ammonium acetate in H₂O/ACN (95/5), B: ACN, 10%]; chiral SFC: 100% *exo* [210 nm; Chiralpak AD-3; 150 × 4.6 mm, 5 µm; flow 3 mL min⁻¹; left 40 °C; right 42 °C; A: 82% CO₂, B: 18% methanol with 0.2% 2-propylamine]; ¹H NMR (600 MHz, DMSO-d₆, 120 °C) δ ppm 7.44 (s, 5 H), 4.29 (br s, 2 H), 3.16 (dt, *J* = 11.1, 5.5 Hz, 1 H), 1.86–2.00 (m, 3 H), 1.79 (ddd, *J* = 13.2, 5.1, 3.0 Hz, 3 H), 1.67–1.75 (m, 3 H), 1.34–1.47 (m, 2 H); LC-MS: 231 (M + H)⁺. CAS registry number: 637018-99-6.

Conclusions

Several variants of a (*S*)-selective transaminase were identified enabling an enzyme-catalyzed synthesis of the pharmaceutically relevant *exo*-3-amino-8-aza-bicyclo[3.2.1]oct-8-yl-phenyl-methanone in good yield and excellent optical purity *via* reductive amination. The key mutations were identified by (a) saturation of the positions known to play a role in the accommodation of bulky substrates, and (b) two rounds of directed evolution. The results represent the first example of the transaminase-catalysed synthesis of an amine containing a

bicyclic bridged moiety. Our study also shows that a combination of rational protein design with random mutagenesis by error-prone PCR was required to identify the most suitable variants, similar to the findings reported by Savile *et al.* for the development of an (*R*)-transaminase for Sitagliptin synthesis.³ Furthermore, our careful analysis of the performance of the 3FCR variants confirms that enzymes found to be active in kinetic resolution must not be suitable for asymmetric synthesis as published earlier for a mutant of the ATA mutant from *Vibrio fluvialis*.¹⁰

Acknowledgements

The authors thank I. Duffour for developing the analysis methods, J. Joerger for the preparative separation of the *exo*- and *endo*-amines, C. Wyss-Gramberg for the NOESY NMR analysis, P. Meier for performing the preparative enzymatic experiments and K.-J. Gutmann for the synthesis of the requisite organic materials.

References

- 1 F. Steffen-Munsberg, C. Vickers, H. Kohls, H. Land, H. Mallin, A. Nobili, L. Skalden, T. van den Bergh, H.-J. Joosten, P. Berglund, M. Höhne and U. T. Bornscheuer, *Biotechnol. Adv.*, 2015, **33**, 566–604.
- 2 (a) D. Koszelewski, K. Tauber, K. Faber and W. Kroutil, *Trends Biotechnol.*, 2010, **28**, 324–332; (b) M. Fuchs, J. E. Farnberger and W. Kroutil, *Eur. J. Org. Chem.*, 2015, 6965–6982.
- 3 C. K. Savile, J. M. Janey, E. C. Mundorff, J. C. Moore, S. Tam, W. R. Jarvis, J. C. Colbeck, A. Krebber, F. J. Fleitz, J. Brands, P. N. Devine, G. W. Huisman and G. J. Hughes, *Science*, 2010, **329**, 305–309.
- 4 A. Korolkovas, in *Essentials of Medicinal Chemistry*, ed. A. Korolkovas, Wiley Interscience, New York, 2nd edn, 1988, pp. 195–283.
- 5 J. Cumming, *Int. Pat.*, WO2003080574A1, 2003.
- 6 I. V. Pavlidis, M. S. Weiß, M. Genz, P. Spurr, S. P. Hanlon, B. Wirz, H. Iding and U. T. Bornscheuer, *Nat. Chem.*, 2016, DOI: 10.1038/NCHEM.2578.
- 7 F. Steffen-Munsberg, C. Vickers, A. Thontowi, S. Schätzle, T. Tumlrirsch, M. Svedendahl Humble, H. Land, P. Berglund, U. T. Bornscheuer and M. Höhne, *ChemCatChem*, 2013, **5**, 150–153.
- 8 M. S. Weiß, I. V. Pavlidis, C. Vickers, M. Höhne and U. T. Bornscheuer, *Anal. Chem.*, 2014, **86**, 11847–11853.
- 9 S. Schätzle, M. Höhne, E. Redestad, K. Robins and U. T. Bornscheuer, *Anal. Chem.*, 2009, **81**, 8244–8248.
- 10 A. Nobili, F. Steffen-Munsberg, H. Kohls, I. Trentin, C. Schulzke, M. Höhne and U. T. Bornscheuer, *ChemCatChem*, 2015, **7**, 757–760.



Amine Transaminase Engineering for Spatially Bulky Substrate Acceptance

Martin S. Weiß,^[a] Ioannis V. Pavlidis,^[a, b] Paul Spurr,^[c] Steven P. Hanlon,^[c] Beat Wirz,^[c] Hans Iding,^{*,[c]} and Uwe T. Bornscheuer^{*,[a]}

Amine transaminase (ATA) catalyzing stereoselective amination of prochiral ketones is an attractive alternative to transition metal catalysis. As wild-type ATAs do not accept sterically hindered ketones, efforts to widen the substrate scope to more challenging targets are of general interest. We recently designed ATAs to accept aromatic and thus planar bulky amines, with a sequence-based motif that supports the identification

of novel enzymes. However, these variants were not active against 2,2-dimethyl-1-phenylpropan-1-one, which carries a bulky *tert*-butyl substituent adjacent to the carbonyl function. Here, we report a solution for this type of substrate. The evolved ATAs perform asymmetric synthesis of the respective *R* amine with high conversions by using either alanine or isopropylamine as amine donor.

Introduction

Amine transaminases (ATAs) are a promising alternative to transition-metal catalysts for the stereoselective synthesis of chiral amines.^[1] Transaminases are pyridoxal-5'-phosphate (PLP)-dependent transferases that catalyse the amino group transfer to ketones or aldehydes, from a donor amine, usually D- or L-alanine or isopropylamine (IPA).^[2] When prochiral ketones are applied for synthesis, amine transaminases perform an asymmetric amino group transfer to provide optical pure amines. This makes ATAs valuable tools for the synthesis of chiral key intermediates for pharmaceutical compounds.^[1b, c] However, the major challenge is their limited substrate scope. Transaminases in general are homodimeric proteins with two active sites, each located at the interface of the two subunits. Thus, each of the two active sites is surrounded by amino acid residues from both monomers thereby encompassing a large and a small binding pocket. In most cases, the small binding pocket accommodates only small moieties such as methyl groups.^[2a, 3] Accordingly, protein engineering is required to expand the active site for larger substrates to enable biosynthesis of chiral amines of high pharmaceutical or synthetic interest. In the past decade, many groups succeeded in bringing

ATAs into the spotlight of organic synthesis. The most prominent example of protein engineering of ATAs was the synthesis of (*R*)-sitagliptin. Codexis introduced 27 mutations into a fold class IV ATA, which exhibited minimal (but detectable) activity towards prositagliptin.^[1c] This engineering effort led to the development of an industrial process. In a more recent and broader study, we identified a sequence-based motif comprising four core mutations in ATAs of fold class I to enable them to accept a set of bulky aromatic and thus planar ketones. We demonstrated their catalytic potential by performing preparative asymmetric synthesis of the corresponding amines, thereby leading to high isolated yields and excellent optical purities.^[1b] The sequence motif was demonstrated to be transferable to fold class I ATAs with at least 70% sequence identity to the enzyme from *Ruegeria* sp. TM1040 (PDB ID: 3FCR) by incorporating the motif in previously uncharacterized putative ATAs. All the synthetic constructs that expressed as soluble protein exhibited activity towards the tested bulky amines (as verified for kinetic resolutions), thus underlining the generality of our sequence motif.^[1b]


The motif we suggested—70% sequence identity to 3FCR and four specific mutations in the active site—provides a toolbox of ATAs for aromatic and aliphatic substrates that have planar bulky substituents, but these variants were not efficient catalysts for spatially bulky ketones. Recently, we reported the first solution for the asymmetric synthesis of a bridged bicyclic amine.^[4] The engineering was based on the same scaffold, but the positions targeted were different, thus showing that bulky substrates require a different approach.

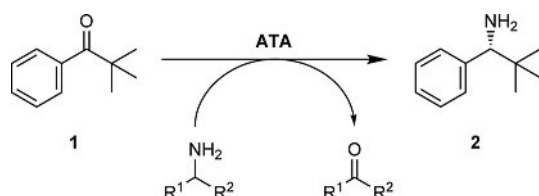
In the current study we investigated the acceptance of the ketone 2,2-dimethyl-1-phenylpropan-1-one (**1**) in the synthesis of the (*R*)-2,2-dimethyl-1-phenylpropan-1-amine (**2**; Scheme 1). This substrate is of interest because of its *tert*-butyl substituent in addition to the aromatic ring. We recently investigated the acceptance of **1** by the ATA from *Vibrio fluvialis* (VF-ATA) in an

[a] M. S. Weiß, Dr. I. V. Pavlidis, Prof. Dr. U. T. Bornscheuer
Department of Biotechnology and Enzyme Catalysis
Institute of Biochemistry, University of Greifswald
Felix-Hausdorff-Strasse 4, 17489 Greifswald (Germany)
E-mail: uwe.bornscheuer@uni-greifswald.de

[b] Dr. I. V. Pavlidis
Group of Biotechnology, Department of Biochemistry, University of Kassel
Heinrich-Plett-Strasse 40, 34132 Kassel (Germany)

[c] Dr. P. Spurr, Dr. S. P. Hanlon, Dr. B. Wirz, Dr. H. Iding
Process Chemistry and Catalysis, Biocatalysis
F. Hoffmann–La Roche Ltd.
Grenzacher Strasse 124, 4070 Basel (Switzerland)
E-mail: hans.iding@roche.com

 The ORCID identification numbers for the authors of this article can be found under <https://doi.org/10.1002/cbic.201700033>.



Scheme 1. Asymmetric synthesis of (*R*)-2,2-dimethyl-1-phenylpropan-1-amine (**2**) by amino group transfer to 2,2-dimethyl-1-phenylpropan-1-one (**1**) catalyzed by ATAs. Isopropylamine ($R^1 = R^2 = \text{CH}_3$) or alanine ($R^1 = \text{CH}_3$, $R^2 = \text{COOH}$) serve as the amine donor.

extensive engineering work, and identified several variants that could perform asymmetric synthesis.^[5] In another recent example VF-ATA was engineered to catalyze the synthesis of (*S*)-1-(1,1'-biphenyl-2-yl)ethanamine.^[6]

The ATA from *Ruegeria* sp. TM1040^[7] (PDB ID: 3FCR; Rsp-ATA) differs significantly from VF-ATA (~33% sequence identity). In a previous report^[1b] we showed that the evolution of the two ATAs of fold class I is different: although several amino acids engineered by us in Rsp-ATA are present as native residues in wild-type VF-ATA, the latter does not exhibit any activity against any of the bulky planar substrates studied.

Thus, in order to facilitate the engineering of the enzymes and understand the features that enable acceptance of this challenging substrate, here we present another engineering solution based on the Rsp-ATA scaffold. We also provide a comparison of the most prominent variants of the two protein scaffolds (with little shared homology) to understand the binding and conversion of its specific target compound, in order to facilitate the engineering of ATA to accept other bulky ketones of this type.

Results and Discussion

Protein engineering for acceptance of amine 2

Wild-type Rsp-ATA has a narrow substrate scope with low activities even for standard substrates such as 1-phenylethylamine. For this reason, our engineering efforts started with the most prominent variant (Y59W/T231A) identified in our previous study^[1b] as this enabled the acceptance of planar bulky substrates. However, this variant did not exhibit any detectable activity towards **2** in kinetic resolution reactions. From *in silico* analysis, we identified Y87 as an important target, as it seems to block the entrance for the sterically demanding *tert*-butyl moiety. We selected hydrophobic residues for this position, as they need to coordinate a hydrophobic group. Variants Y59W/Y87V/T231A and Y59W/Y87L/T231A exhibited, for the first time, activity towards the desired amine (Table 1). These findings were quite interesting. Firstly variant Y59W/Y87F/T231 (developed in our previous work for activity towards aromatic bulky substrates)^[1b] was not active, thus supporting our belief that a different engineering approach was needed. More interestingly, the leucine variant was more active than the valine mutant. This is striking, as one would expect that smaller residues would be preferred to accommodate a sterically challeng-

Table 1. Specific activities of Rsp-ATA variants towards *rac*-amine **2** (1 mM) determined in kinetic resolution mode by using pyruvate as amine acceptor (2 mM) at 30 °C, pH 9.0 (*N*-cyclohexyl-2-aminoethanesulfonic acid (CHES), 50 mM).

Variant	Activity [mU mg ⁻¹]
Rsp-ATA_Y59W/T231A	n.a.
Rsp-ATA_Y59W/Y87F/T231A	n.a.
Rsp-ATA_Y59W/Y87V/T231A	6.5 ± 0.4
Rsp-ATA_Y59W/Y87L/T231A	11.5 ± 0.8
Rsp-ATA_Y59W/Y87L/T231A/L382M	19.0 ± 1.9
Rsp-ATA_Y59W/Y87L/T231A/P281S/G429A	32.4 ± 0.1
Rsp-ATA_Y59W/Y87L/T231A/G429A	44.8 ± 0.9
Rsp-ATA_Y59W/Y87L/T231A/L382M/G429A	77.1 ± 5.5
(Rsp-ATA_WLAMA)	
n.a.: Not active (below the detection limit, 1 mU mg ⁻¹).	

ing substrate. However, it seems that the hydrophobicity of the residue plays a role. Smaller residues might provide more space, but this extra space might be occupied by water molecules and thus disfavour diffusion of hydrophobic substrates in the binding pocket. When the mutation provides just enough space for the binding, then hydrophobic interactions between position 87 and the substrate can take place, thereby leading to higher specific activity.

Our rational analysis on the quinonoid intermediate of PLP and compound **1** did not suggest any other position of interest. In this scaffold—for which we observed the first measurable activity—we incorporated mutation L382M, which was identified as beneficial in our previous work dealing with a bridged bicyclic amine.^[4] In parallel, we performed error-prone PCR on variant Rsp-ATA_Y59W/Y87L/T231A. After screening about 5000 colonies of three different ep-PCR libraries with our solid-phase assay^[8] with **2** as the amine donor, we identified a variant with increased activity in kinetic resolution (Table 1). Variant Rsp-ATA_Y59W/Y87L/T231A/P281S/G429A exhibited almost threefold increased activity compared to Rsp-ATA_Y59W/Y87L/T231A (incorporation of just two additional mutations).

Position 429 is close to the large binding pocket, thus we focused on this mutation. Mutation P281S seemed to have a negative effect on specific activity (Table 1) and thus it was discarded. When mutation G429A was incorporated into Rsp-ATA_Y59W/Y87L/T231A/L382M, the effect was almost the same: a fourfold increase (Table 1). As the mechanism of the effect of the mutation at position 429 on the specific activity of the ATA is not clear, and the epPCR random mutagenesis might not provide the best mutation at a given position, we performed saturation mutagenesis at position 429. No variant was better than G429A (data not shown).

In parallel to the protein engineering experiments, we investigated the synthetic usefulness of the identified variants. First, we performed a preparative scale (100 mg) experiment in kinetic resolution mode for Rsp-ATA_Y59W/Y87L/T231A. The findings were striking, as the isolated residual enantiomer of **2** (38 mg) had *S* configuration with 96.2% *ee*. This shows that the enzyme did not prefer the *S* enantiomer for this specific

compound as one would have assumed for an enzyme of fold class I. With this result, we performed another round of in silico analysis: we docked the *tert*-butyl moiety in the large binding pocket, in a conformation that is in line with the preferentially converted *R* enantiomer. In this position the hydrophobic group interacts with the positions 58, 59, 85, 231 and 422. Based on the best variant created so far (Rsp-ATA_WLAMA, Figure 1) further saturation mutagenesis libraries were designed. Position 59 was fully saturated with a NNK codons, and L58 was mutated to alanine, valine, methionine, isoleucine, and cysteine, in order to provide more space and potentially trigger specific interactions with the substrate in the large binding pocket. Two hydrophobic residues (valine or leucine) were incorporated at H85, but these variants did not exhibit improved activity (data not shown).

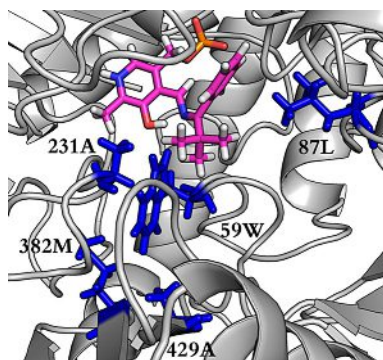


Figure 1. A in silico model of Rsp-ATA_WLAMA with the quinonoid of 2,2-dimethyl-1-phenylpropan-1-one (**1**), based on 3FCR structure. The side chains of the engineered positions are colored in blue.

Next, all interesting variants were applied in analytical scale asymmetric synthesis reactions; this is the desired mode as it theoretically can yield 100% product. We used L-alanine ((S)-alanine) or IPA as amine donors. Despite the low activity in kinetic resolution assays, all variants were active in asymmetric synthesis. Interestingly, the use of L-alanine as amine donor with lactate dehydrogenase (LDH)/glucose dehydrogenase (GDH) cascade for the removal of pyruvate^[9] led to full conversion after 42 h. Isopropylamine was also accepted as an amine donor, but at lower conversions (Table 2). As expected from the kinetic resolution experiments, Rsp-ATA_WLAMA exhibited the highest conversion rates. In order to increase the productivity of the best variant, we incorporated the mutation Y152F, as in previous studies this was related to significant stabilization of the enzyme under the experimental conditions.^[1b] However, this mutation did not provide any benefit for the current reaction; indeed, it decreased the specific activity towards the desired amine.

Next, we compared our most active Rsp-ATA variants under identical conditions with the two most active VF-ATA variants:^[5] VF-ATA_H1_A was the most active variant in kinetic resolution with pentanal as amine acceptor; VF-ATA_H3_RAV was the only variant that reached full conversion in asymmetric synthesis of 10 mM **1** with alanine as amine donor, however

Table 2. Asymmetric synthesis of (*R*)-amine **2** catalysed by the most interesting variants.

Variant	Conversion [%] (ee)	
	with L-alanine	with IPA
Rsp-ATA_Y59W/Y87L/T231A	100 (> 99)	22 ± 2.3 (n.d.)
Rsp-ATA_Y59W/Y87L/T231A/L382M	100 (> 99)	38 ± 1.4 (> 99)
Rsp-ATA_Y59W/Y87L/T231A/G429A	100 (> 99)	45 ± 0.8 (> 99)
Rsp-ATA_Y59W/Y87L/T231A/L382M/G429A (Rsp-ATA_WLAMA)	100 (> 99)	71 ± 3.5 (> 99)
Rsp-ATA_Y59W/Y87L/Y152F/T231A/L382M/G429A	100 (> 99)	40 ± 2.8 (> 99)

Reaction conditions: 4 mM ketone (**1**), HEPES buffer (50 mM, pH 8.0), 5% (v/v) DMSO, 1.35 mg mL⁻¹ ATA, 1 mM PLP at 30 °C and 600 rpm. The amine donor was 200 mM IPA or 200 mM L-alanine. In the case of L-alanine, 150 mM D-glucose, 45 U mg⁻¹ LDH, 15 U mg⁻¹ GDH and 1 mM NADH were added. Samples were taken after 42 h incubation at 30 °C and 600 rpm.

Table 3. Comparison of the most active Rsp-ATA variants with the most active variants of VF-ATA in analytical scale asymmetric synthesis reactions with alanine or isopropylamine as amine donors.

Variant	Conversion [%]	
	with L-alanine	with isopropylamine
VF-ATA_H3_RAV	24 ± 2	3 ± 0.4
VF-ATA_H1_A	0 ± 0	17 ± 1
Rsp-ATA_WLAMA	75 ± 7	28 ± 1
Rsp-ATA_WLAMA/152F	69 ± 4	15 ± 1.7

Reaction conditions: 4 mM ketone (**1**), HEPES buffer (50 mM, pH 8.0), 5% (v/v) DMSO, 1 mM PLP at 30 °C and 600 rpm. In case of isopropylamine as amine donor 0.725 mg mL⁻¹ ATA and 200 mM isopropylamine were applied. In the case of alanine as amine donor, 0.25 mg mL⁻¹ ATA, 200 mM L-alanine, 150 mM D-glucose, 45 U mg⁻¹ LDH, 15 U mg⁻¹ GDH, and 1 mM NADH were applied. Samples were taken after 23 h.

with a significantly higher enzyme concentration (3.8–4.6 mg mL⁻¹).^[5] The Rsp-ATA variants reached significantly higher conversions than the VF-ATA variants (Table 3).

We were interested to compare the stability of Rsp-ATA_WLAMA to that of the Rsp-ATA variant with mutation Y152F (previously reported to stabilize Rsp-ATA). We performed asymmetric synthesis reactions either without pre-incubation or with a six-hour pre-incubation before addition of the keto substrate to start the reaction. Both enzymes lost some activity during the six-hour incubation with 200 mM isopropylamine: 4% lower conversion for Y152F, and 8% for Rsp-ATA_WLAMA. However, Rsp-ATA_WLAMA still provided the highest overall conversions despite six hours of pre-incubation (Table 4).

Bioinformatics and structural comparison of active variants of Rsp-ATA and VF-ATA

We established two solutions to synthesize (*R*)-2,2-dimethyl-1-phenylpropan-1-amine with engineered ATAs: one based on Rsp-ATA and the other based on VF-ATA. It was interesting to analyze in detail which mutations lead to active enzyme variants in the two ATA scaffolds. Rsp-ATA and VF-ATA share only

Table 4. The effect of mutation Y152F on the Rsp-ATA_WLAMA stability was evaluated in terms of conversion after 42 h reaction time with or without six hours pre-incubation (one sample at 30 °C (shaking at 600 rpm) without isopropylamine and another sample with 200 mM isopropylamine).

Conditions	Conversion [%]	
	Rsp-ATA_WLAMA	Rsp-ATA_WLAMA/Y152F
no pre-incubation	43 ± 2.5 %	30 ± 1.9 %
pre-incubation without IPA (6 h)	41 ± 2.0 %	30 ± 2.0 %
pre-incubation with IPA (6 h)	35 ± 0.0 %	26 ± 1.8 %

Final reaction conditions: 4 mM ketone (**1**), HEPES buffer (50 mM, pH 8.0), 5% (v/v) DMSO, 1 mM PLP, 200 mM IPA and 1.15 mg mL⁻¹ TA at 30 °C, 600 rpm for 42 h.

33% sequence identity and only 54% sequence similarity. However, their structures (PDB IDs: 3FCR and 4E3Q, respectively) are quite similar as the alignment of their monomers results in an RMSD of only 1.154 Å. Moreover, most of the residues that are 10 Å from the enamine nitrogen atom of the external aldimine of PLP and the substrate (and thus are supposed to form the active-site), as defined from our in silico modeling studies, are conserved. Aligning the predicted dimeric structures of Rsp-ATA_WLAMA and crystal structure of wild-type VF-ATA returned 49 amino acids with the above-mentioned criteria (25 identical, 32 similar). Notably, both wild-type enzymes did not accept the bulky **2**.

The best VF-ATA variants had mutations L56V, W57C, F85V, and V153A (H3_RAV), or L56V, W57F, F85V, V153A, and R415C (H1_A),^[5] the latter correspond to L58, W59, L87, S155, and R420 in Rsp-ATA_WLAMA. It is interesting to note that in the previous study^[5] the library theoretically comprised 16384 different variants (including wild-type codons at each position), but in fact only 2240 variants needed to be screened to find improved variants. L58 was already targeted in Rsp-ATA in the current study and no mutation to L58 resulted in improved activity. An interesting position in Rsp-ATA is residue 59: in this position in VF-ATA mutation to cysteine was found to be beneficial. Interestingly, in Rsp-ATA the Y59W mutation was found to be the best (this residue is tryptophan in wild-type VF-ATA). Saturation mutagenesis of this position in Rsp-ATA_Y59W/Y87L/T231A and Rsp-ATA_WLAMA did not identify any residue resulting in higher activity than for tryptophan. The most important mutation however was at position 87. Mutations Y87L or Y87V were the ones that created activity for amine **2** in the first place in the Rsp-ATA_Y59W/231A variant. In VF-ATA this mutation is not crucial, as there are variants that accept the amine without the mutation F85V, although the variants that included this mutation showed higher conversion in asymmetric synthesis. So, although the side chain at this position does not interact directly with the *tert*-butyl moiety of compound **1** as the quinonoid intermediate, an aliphatic hydrophobic side chain is required. This can be related to the hydrophobicity of the microenvironment and the diffusion of the substrate to the large binding pocket.

Finally, mutation V153A was previously incorporated into the mutants of VF-ATA,^[5] based on literature reports.^[10] The effect seemed to be specific for this template, as the residue is in the second sphere of interactions and does not interact directly with the quinonoid.^[10a] Indeed, introduction of this alanine mutation at the corresponding position in Rsp-ATA (Rsp-ATA_WLAMA/S155A) reduced the activity in kinetic resolution (data not shown). Three out of the five mutations identified in our best variant Rsp-ATA_WLAMA (Y59W, T231A, and L382M) are found in wild-type VF-ATA. The mutation G429A is also a second shell residue, and seems to be specific for the Rsp-ATA scaffold.

From this analysis it can be seen that despite the structural similarity and conservation of the residues of the active site, no motif can be easily identified. The most crucial position for substrates with a *tert*-butyl substituent is position Y87 (Rsp-ATA)/F85 (VF-ATA), as its mutation to aliphatic hydrophobic residues had a beneficial effect in both enzymes.

Conclusion

The amine transaminase of *Ruegeria* sp. TM1040 (Rsp-ATA) was engineered to enable the synthesis of the bulky amine (*R*)-2,2-dimethyl-1-phenylpropan-1-amine. Although the wild-type enzyme did not exhibit activity towards this substrate, incorporation of five mutations led to the acceptance of the corresponding bulky ketone and allowed the asymmetric synthesis of (*R*)-amine **2**, even with isopropylamine as the amine donor. We show that these mutations are different from those required to convert planar bulky compounds, and hence a different protein-engineering strategy was needed. The most critical mutation to enable acceptance of the bulky substrate was Y87L, a position that was also important for VF-ATA; thus, this seems to be a critical residue for the identification of ATAs that are active towards compounds with a tertiary carbon substituent.

Experimental Section

Materials: Ketone **1** and amine **2** (racemic mixtures and individual enantiomers) were made available by F. Hoffmann-La Roche. All other reagents were of analytical grade. Recombinant expression of ATA from *Ruegeria* sp. TM1040 (Rsp-ATA) and all variants was as described previously.^[1b] The glycine oxidase was produced as described previously.^[8]

Directed evolution libraries—point and site-saturation mutagenesis: For the preparation of error-prone PCR libraries, the gene of the respective template of the ATA from *Ruegeria* sp. TM1040 was amplified by using a GeneMorph II Random Mutagenesis Kit (Agilent Technologies) according to the instructions and with the previously described flanking primers,^[4] and 40, 50, and 60 ng of plasmid DNA template. All other variants were prepared by using a modified version of the QuikChange PCR method as described before.^[4]

Protein expression and purification: Protein expression and purification were performed as described previously.^[4]

Kinetic resolution experiments: For determination of specific activities and for screening libraries in crude lysate, a direct spectrophotometric assay was applied as described previously.^[1b] Formation of the ketone (**1**) was monitored at 245 nm ($\epsilon = 7953 \text{ M}^{-1} \text{ cm}^{-1}$). Saturation libraries based on Rsp-ATA_59W/87L/231A were screened in crude lysate by a glycine oxidase assay as described previously.^[4]

Solid-phase assay screening of error-prone PCR libraries: The ep-PCR libraries were screened by using the glycine oxidase solid-phase assay^[4] with all subsequent steps performed as described before.^[4] The assay plates contained racemic 2,2-dimethyl-1-phenylpropan-1-amine (4.44 mm) and glyoxylate (10 mm) as transaminase substrates.

Asymmetric synthesis experiments: These were performed in analytical scale (0.5 or 1 mL) in glass vials on an Eppendorf shaker. Detailed final concentrations and conditions are given in the main text. For HPLC analysis, a sample (65 μL) was mixed with acetonitrile (65 μL) including diethylamine (0.1%) and passed through a filter tip before injection into the HPLC instrument. For chiral analysis, a sample (150 μL) was used for extraction as described previously.^[5] Chiral GC-analysis was performed as described previously.^[5] In GC the ketone eluted after 35.26 min, the (*S*)-amine eluted after 35.9 min, and the (*R*)-amine eluted after 37.58 min. Conversions were determined by HPLC analysis on a Luna C₈ column (150 \times 4.6 mm; Phenomenex) with a gradient of acetonitrile containing TFA (0.1%) and water containing TFA (0.1%): 0–4 min, 10% acetonitrile; 8–12 min, 60% acetonitrile; 12–25 min, 10% acetonitrile (1 mL min⁻¹; oven temperature 45 °C; detection at 210 nm). A standard curve for amine (**2**, 0–4 mm) returned a slope of 10094443 AU mm⁻¹ for an injection volume of 15 μL . In achiral HPLC the amine peak eluted after 9.38 min. For each reaction with full conversion, it was confirmed by GC that the ketone was entirely consumed.

Preparative scale preparation of (*S*)-amine **2:** sodium pyruvate (129 mg) and purified mutant transaminase Rsp-ATA_Y59W/Y87L/T231A (18.5 mL, protein 2.47 mg mL⁻¹) were added to TRIS buffer (89.75 mL, 50 mM, pH 8.5) containing PLP (Sigma–Aldrich, 1 mM) and stirred for 5 min at 30 °C. The reaction was started by the addition of *rac*-**2** (100 mg in DMSO (1 mL)). After 48 h and a conversion of roughly 55 area% (IPC-chiral HPLC), the reaction was acidified to pH 2.0 to precipitate the enzymes, and stirred for 20 min. Subsequently, the reaction mixture was filtrated through 25 g filter aid (Dicalite) bed, then the filter cake was washed with deionized water and MTBE (50 mL). After phase separation the aqueous phase was extracted with MTBE (50 mL) to remove the 2,2-dimethyl-1-phenylpropan-1-one (**1**). The combined organic phases were dried over anhydrous MgSO₄, filtered, and evaporated in a vacuum at 40 °C thereby yielding **1** as yellow viscous oil (25 mg, 26.5%; chiral HPLC: 99 area %). The pH of the aqueous phase was adjusted to pH 12 with NaOH (2 N) then the mixture was extracted with MTBE (2 \times 50 mL). The combined organic phases were dried over anhydrous MgSO₄, filtered, and evaporated in a vacuum at 40 °C thereby yielding 38 mg (40%) (*S*)-2,2-dimethyl-1-phenylpropan-1-amine (**2**) as yellow oil.

Chiral HPLC: 98.1 area% (*S* enantiomer), 1.9 area % (*R* enantiomer) [220 nm; Chiracel OD-3R; 150 \times 4.6 mm, 3 μm , flow 1.0 mL, 25 °C,

A) 50% acetonitrile (ACN), B) 50% 6.3 g ammonium formate in 950 mL H₂O : 50 mL ACN]; ¹H NMR (600 MHz, CDCl₃): δ = 7.27–7.31 (m, 4H), 7.24 (dt, *J* = 6.0, 2.6 Hz, 1H), 3.71 (s, 1H), 0.91 ppm (s, 9H); GC-MS: 162 (M).

Acknowledgements

We would like to thank Ina Menyes for her support in the HPLC and GC analysis.

Conflict of Interest

The biocatalysis group of Roche has a committed interest over the long term in establishing a set of technically applicable TAs with broad substrate acceptance to assist in devising more attractive, shorter, economical and greener synthetic routes to investigational drugs and beyond.

Keywords: amine transaminase • asymmetric synthesis • enzyme catalysis • protein engineering

- [1] a) M. Fuchs, J. E. Farnberger, W. Kroutil, *Eur. J. Org. Chem.* **2015**, 6965–6982; b) I. V. Pavlidis, M. S. Weiß, M. Genz, P. Spurr, S. P. Hanlon, B. Wirz, H. Iding, U. T. Bornscheuer, *Nat. Chem.* **2016**, *8*, 1076–1082; c) C. K. Savile, J. M. Janey, E. C. Mundorff, J. C. Moore, S. Tam, W. R. Jarvis, J. C. Colbeck, A. Krebber, F. J. Fleitz, J. Brands, P. N. Devine, G. W. Huisman, G. J. Hughes, *Science* **2010**, *329*, 305–309; d) M. D. Truppo, J. D. Rozzell, N. J. Turner, *Org. Process Res. Dev.* **2010**, *14*, 234–237.
- [2] a) F. Steffen-Munsberg, C. Vickers, H. Kohls, H. Land, H. Mallin, A. Nobili, L. Skalden, T. van den Bergh, H.-J. Joosten, P. Berglund, M. Höhne, U. T. Bornscheuer, *Biotechnol. Adv.* **2015**, *33*, 566–604; b) D. Koszelewski, K. Tauber, K. Faber, W. Kroutil, *Trends Biotechnol.* **2010**, *28*, 324–332.
- [3] M. Höhne, S. Schätzle, H. Jochens, K. Robins, U. T. Bornscheuer, *Nat. Chem. Biol.* **2010**, *6*, 807–813.
- [4] M. S. Weiß, I. V. Pavlidis, P. Spurr, S. P. Hanlon, B. Wirz, H. Iding, U. T. Bornscheuer, *Org. Biomol. Chem.* **2016**, *14*, 10249–10254.
- [5] M. Genz, O. Melse, S. Schmidt, C. Vickers, M. Dörr, T. van den Bergh, H.-J. Joosten, U. T. Bornscheuer, *ChemCatChem* **2016**, *8*, 3199–3202.
- [6] D. F. A. R. Dourado, S. Pohle, A. T. P. Carvalho, D. S. Dheeman, J. M. Caswell, T. Skvortsov, I. Miskelly, R. T. Brown, D. J. Quinn, C. C. R. Allen, L. Kulakov, M. Huang, T. S. Moody, *ACS Catal.* **2016**, *6*, 7749–7759.
- [7] F. Steffen-Munsberg, C. Vickers, A. Thontowi, S. Schätzle, T. Tumlrirsch, M. Svedendahl-Humble, H. Land, P. Berglund, U. T. Bornscheuer, M. Höhne, *ChemCatChem* **2013**, *5*, 150–153.
- [8] M. S. Weiß, I. V. Pavlidis, C. Vickers, M. Höhne, U. T. Bornscheuer, *Anal. Chem.* **2014**, *86*, 11847–11853.
- [9] D. Koszelewski, I. Lavandera, D. Clay, D. Rozzell, W. Kroutil, *Adv. Synth. Catal.* **2008**, *350*, 2761–2766.
- [10] a) A. Nobili, F. Steffen-Munsberg, H. Kohls, I. Trentin, C. Schulzke, M. Höhne, U. T. Bornscheuer, *ChemCatChem* **2015**, *7*, 757–760; b) E.-S. Park, S.-R. Park, S.-W. Han, J.-Y. Dong, J.-S. Shin, *Adv. Synth. Catal.* **2014**, *356*, 212–220.

Manuscript received: January 23, 2017

Accepted manuscript online: March 23, 2017

Version of record online: April 27, 2017

Solid Phase Agar Plate Assay for Screening Amine Transaminases

Martin S. Weiß¹, Matthias Höhne² and Uwe T. Bornscheuer¹

¹Institute of Biochemistry, Department of Biotechnology and Enzyme Catalysis, Greifswald University, Germany

²Institute of Biochemistry, Greifswald University, Germany

Email: uwe.bornscheuer@uni-greifswald.de, Matthias.Hoehne@uni-greifswald.de

Running Head

Plate assays

i. Summary

Agar plate assays represent a useful method for high-throughput prescreening of larger enzyme libraries derived from e.g. error-prone PCR or multiple site saturation mutagenesis to decrease screening effort by separating promising variants from less active, inactive or neutral variants. In order to do so, colonies are directly applied for enzyme expression and screening on adsorbent and micro porous membranes instead of elaborately preparing cell lysates in 96-well plates. This way, 400 to 800 enzyme variants can be prescreened on a single membrane, 10000 – 20000 variants per week and per single researcher respectively (calculating 25 membranes per week).

The following chapter gives a detailed protocol of how to screen transaminase libraries in solid-phase, but it also intends to provide inspiration to establish a direct or coupled agar plate assay for screening variable enzymatic activities by interchanging assay enzymes and adapting assay conditions to individual needs.

ii. Key words (5-10 key words)

Agar plate assay, solid-phase assay, high-throughput screening assay, directed evolution, transaminase, horseradish-peroxidase, glycine oxidase

1. Introduction

Random mutagenesis or multiple site saturation mutagenesis still represent key methods for evolving biocatalysts to fit the desired process conditions such as high solvent, substrate and product titers or elevated temperatures [1]. In most of the cases random mutagenesis methods are applied to improve an already existing enzyme property by mimicking nature's evolution process and simply screening a large number of random variants [2]. To reduce the screening effort by sorting out less active or inactive variants and to focus only on the promising ones, various assay systems with different throughput levels are available. Among those, 96-well microtiter plate assays are commonly used and allow growth of the expression host, expression and screening of the variants. This way the screening throughput is more or less restricted to screening not significantly more than 1000 variants per week and researcher without any robotic support [2].

Solid-phase assay screening intends to increase the throughput by circumventing the laborious inoculation of single variants from agar plates in microtiter plates. Instead, colonies carrying the plasmids with the mutated genes are directly transferred from the master agar plate to micro porous membranes. Placing the membranes – colonies facing up – on different agar plates (containing appropriate inducer and assay substances) allows expression and screening of the enzyme variants by diffusion of the assay compounds from the agar into the membrane. In general, agar plate assays comprise the same principle steps as microtiter plate assays do: (i) Transfer of the colonies to a microporous membrane, (ii) enzyme expression on an induction plate, (iii) cell permeabilization, e.g. by chloroform treatment and (iv) finally assaying the desired reaction by placing the membrane on an assay plate containing all the reagents necessary for the detection of the desired activity. Thus, up to ~800 colonies can be prescreened on a single membrane and as handling of the membranes does not involve any time consuming and elaborate processing steps, such as centrifugation of microtiter plates after cell disruption, it is easily feasible to prescreen 25 membranes representing 10000–20000 different variants per week and researcher. However, not only the throughput is relevant for efficient catalyst evolution, but also a well prepared library, which should not contain too many wild-type clones and optimal mutation frequency is crucial for success. Using an agar plate assay allows preparation and investigation of several different libraries in parallel. Observation of the ratio of

active to inactive variants on a membrane can help to adjust the mutation frequency to the individual needs or can help to select one of the investigated libraries for further screening.

There are various interchangeable principle assay reactions available that allow translation of the desired enzyme activity into a detectable signal, most frequently by formation of a dye to visualize colonies containing the desired enzyme variants on agar plates or membranes (*see* Table 1) [3].

For coupled assay systems, co-expression of one or more assay enzymes together with the variant of interest allows efficient screening in solid-phase without any need to apply purified enzymes and taking advantage of very close proximity of all involved assay enzymes [4, 5]. Application of externally applied purified assay enzymes may lead to diffuse color formation due to diffusion of the intermediate products before its local concentrations are high enough to allow fast subsequent conversion by the assay enzymes *in situ*, if the activity of the assay enzymes is insufficient [4, 5]. For co-expression of multiple enzymes on different plasmids, subcloning in compatible plasmids exhibiting independently regulated plasmid replication origins is required [6].

Horseradish-peroxidase coupled assays allow screening of a variety of different enzymatic activities by detection of hydrogen peroxide and subsequent formation of a dye [4, 5, 7-10]. There are several chromogenic substrates for horseradish peroxidases that lead to soluble or insoluble products.

However, the pH-working range is different for each substrate due to changes in the absorbance spectra, altered stability or specific reactivities leading to the proper formation of the dye at different pH-values (*see* Table 2).

The following chapter intends to provide general inspiration to establish a direct or coupled agar plate assay for screening variable enzymatic activities. Thus, we exemplarily describe a glycine oxidase and horseradish-peroxidase double-coupled agar plate assay for detection of transaminase activities towards amines by following the formation of the by-product glycine, which is oxidized *in situ*, generating hydrogen peroxide and finally leading to the formation of a red quinone imine dye (*see* Figure 1) [4].

The solid-phase assay screening procedure consists of several consecutive steps depicted in Figure 2. *E. coli* BL21 carrying the plasmid coding for glycine oxidase (Figure 2.1) is transformed with the plasmid mixture obtained from the mutagenesis experiment. Transformed cells are spread out on agar

plates and are incubated overnight for colony growth on the plates (Figure 2.2). Transfer of the colonies on a microporous membrane (Figure 2.3) allows induction of the colonies on agar plates containing suitable inducers (Figure 2.4), while the original plate is kept to serve as a master plate. After expression, the membrane is treated with chloroform for cell permeabilization (Figure 2.5). To reduce possible background reactions the membrane is placed on dialysis plates overnight allowing low molecular weight compounds to diffuse into the dialysis agar (Figure 2.6). Finally, incubation of the membranes on assay plates containing all the substrates and reagents for the assay reaction allows screening of the library of interest by selecting most colored colonies for further investigation (Figure 2.7). In Table 3 we suggest a possible time-table for the assay procedure for screening 25 agar plates per week.

2. Materials

2.1. Biological and Chemical Materials

1. A transaminase gene of choice subcloned in a suitable plasmid, such as pET22b(+) as described in [11].
2. The glycine oxidase gene should be subcloned in a plasmid, which is compatible to the one containing the transaminase. The two plasmids should contain different antibiotics selection markers. In our hands, a codon-optimized glycin oxidase gene [4] subcloned in the compatible vector pCDF-1b worked well for co-expression with the transaminase.
3. Expression strain: *E. coli* BL21 (DE3) *fhuA2* [*lon*] *ompT* *gal* (λ DE3) [*dcm*] Δ *hdsS* λ DE3 = λ *sBamHI*o Δ *EcoRI*-B *int::*(*lacI::PlacUV5::T7 gene1*) *i21* Δ *in5*
4. LB medium and LB agar from any supplier
5. Sterile SOC medium: 20 g/L tryptone; 5 g/L yeast extract; 10 mM NaCl; 2.5 mM KCl; 20 mM glucose.
6. 10% glycerol (autoclaved)
7. Suitable antibiotics stock solutions. We used ampicillin stock solution (100 mg/mL ampicillin in deionized water) and spectinomycin stock solution (50 mg/mL spectinomycin in deionized

water) after sterilization by filtration (0.2 μm pore size filter), aliquots can be stored at -20°C for several months.

8. IPTG stock solution: Dissolve 238 mg/mL IPTG in distilled water and sterilize by filtration. Aliquots can be stored at -20°C for several months.
9. Agarose: Standard agarose for DNA electrophoresis
10. 30 mM Tris-HCl buffer, pH 8.5 for dialysis plates
11. 50 mM CHES buffer, pH 9.5. Adjust the pH to 9.5 with NaOH.
12. Glyoxylate stock solution: 1 M glyoxylic acid solution in ultra-pure water. Weigh 920 mg of glyoxylic acid monohydrate, add 10 mL of ultra-pure water, mix and store at 4°C
13. 4-AAP stock solution: 0.3 g/mL 4-aminoantipyrine in pure ethanol. Store at room temperature.
14. Vanillic acid stock solution: 0.13 g/mL vanillic acid in methanol. Store at room temperature.
15. Amine donor stock solution: 1 M (S)-1-phenylethylamine in pure ethanol. Pipette 262.67 μL of (S)-(-)-1-phenylethylamine, add 1737.33 μL of pure ethanol, mix and store at room temperature.
16. HRP-solution (1200 U/mL): Carefully dissolve 3000 U horseradish peroxidase lyophilisate in 2.5 mL ultra-pure water. Keep on ice and do not store the solution longer than necessary. Always prepare it fresh directly before usage.
17. Nitrocellulose membranes: Binding capacity for proteins $> 200 \mu\text{g}/\text{cm}^2$, pore size 0.2 μm , membrane strength $0.15 \text{ mm} \pm 0.05 \text{ mm}$.

2.2 Equipment

1. Electroporation device:
2. Desiccator: Fill up a desiccator with chloroform to 1 cm height, close the lid and store it for at least five hours at room temperature
3. Sieve: A usual steel strainer used in the kitchen, remove the handle in order to fit it in the desiccator

3. Methods

3.1 Preparation of Plates for Selection, Induction, Dialysis and Assaying

1. Add 12 g of agar-agar and 20 g LB-medium to 800 mL of deionized water and autoclave the mixture (sufficient for 30-35 plates à 20-25 mL). Cool down to $\approx 45^{\circ}\text{C}$ while stirring. For preparation of selection plates for the simultaneous selection of cells that harbor both plasmids (the glycine oxidase and the transaminase library of interest) add 800 μL of ampicillin stock solution and 800 μL of spectinomycin stock solution (*see Note 1*). For preparation of induction plates add the corresponding antibiotics and additionally 800 μL of the IPTG stock solution. After mixing, aliquot the solution in sterile petri dishes and store them at 4°C after solidification.
2. For preparing dialysis plates add 800 mL of TRIS buffer (sufficient for 30–35 plates à 20–25 mL) and 3.2 g of agarose (0.4 %) and boil the suspension by microwave heating or on a hot plate until the agarose is completely dissolved. Cool down the solution to 38°C while stirring. Add 19.77 mg PLP and 6.28 mg FAD to achieve an end concentration of 100 μM and 10 μM . Aliquot the homogenous solution into petri-dishes (*see Note 2*).
3. For preparation of assay plates add 200 mL of CHES buffer (sufficient for 8–10 assay plates à 20–25 mL) and 2 g of agarose (1 %) and boil the suspension by application of a microwave or a hot plate until the agarose is completely dissolved. Cool down the solution to 38°C while stirring. Add 160 μL 4-AAP stock solution, 1 mL vanillic acid stock solution, 2 mL glyoxylic acid stock solution and 0.2–2 mL of amine donor stock solution to achieve an amino donor end concentration of 1–10 mM (*see Note 3*). Horseradish peroxidase application on the assay plates takes place right before the membranes are applied as described below.

3.2 Electrocompetent Cells / Multiple plasmids

1. Inoculate 500 mL of LB-medium with 5 mL of a fresh overnight culture of *E. coli* BL21(DE3) and let them grow at 37°C and 180 rpm until OD_{600} of 0.5–0.7. Cool them on ice for 20 min. Centrifugation of the suspension at 4000 g and 4°C allows sequential washing of the cells. To do so resuspend the cell pellets in 500, 250, 20 and finally 1.5 mL ice-cold ultra-pure and sterile water containing 10 % glycerol. Aliquot 50 μL in 1.5 mL tubes and immediately deep-freeze in liquid nitrogen. Store the competent cells at -80°C .

2. The plasmids for co-expression of the assay enzymes (in this case coding for glycine oxidase) are transformed and corresponding transformants are made electro-competent again to achieve high transformation efficiencies for multiple plasmid transformations. Repeat the protocol for the preparation of electro-competent cells for the cells carrying the plasmids needed for the assay. Do not forget to add the corresponding antibiotics in the culture media.

3.3 Transformation and Colony Transfer to the Membranes, Induction

1. Thaw a sample of electro-competent cells containing plasmids necessary for the assay on ice for 5–10 min. Add 0.5 μL of plasmid DNA from your library of interest having a plasmid DNA concentration of around 20 ng/ μL (*see Note 4*). Add the aliquot containing the DNA in a precooled 0.2 mm electroporation cuvette and pulse with 1.8 kV (*see Note 5*). Immediately afterwards, add 1 mL of LB-SOC medium and carefully transfer the suspension in a sterile 1.5 mL tube. Cure the cells for 1 h at 37 °C and 180 rpm. To achieve suitable colony numbers on the plates, plate out 10, 20, 30, 40 and 50 μL of the suspension on agar plates (room temperature) containing ampicillin and spectinomycin. Incubate the plates at 30 °C overnight. The next morning, incubate the plates at 37°C, if the colonies are not big enough until the desired size is obtained (*see Note 6*).
2. Use a water-proof pen to label the nitrocellulose membranes with a membrane number and the current date. Additionally, put three different check marks on the margin of each membrane (ideally in a triangle), to be able to document the orientation of the membrane on the agar plate. Place one labeled nitrocellulose membrane, labeling facing down, on an agar plate covered with colonies of reasonable size (*see Note 7*). Make sure the membrane has contact to the assay agar over the whole plate. Use a water-proof pen to label the agar plate with the same check marks in the same orientation, plate number and date.
3. Take off the membrane from the agar plate using tweezers and place it, colonies facing up, on an induction plate. Make sure the membrane is in contact with the induction medium over the whole plate. For co-expression of the variants of interest and the assay enzymes, incubate the membrane for 6–7 hours at 30 °C (*see Note 8*).

4. The selection plates where the colonies were transferred from are incubated for 6 hours at 37 °C for regrowth of the colonies. By doing so, an exact copy of the colonies on the membranes is generated that can serve as a master plates for further investigation of the interesting variants. Seal the master plates and store them at 4 °C.

3.3. Cell Permeabilization, Dialysis and Assaying

1. After expression, the membranes are placed on a mesh in the desiccator saturated with chloroform vapor for 60 seconds at room temperature (*see Note 9*, Figure 3 and 4) to permeabilize the cells.
2. After cell permeabilization place the membranes on precooled dialysis plates and store them overnight at 4 °C (*see Note 10*).
3. Spread 100 µL of horseradish peroxidase solution on an assay plate (*see Note 11*). Immediately afterwards place a membrane covered with chloroform treated and dialysed colonies, colonies facing up, on the assay plate with horseradish peroxidase. If necessary strip off remaining liquid of the membrane at the lid of the petri dish. Make sure the whole membrane is in contact with the assay agar. Incubate the assay plates at 37°C and monitor color formation for up to six hours (*see Note 12*).
4. Select the most colored colonies on each membrane and locate them on the corresponding master plate for regrowth on a hit-agar plate or for rescreening in microtiter plates, depending on the number of interesting variants for further investigation (*see Note 13*).

2. Notes

1. In this case selection on two plasmids is carried out by ampicillin (transaminase of interest) and spectinomycine (glycine oxidase, assay enzyme). Substitute these antibiotics according to your needs. For three or more different plasmids reduce the amount of each antibiotic.

2. Do not dry the dialysis plates after aliquoting. They are supposed to be wet enough to facilitate diffusion during the dialysis step.
3. Do not stir the assay agar too strongly to avoid air intake and air bubble formation. The amount of substrate for the protein of interest (here transaminases) is depending on the activity of your template and the cost of the amine substrates. For higher amine substrate concentrations it is important to check, whether the pH-value is affected. Readjust the pH, if necessary. For other assay systems substitute all reagents to assay your reaction of interest. Be advised: Depending on both the substrates and your protein of interest the choice of buffer compound and the adjusted pH value is crucial. For transaminases even pH 9.0 instead of pH 9.5 will dramatically affect the signal strength. Make sure that all assay enzymes (here glycine oxidase and horseradish peroxidase) at least tolerate or are compatible to the conditions required by your enzyme of interest. Make sure to use chromogenic dyes that are suitable for the desired pH-value of the assay agar. Besides of the desired assay reaction, a background color formation might occur which often also has a certain pH optimum. Do not store the assay plates for more than a few hours to avoid auto-oxidation or other side reactions.
4. Please consult further literature for preparation of random mutagenesis libraries or saturation libraries [12, 13], as it would go beyond the scope of this chapter to discuss this in details here.
5. In our hands, transformation by electroporation provided highest and quite reproducible transformation efficiencies. Both properties are crucial for efficient screening of large libraries. However, despite all efforts, transformation efficiency varies. In order to be able to distinguish each colony on the membrane and to be able to assign interesting colonies on the membrane to the corresponding colonies on the master plates, less than 800 colonies should be plated out per membrane. Too few colonies per membrane are not worth the screening effort. The amount of colonies obtained is very dependent on the amount of DNA added. Try to add always the same amount of DNA (e.g. 20 ng) and find out the individual

transformation efficiency for each batch of competent cells. With some experience it is easily possible to get the ideal amounts of colonies.

6. Do not grow the plates too long, as too large colonies cannot be discriminated from each another. This will decrease the screening efficiency. Too small colonies are difficult to transfer to the membrane and later on are more difficult to locate on the master plate, when interesting colonies are supposed to be selected for further investigation. As well consider that during expression the colonies still continue to grow. For these reasons colonies should not be larger than the head of a pin (< 1 mm diameter) when they are transferred to the nitrocellulose membrane.
7. Whenever possible try to implement a positive control on each membrane. In best cases the template already shows initial activity against the target substrate. This way properly working assay reagents and procedure can be monitored for each membrane. It is as well possible to apply a positive control from a different plate. To do so cut out a piece of agar from a plate covered with colonies carrying wild-type or reference plasmids and transfer the colonies to the membrane before placing the membrane on the plate with the target library. However, this positive control will not exactly behave as the colonies obtained from placing the membrane on the agar containing the colonies of the library of interest as cell material will remain on the master-plate.
8. Expression conditions such as temperature, duration, kind of inducer and inducer concentration need to be adapted to the need of both your assay enzymes and your protein of interest, as well as to your expression system. We recommend elaborating the expression conditions for the assay enzymes in a first step (in this case expression of cells containing only glycine oxidase and incubation on glycine containing assay agar). In parallel, expression conditions for the protein of interest can be investigated in shake flasks to get an idea where to start. In every case a good compromise needs to be made for all enzymes involved in the assay reaction. Investigation of the whole enzymatic setup is possible by application of characterized wild-type proteins (here transaminases) and application of different substrates

being accepted with different activities. Thus, determine the limit of detection for your individual assay conditions.

9. In our hands, cell permeabilization using chloroform was most straightforward to serve its purpose. Freeze-thawing cycles or liquid nitrogen might be possible as well, but we observed that the nitrocellulose membranes broke into pieces and we did not put further effort for investigation. Membranes from different suppliers might behave differently.
10. In every case a negative control experiment employing assay plates without the substrate of interest (in this case 1-phenylethylamine) is required to investigate if any compounds in the cell lysate lead to a false positive signal in the assay. In our exemplary case a background signal could arise from intracellular glycine, or other amino acids that are converted to glycine by the transaminase. Incubating the membranes in a dialysis step helped to remove most of the background signal.
11. Make sure to apply the membrane immediately after application of horseradish peroxidase solution in order to avoid diffusion into the assay agar and to allow the membrane to soak in the solution. Make sure there is not too much liquid between the membrane and the assay agar. The amount of humidity should be enough for the substrates to diffuse into the nitrocellulose membrane when placed on the agar but few enough to avoid any easy diffusion of reaction products.
12. Too long incubation of the plates lead to color formation that is potentially not correlated to the desired enzyme activity. As well, diffusion of the dye plays a bigger role for longer incubations. Investigate the maximum duration of incubation by application of positive and negative controls. We recommend application of insoluble dyes for long-term incubations.
13. According to our experiences variants with more than 5-fold increased activity compared to the reference can be discriminated in solid-phase on a hit plate. For more accurate investigation most colored colonies should be expressed in deep-well blocks and subsequent screening of the crude lysates. For multiple plasmids in the cells, add both antibiotics and express all cascade enzymes. As a reference, apply *E. coli* BL21 cells transformed as well

with all the plasmids necessary for the assay cascade and the protein of interest to guarantee comparability.

3. References

1. Bornscheuer UT, Huisman GW, Kazlauskas RJ et al (2012) Engineering the third wave of biocatalysis. *Nature* 485:185–194
2. Leemhuis H, Kelly RM, Dijkhuizen L (2009) Directed evolution of enzymes: Library screening strategies. *IUBMB Life* 61:222–228
3. Reymond, JL (2006) *Enzyme Assays*. Wiley-VCH, Weinheim
4. Weiß MS, Pavlidis IV, Vickers C et al (2014) Glycine oxidase based high-throughput solid-phase assay for substrate profiling and directed evolution of (R)- and (S)-selective amine transaminases. *Anal. Chem.* 86:11847–11853
5. Willies SC, White JL, Turner NJ (2012) Development of a high-throughput screening method for racemase activity and its application to the identification of alanine racemase variants with activity towards L-arginine. *Tetrahedron* 68:7564–7567
6. Tolia NH, Joshua-Tor L (2006) Strategies for protein coexpression in *Escherichia coli*. *Nat Methods* 3:55–64
7. Delagrave S, Murphy DJ, Pruss JL et al (2001) Application of a very high-throughput digital imaging screen to evolve the enzyme galactose oxidase. *Protein Eng* 14:261–267
8. Escalettes F, Turner NJ (2008) Directed evolution of galactose oxidase: generation of enantioselective secondary alcohol oxidases. *ChemBioChem* 9:857–860
9. Alexeeva M, Enright A, Dawson MJ (2002) Deracemization of α -methylbenzylamine using an enzyme obtained by in vitro evolution. *Angew Chem Int Ed* 41:3177–3180
10. Rowles I, Malone KJ, Etchells LL et al (2012) Directed evolution of the enzyme monoamineoxidase (MAO-N): Highly efficient chemo-enzymatic deracemisation of the alkaloid (\pm)-crispine A. *ChemCatChem* 4:1259–1261
11. Steffen-Munsberg, F, Vickers C, Thontowi A et al (2013) Connecting unexplored protein crystal structures to enzymatic function. *ChemCatChem* 5:150–153

12. Tee KL, Wong TS (2013) Polishing the craft of genetic diversity creation in directed evolution. *Biotechnol Adv* 31:1707–1721
13. Gillam EMJ, Copp JN, Ackerley DF (eds) (2014) Directed evolution library creation: methods and protocols. Springer, New York
14. Bornscheuer UT, Altenbuchner J, Meyer HH (1998) Directed evolution of an esterase for the stereoselective resolution of a key intermediate in the synthesis of epothilones. *Biotechnol Bioeng* 58:554–559
15. Green AP, Turner NJ, O'Reilly E (2014) Chiral amine synthesis using ω -transaminases: An amine donor that displaces equilibria and enables high-throughput screening. *Angew Chem Int Ed* 53:10714–10717
16. Martin AR, DiSanto R, Plotnikov I et al (2007) Improved activity and thermostability of (S)-aminotransferase by error-prone polymerase chain reaction for the production of a chiral amine. *Biochem Eng J* 37:246–255
17. Hailes H, Baud D, Ladkau N et al (2015) A rapid, sensitive colorimetric assay for the high-throughput screening of transaminases in liquid or solid-phase. *Chem Commun* 51:17225–17228
18. Mayer C, Jakeman DL, Mah M et al (2001) Directed evolution of new glycosynthases from *Agrobacterium* β -glucosidase: a general screen to detect enzymes for oligosaccharide synthesis. *Chem Biol* 8:437–443

4. Figure Captions

1. Figure 1: Application of glyoxylate as amino acceptor substrate allows screening for activity towards different amines by either (*R*)- or (*S*)-selective transaminases. Production of achiral glycine is then followed by oxidation and hydrogen peroxide formation leading to the formation of a red quinone imine dye [4]. Toxic phenol can be substituted by vanillic acid [4].
Link: <http://pubs.acs.org/doi/pdf/10.1021/ac503445y>
2. Figure 2: General procedure of the solid-phase assay. *E. coli* BL21(DE3) cells are transformed with both plasmids coding for glycine oxidase and the transaminase library of interest (1) and colonies are grown on dual selection LB agar plates (2). Afterwards, colonies

are transferred to nitrocellulose membranes (3) that are placed—colonies facing up—on induction plates containing IPTG for expression of the proteins (4). Then, cells are permeabilized by chloroform treatment (5). To eliminate false positive background color formation, permeabilized cell colonies are dialyzed overnight by placing the membranes on dialysis plates (6). Finally, screening is conducted by incubation of the membranes on assay plates (7) [4]. Link: <http://pubs.acs.org/doi/pdf/10.1021/ac503445y>

3. Figure 3: a) Arrangement of the membranes on a mesh and b) chloroform treatment of the mesh in a desiccator filled with chloroform to 1 cm of height.

5. Table Captions

Table 1: Selected exemplary literature using the most commonly used assay principles in agar plate screening.

Table 2: Suitable horseradish-peroxidase substrates for agar plate screenings at different pH-working ranges.

Table 3: Suggested schedule for solid-phase assaying.

6. Tables

Table 1

Enzyme activity	Principle	References
Hydrolases, decarboxylases, kinases glycosyltransferases	Detection of pH-change	[14]
Transaminases	Direct formation of a colored product	[15–17]
Glycosynthase	Coupled assay using chromogenic substrates	[18]
Oxidases	Direct detection of hydrogen peroxide	[7–10]
Racemases, transaminases	Coupled assays detecting hydrogen peroxide	[4,5]

Table 2

Compound name	pH-working range	Dye solubility
3-amino-9-ethylcarbazole (AEC)	< 6.0	insoluble
4-Chloro-1-naphthol (4-CN)	7.0 – 8.0	insoluble
3,3'-Diaminobenzidine (DAB)	7.0 – 7.6	insoluble
4-Aminoantipyrine (4-AAP) and vanillic acid or phenol	> 8.0	soluble

Table 3

Monday	Tuesday	Wednesday	Thursday	Friday
Preparation of agar plates, induction plates, dialysis plates, buffers and stock solutions	Transformation of the libraries and plating out 75 plates for incubation overnight	If no suitable colony density on the plates was achieved, repeat the program of yesterday	Preparation of fresh assay plates	Reserved for repetitions and organization of the next week's experiments
Preparation of 1 % agarose in screening buffer and storage at 60 °C		Labeling of 25 membranes, transfer of the colonies to the membranes, induction and regrowth of the colonies on the master plates	Screening of the membranes: 45 minutes time-delayed for every five or ten membranes	
		After at least 6 hours of expression on induction plates chloroform treatment and overnight dialysis	Following color formation of the colonies and selection of the most colored colonies on the master plates	
			Arrangement of a hit plate	

Eigenständigkeitserklärung

Hiermit erkläre ich, dass diese Arbeit bisher von mir weder an der Mathematisch-Naturwissenschaftlichen Fakultät der Ernst-Moritz-Arndt-Universität Greifswald noch einer anderen wissenschaftlichen Einrichtung zum Zwecke der Promotion eingereicht wurde.

Ferner erkläre ich, dass ich diese Arbeit selbstständig verfasst und keine anderen als die darin angegebenen Hilfsmittel und Hilfen benutzt und keine Textabschnitte eines Dritten ohne Kennzeichnung übernommen habe.

Martin Weiß

Martin Steffen Weiß

NATURAL SCIENTIST · BIOCHEMISTRY & BIOTECHNOLOGY

Vulkanstraße 27, 17489 Greifswald, Federal Republic of Germany

☎ (+49) 151-1444-0649 | ✉ martin_in_ladenburg@hotmail.com | 📠 martinladenburg | 📺 weiß-martin-97a59776 | 📧 martinladenburg

“Curiosity is the key to problem solving.” - Galileo Galilei

Education

Ernst-Moritz-Arndt-Universität Greifswald

Greifswald, Germany

PHD-THESIS

Dec. 2013 - present

- Joint industry project with F. Hoffmann-La Roche AG and Prof. Dr. Uwe T. Bornscheuer
Thesis title: *Novel Transaminases for the Preparation of Pharmaceutically Relevant Chiral Amines*

Technische Universität Darmstadt

Darmstadt, Germany

M.Sc. IN BIOMOLECULAR ENGINEERING

Oct. 2011 - Nov. 2013

- Specialization: *White Biotechnology*
- Master-thesis in the working group of Prof. Dr. T. Uwe Bornscheuer in Greifswald
Thesis title: *Development of a New Solid-phase Assay for High-throughput-screening of Both (R)- and (S)-Selective Transaminases*

Technische Universität Darmstadt

Darmstadt, Germany

B.Sc. IN BIOMOLECULAR ENGINEERING

Oct. 2008 - Oct. 2011

- Seminar tutor for chemistry, organic chemistry & physics for students of biology since 2009
Initiated and employed by study dean Prof. Dr. Heribert Warzecha
- Bachelor-thesis in the working group of Prof. Dr. Harald Kolmar in Darmstadt
Thesis topic: *Development of a Yeast Cell Surface Display*

Alternative Civilian Service

Nierenzentrum Heidelberg e.V.

Heidelberg, Germany

CIVILIAN SERVICE

Dec. 2007 - Aug. 2008

- Support on Nephrology Hospital Ward
www.nierenzentrum-heidelberg.com

Secondary School

Carl-Benz-Gymnasium Ladenburg

Ladenburg, Germany

ABITUR

Sept. 1998 - Sept. 2007

- Abitur, general qualification for university entrance, 2007
- Private School St. Raphael in Heidelberg, 2004 - 2005

Publications & Patents

Ernst-Moritz-Arndt-Universität Greifswald

Greifswald, Germany

PUBLICATIONS

2014 - 2017

- **Glycine oxidase based high-throughput solid-phase assay for substrate profiling and directed evolution of (*R*)- and (*S*)-selective amine transaminases.**
Martin S. Weiß, Ioannis V. Pavlidis, Clare Vickers, Matthias Höhne and Uwe T. Bornscheuer.
Anal. Chem., **2014**, 86, 11847–11853.
- **Identification of (*S*)-selective transaminases for the asymmetric synthesis of bulky chiral amines.**
Ioannis V. Pavlidis, Martin S. Weiß, Maika Genz, Paul Spurr, Steven P. Hanlon, Beat Wirz, Hans Iding and Uwe T. Bornscheuer.
Nat. Chem., **2016**, 8, 1076–1082.
- **Protein-engineering of an amine transaminase for the stereoselective synthesis of a pharmaceutically relevant bicyclic amine.**
Martin S. Weiß, Ioannis V. Pavlidis, Paul Spurr, Steven P. Hanlon, Beat Wirz, Hans Iding and Uwe T. Bornscheuer.
Org. Biomol. Chem., **2016**, 14, 10249–10254.
- **Amine transaminase engineering for spatially bulky substrate acceptance.**
Martin S. Weiß, Ioannis V. Pavlidis, Paul Spurr, Steven P. Hanlon, Beat Wirz, Hans Iding and Uwe T. Bornscheuer.
ChemBioChem, **2017**, 18, 1022–1026.

PATENT

- **Mutant transaminases as well as methods and uses relating thereto.**
Bornscheuer Uwe T., Hanlon Steven P., Iding Hans, Pavlidis Ioannis V., Spurr Paul, Weiß Martin S., Wirz Beat.
PCT Patent Application, **2016**, WO2016/166120; US 2016/0304843.

BOOK CHAPTER

- **Solid Phase Agar Plate Assay for Screening Amine Transaminases.**
In: Protein Engineering: Methods and Protocols, ISBN: 978-1-4939-7364-4,
Martin S. Weiß, Matthias Höhne and Uwe T. Bornscheuer.
Springer Publishing (In press)

Technische Universität Darmstadt

Darmstadt, Germany

PUBLICATIONS

2013

- **Engineering of a cytidine 5'-monophosphate-sialic acid synthetase for improved tolerance to functional sialic acids.**
Dong Yi, Ning He, Michael Kickstein, Julia Metzner, Martin S. Weiß, Alan Berry and Wolf-Dieter Fessner.
Adv. Synth. Catal., **2013**, 355: 3597–3612.

(Martin Weiß)

Acknowledgements

Zu aller erst möchte ich mich bei Herrn Prof. Dr. Bornscheuer dafür bedanken, dass er mich in seine Arbeitsgruppe aufgenommen hat und mir so nicht nur ermöglicht hat zu promovieren, sondern darüber hinaus auch auf diesem internationalen Industrieprojekt sehr wertvolle Erfahrungen zu sammeln, die mich in vielerlei Hinsicht enorm weiter gebracht haben.

Ganz besonderer Dank gilt natürlich Herrn Dr. Beat Wirtz und Herrn Dr. Hans Iding der Firma Hoffmann-La Roche, die gemeinsam mit Herrn Prof. Bornscheuer das Industrieprojekt geplant, geleitet und ermöglicht haben! Ebenso verdanke ich Herrn Dr. Ioannis Pavlidis, der als verantwortlicher Post-Doc das Projekt geleitet hat, dass dieses Projekt durch seinen unermüdlichen Einsatz in so kurzer Zeit zu so vielen Publikationen und Patenten geführt hat! Ferner diene mir Herr Dr. Pavlidis in vielen Dingen als großes Vorbild insbesondere was effizientes und strukturiertes Arbeiten anbelangt, sowie seine herausragenden Fähigkeiten wirklich elegant und kondensiert zu formulieren. Ich danke ihm sehr für alles was ich von ihm lernen konnte! Vielen herzlichen Dank sei an dieser Stelle auch an alle jenen Wissenschaftler von Roche ausgesprochen, die im Hintergrund zum Erfolg des Projektes beigetragen haben, beispielsweise durch die Substratsynthese und Charakterisierung, Hilfestellung bei der Analytik, Durchführung von präparativen Synthesen, deren Aufarbeitung und Analytik, oder die Bestimmung der absoluten Konfiguration unserer Produkte.

Besonderes dankbar bin ich, dass ich hier in dieser Arbeitsgruppe die Gelegenheit erhalten habe, so viele verschiedene Menschen aus aller Herren Länder näher kennen lernen zu können. So waren unter diesen Kollegen Leute aus z.B. Afrika (Chris), Brasilien (Ingrid), China (Qing-Yun und Yi-Feng), England (Clare), Griechenland (Ioannis), Indien (Vishnu), Italien (Alberto und Claudia), der Schweiz (Beat und Hans), Spanien (Javier und Isabelle) und aus den USA (Anders und Ivan)). Alle diese Begegnungen haben mich sehr inspiriert, meinen Horizont enorm erweitert und mich auf ihre Weise sehr beeindruckt. Besonders die internationalen Gastwissenschaftler und Stipendiaten, die an so großer Zahl auch für längere Zeit bei uns zu Besuch waren und die man zum Teil auf den zahlreichen Laborausflügen oder bei anderen Gelegenheiten näher kennenlernen konnte waren sehr wertvolle Begegnungen, zu denen man sonst selten die Gelegenheit bekommen hätte.

Der gesamten Arbeitsgruppe möchte ich dafür danken, dass alle gemeinsam die Infrastruktur bereitgestellt haben um derartige Projekte durchzuführen. Insbesondere danke ich den technischen Assistenten Frau Menyes und Frau Eisner, sowie Frau Dr. Böttcher und Herrn Dr. Dörr für die praktische Organisation des Labors. Im speziellen danke ich mich bei Frau Menyes und Herrn Dr. Dörr für ihre Unterstützung in allen Belangen der HPLC- und GC-Analytik. Dankbar bin ich Herrn Dr. Kabisch und Herrn Dr. Dörr dafür, dass sie mich durch ihre Anregungen und Inspirationen in allen Dingen, die mit elektronischer Datenverarbeitung zu tun haben unglaublich weitergebracht haben!

Ganz besonders möchte ich mich bei Herrn Dr. Dörr, Herrn Dr. Höhne und Frau Dr. Böttcher für ihre allgemeine, große Unterstützung bedanken und dafür, dass sie mir als Ansprechpartner zur Verfügung standen. Ebenso Danke ich allen meinen Freunden, meiner Freundin Vivi, meiner Familie und meinen Kollegen für ihre so wertvolle Unterstützung!